Pharmacological Research 224 (2026) 108107

Contents lists available at ScienceDirect

Pharmacological Research

journal homepage: www.elsevier.com/locate/yphrs

Properties of FDA-approved small molecule protein kinase inhibitors: A 2026 update

Robert Roskoski Jr.

Blue Ridge Institute for Medical Research, 221 Haywood Knolls Drive, Hendersonville, NC 28791, United States

ARTICLE INFO

Keywords:
Chronic immune thrombocytopenia
Chronic spontaneous urticaria
Hand eczema
Mutant *EGFR, HER2,* and *ROS1* non-small cell lung cancer
Ovarian cancer
Tenosynovial giant cell tumors

Chemical compounds studied in this article:
Avutometinib (PubChem CID: 16719221)
Defactinib (PubChem CID: 25117126)
Delgocitinib (PubChem CID: 50914062)
Mirdametinib (PubChem CID: 9826528)
Remibrutinib (PubChem CID: 118107483)
Rilzabrutinib (PubChem CID: 73388818)
Sunvozertinib (PubChem CID: 139377809)
Taletrectinib (PubChem CID: 72202474)
Vimseltinib (PubChem CID: 86267612)
Zongertinib (PubChem CID: 160283094)

ABSTRACT

Because of the dysregulation of protein kinase activity in many neoplastic and inflammatory diseases, protein kinases are among the most significant drug targets in the 21st century. Of the 94 FDA-approved protein kinase inhibitors, ten were approved in 2025. Of these drugs, six target dual specificity protein kinases (MEK1/2), fourteen inhibit protein-serine/threonine kinases, twenty-six block nonreceptor protein-tyrosine kinases, and 48 target receptor protein-tyrosine kinases. Most of these drugs (≈ 80) are prescribed for the management of neoplasms and others are used for the treatment of inflammatory and miscellaneous diseases. Of the 94 FDA-approved agents, about two dozen are used in the treatment of multiple diseases. The following ten drugs received FDA approval in 2025 – avutometinib (inhibiting MEK1/2 in serous ovarian carcinomas), defactinib (blocking FAK in low grade serous ovarian carcinomas), delgocitinib (antagonizing the JAK family in hand eczema), mirdametinib (inhibiting MEK1/2 in type I neurofibromatosis), remibrutinib (blocking BTK in chronic spontaneous urticaria), rilzabrutinib (antagonizing BTK in chronic immune thrombocytopenia), sunvozertinib (blocking mutant exon 21 insertion EGFR NSCLC), taletrectinib (inhibiting mutant *ROS1* in NSCLC), vimseltinib (blocking CSF1R in tenosynovial giant cell tumors), and zongertinib (antagonizing mutant *HER2* in NSCLC). Ninety of the approved protein kinase blockers are orally bioavailable. This article summarizes the physicochemical properties of all 94 FDA-approved small molecule protein kinase inhibitors including the molecular weight, number of hydrogen bond donors/acceptors, ligand efficiency, lipophilic efficiency, polar surface area, and solubility. A total of 45 of the 94 FDA-approved drugs have a least one Lipinski rule of five violation.

1. An overview of therapeutic protein kinase inhibitors

Because of various mutations, genetic translocations, and overexpression, the dysregulation of protein kinase activity constitutes a pivotal role in the pathogenesis of autoimmune, cardiovascular, inflammatory, and nervous diseases as well as a host of neoplasms. It is not surprising that these protein kinases are among the most important therapeutic targets in the 21st century [1,2]. Back-of-the envelope calculations suggest that between one-fourth and one-third of drug development programs in the United States and throughout the world target these enzymes. The clinical efficacy of imatinib in the treatment of Philadelphia chromosome-positive CML (chronic myelogenous leukemia), which received FDA approval in 2001, stimulated the quest for orally efficacious therapeutic protein kinase blockers [3–5]. This therapeutic achievement ensued from the imatinib inhibition of the activated chimeric BCR-Abl nonreceptor protein-tyrosine kinase, the

Abbreviations: ADME, Absorption, Distribution, Metabolism, Excretion; ALL, Acute lymphocytic leukemia; AS, Activation segment; BBB, Blood Brain Barier; BP, Back Pocket; bRo5, Beyond Lipinski's rule of five; BTK, Bruton Tyrosine Kinase; C-spine, Catalytic spine; cIPP, Chronic immune thrombocytopenia; CNS, Central Nervous System; CS1, Catalytic spine residue 1; CML, Chronic myelogenous leukemia; CL, Catalytic loop; CLL, Chronic lymphocytic leukemia; CSF1R, Colony stimulating factor-1 receptor; DS, Dual specificity; EGFR, Epidermal growth factor receptor; FDA, The Food and Drug Administration of the United States; FP, Front pocket; GEF, Guanine nucleotide exchange factor; GK, Gatekeeper; GRL, Glycine-rich loop; HCC, Hepatocellular carcinoma; HTS, High throughput screening; IFN, Interferon; IL, Interleukin; JAK, Janus kinase; KLIFS-3, Kinase-ligand interaction fingerprint and structure residue-3; LGSC, Low grade serous carcinoma of the ovary; LE, Ligand efficiency; LipE, Lipophilic efficiency; NF1, Neurofibromatosis type 1; NTRK, Neurotrophic Tyrosine Receptor Kinase; NSCLC, Non-small cell lung cancer; PI3K, Phosphatidylinositol 3-kinase; PKA, Protein kinase A; PSA, Polar surface area; RCC, Renal cell carcinoma; Ro5, Lipinski's rule of five; R-spine, Regulatory spine; RS1, Regulatory spine residue 1; SBN, Serous borderline neoplasm; Sh2, Shell residue 2; TGCT, Tenosynovial giant cell tumor; VEGFR, Vascular endothelial growth factor receptor.

E-mail address: rrj@brimr.org.

https://doi.org/10.1016/j.phrs.2026.108107
Received 20 January 2026; Accepted 20 January 2026
Available online 24 January 2026

causative biochemical agent that produces these leukemias.

The existence of nearly eight thousand protein kinase X-ray crystal structures in the public domain has played a significant role in structure-based drug development. More than 425 orally bioavailable protein kinase antagonists are in or have been in clinical trials worldwide [6]. A complete directory of these drugs can be accessed from www.icoa.fr/pkidb/. The FDA has approved 94 agents that target about two dozen different wild-type and mutant protein kinases (Table 1, Fig. 1, supplementary material). However, these enzymes constitute a small portion of the 518-member protein kinase superfamily. Other drugs that target these protein kinases and underrepresented protein kinases are in clinical trials worldwide [4–7].

Manning et al. reported that the human protein kinase enzyme superfamily consists of 478 typical and 40 atypical kinases [8]; phosphatidylinositol 3-kinase (PI3K) is among the atypical enzymes with a lipid and not a protein substrate [5,9]. Typical protein kinases catalyze the following reaction;

$$MgATP^{1-} + \text{protein–O:H} \rightarrow \text{protein–O:}PO_3^{2-} + MgADP + H^+$$

Note that the kinase catalyzes the transfer of the phosphoryl group or phosphorylium ion ($:PO_3^{2-}$) and not the phosphate group (OPO_3^{2-}) as stated in numerous publications (I thank the late Fritz Lipmann (1899–1986) for drawing my attention to this distinction). This superfamily is made up of protein-serine/threonine kinases (385 members), protein-tyrosine kinases (90), and protein-tyrosine kinase–like enzymes (43). The protein-tyrosine kinase group consists of both transmembrane receptor (58) and intracellular nonreceptor (32) proteins. The protein-tyrosine kinase like group includes the TGF-β receptor (a transmembrane protein-threonine kinase) and A/B/C-Raf (protein-serine kinases), enzymes with protein-tyrosine kinase structural features. Moreover, the protein kinase family includes a small group of enzymes such as MEK1/2 that catalyze the phosphorylation of tyrosine and then threonine residues that occur in the activation segment of their target protein kinases. Owing to this distinctive process, MEK1/2 and related enzymes are classified as dual specificity (DS) protein kinases. An additional sign of the prominence of protein kinases in biology is the observation that about one in every 40 human genes (518 protein kinase genes out of an estimated 20,000 human protein-encoding genes) corresponds to a protein kinase amounting to ≈ 2.5 % of the human genome. Enrico Fermi type back-of-the envelop calculations indicate that these enzymes catalyze the phosphorylation of up to one-third of the proteome. Other information confirming the significance of protein kinases as drug targets is the discovery of Manning et al. that 244 protein kinase genes are linked to cancer amplicons and other disease loci [8]. Accordingly, as further research on the development of various disorders is undertaken, we can anticipate that there will be a substantial growth in protein kinase therapeutic targets.

Table 1
Principal FDA-approved protein kinase inhibitor drug targets[a].

Kinase family	Class of Kinase	US FDA approved
JAK	NRY	11
EGFR/ErbB	RY	9
VEGFR	RY	8
ALK	RY	6
BCR-Abl	NRY	6
BTK	NRY	6
MEK1/2	DS	6
FGFR	RY	5
B-RAF	S/T	4
CDK4/6	S/T	4
RET	RY	4
ErbB2/HER2	RY	3
FKBP	S/T	3
Flt3	RY	3
CSF1	RY	2
c-MET	RY	2
ROCK	S/T	2
ROS1	RY	2
TRKA	RY	2
AKT	S/T	1
FAK	NRY	1
Kit	RY	1
PDGFR	RY	1
Syk	RY	1
TYK2	NRY	1
Total		94

[a] DS, Dual specificity protein kinase; NYR, nonreceptor protein-tyrosine kinase; RY, receptor protein-tyrosine kinase; S/T, protein-serine/threonine kinase

As of January 2026, the FDA has approved 94 small molecule therapeutic protein kinase blockers (Table 1) [10–16]. Except for delgocitinib (a cream), netarsudil (an eye drop) and temsirolimus and trilaciclib (which are given intravenously), all kinase blockers are orally bioavailable. Ruxolitinib, which is a JAK1/2 orally active blocker that was FDA-approved for the treatment of polycythemia vera and myelofibrosis in 2011, is also prescribed as a topically active cream as approved by the FDA in 2021 for the management of atopic dermatitis. Of the 94 approved drugs, forty-eight target receptor protein-tyrosine kinases, twenty-six block nonreceptor protein-tyrosine kinases, fourteen inhibit protein-serine/threonine protein kinases, and six block dual specificity protein kinases (MEK1/2) (Table 2). The majority of the small molecule blockers (≈ 80) are approved for the treatment of solid and nonsolid neoplasms. About four dozen of these approved drugs are multikinase antagonists. The concurrent inhibition of multiple protein kinases has possible benefits as well as shortcomings. For example, the therapeutic effectiveness of multikinase antagonists may be linked to the inhibition of two or more targets. For example, gilteritinib, sunitinib, and cabozantinib have documented off-target activity against the Axl receptor protein-tyrosine kinase and this activity may add to their therapeutic usefulness [17]. In contrast, the antagonism of off-target protein kinases may elicit adventitious side effects. Accordingly, we have the dilemma of whether a magic shotgun multienzyme inhibitor ought to be preferred over Paul Ehrlich's enzyme-specific magic bullet [18].

More than a dozen of the FDA-approved protein kinase antagonists are used for the treatment of nonneoplastic diseases. These include (i) the recently approved delgocitinib for the management of hand eczema, (ii) the newly approved remibrutinib for the treatment of chronic spontaneous urticaria, (iii) upadacitinib for the treatment of psoriatic arthritis, rheumatoid arthritis, and atopic dermatitis, (iv) tofacitinib for the management of psoriatic arthritis, rheumatoid arthritis, and ulcerative colitis, (v) baricitinib and upadacitinib for the treatment of rheumatoid arthritis, (vi) ruxolitinib and abrocitinib for the management of atopic dermatitis, (vii) belumosudil, ibrutinib, and ruxolitinib for the treatment of graft vs. host disease, (viii) fostamatinib and the recently approved rilzabrutinib for the management of chronic immune thrombocytopenia, (ix) deuruxolitinib and ritlecitinib for the management of alopecia areata, and (x) netarsudil for the treatment of glaucoma [10–17]. The 2025 approvals of rilzabrutinib and remibrutinib represent the first nononcologic approvals for BTK blockers. Moreover, sirolimus, ruxolitinb, and ibrutinib are approved therapies for both neoplastic and nonneoplastic diseases.

Fifteen of the FDA-approved kinase antagonists form a covalent bond with their targets and are consequently categorized as TCIs (targeted covalent inhibitors) [19,20]. These agents include ibrutinib (inhibiting BTK in chronic graft vs. host disease, mantle cell lymphoma, CLL, marginal zone lymphoma, and Waldenström macroglobulinemia, acalabrutinib (blocking BTK in mantle cell lymphoma and CLL), remibrutinib (inhibiting BTK in patients with chronic spontaneous urticaria), rilzabrutinib (forming a reversible covalent bond with BTK in chronic immune thrombocytopenia), zanubrutinib (antagonizing BTK in mantle cell lymphoma), afatinib, dacomitinib, lazertinib, mobocertinib, osimertinib, and sunvozertinib (all six targeting mutant *EGFR* in NSCLC), neratinib (blocking ErbB2 in HER2-positive breast cancer), zongertinib (targeting mutant *ErbB2/HER2* in NSCLC), ritlecitinib (blocking JAK3 in alopecia areata), and futibatinib (antagonizing FGFR2 fusions or

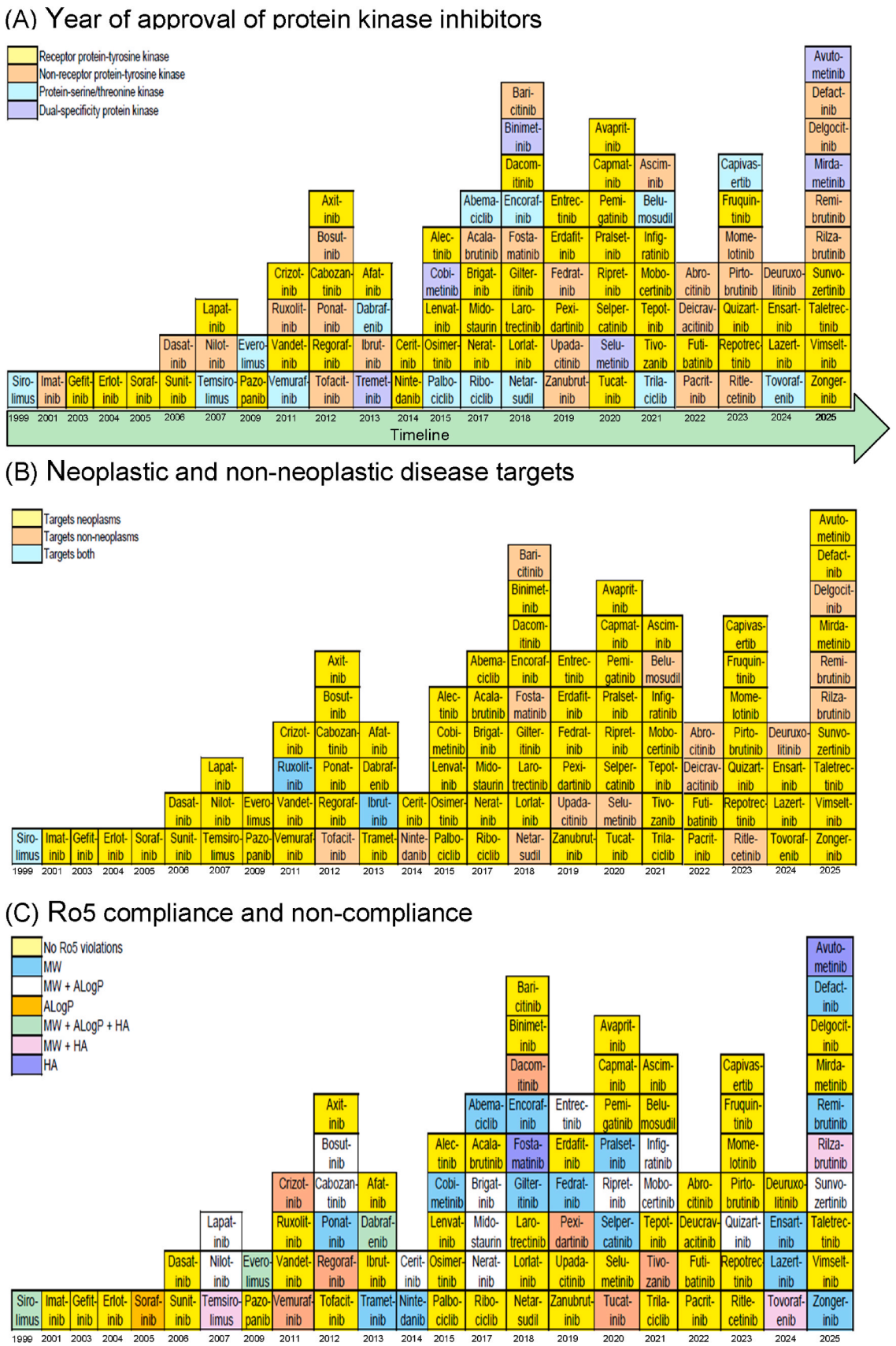

Fig. 1. (A) Year of approval of receptor and nonreceptor protein-tyrosine kinase inhibitors, protein-serine/threonine kinase antagonists, and dual specificity protein kinase blockers. (B) Protein kinase inhibitors that target neoplastic disorders, nonneoplastic disorders, and both classes of diseases. (C) Ro5 compliant and non-compliant protein kinase antagonists. MW, molecular weight; AlogP, atom-based logarithm of the partition coefficient violation; HA, Hydrogen bond Acceptor; HD, Hydrogen bond Donor.

Table 2
FDA-approved small molecule protein kinase inhibitors, their protein kinase targets, and therapeutic indications[a].

Drug	Code	Company	Trade name	Year approved	Primary targets[b]	Therapeutic indications[c]
Abemaciclib	LY2835219	Lilly	Verzenio	2017	CDK4/6	$HER2^+$ breast cancer, both monotherapy and combination therapy
Abrocitinib	PF04965842	Pfizer	Cibinqo	2022	JAK family	Atopic dermatitis in adults and children 12 years of age and older
Acalabrutinib	ACP-196	Acerta Pharma	Calquence	2017	BTK	Mantle cell lymphoma, chronic lymphocytic leukemia (CLL), small lymphocytic lymphoma (SLL)
Afatinib	BIBW2992	Boehringer Ingelheim	Tovok	2013	ErbB1/2/4	NSCLC (non-small cell lung cancer) and squamous NSCLC
Alectinib	CH5424802	Roche	Alecensa	2015	ALK, RET	ALK^+ NSCLC
Asciminib	ABL001	Novartis	Scemblix	2021	BCR-Abl	First or second-line treatment of Ph^+ CML with or without a T315I mutation
Avapritinib	BLU285	Blueprint Medicines	Ayvakit	2020	PDGFRα	Gastrointestinal stromal tumors (GIST) with a *PDGFRα* exon 18 mutations; indolent and advanced systemic mastocytosis
Avutometinib	RO-5126766 & VS-6766	Verastem	Avmapki	2025	A/B/C-Raf & MEK1/2	Second-line treatment of *KRAS* mutant low grade serous ovarian carcinoma in combination with defactinib
Axitinib	AG013736	Pfizer	Inlyta	2012	VEGFR1/2/3	Single agent and combination therapy for renal cell carcinoma (RCC)
Baricitinib	LY3009104	Lilly	Olumiant	2018	JAK family	Rheumatoid arthritis
Belumosudil	KD025	Kadmon Pharma	Rezurock	2021	ROCK2	Graft vs. host disease in adults and pediatric patients 12 years of age and older
Binimetinib	MEK162	Array BioPharma	Mektovi	2018	MEK1/2	Melanoma with *BRAF V600E/K* and NSCLC with *BRAF* V600E mutations with encorafenib
Bosutinib	SKI-606	Pfizer	Bosulif	2012	BCR-Abl	Ph^+ CML
Brigatinib	AP 26113	Ariad Pharm	Alunbrig	2017	ALK	ALK^+ NSCLC
Cabozantinib	BMS907351	Exelixis	Cometriq & Cabometyx	2012	RET, VEGFR2	Differentiated thyroid cancer, RCC, HCC
Capivasertib	AZD5363	AstraZeneca	Truqap	2023	AKT	Hormone receptor (HR)-positive, human epidermal growth factor receptor 2 (HER2)-negative breast cancer bearing *PIK3CA/AKT1/PTEN* mutations
Capmatinib	INC280	Novartis	Tabrecta	2020	c-MET (HGFR)	NSCLC with *MET* exon 14 skipping mutations
Ceritinib	LDK378	Novartis	Zykadia	2014	ALK	ALK^+ NSCLC
Cobimetinib	GDC-0973	Genentech	Cotellic	2015	MEK1/2	$BRAF^{V600E/K}$ melanomas in combination with vemurafenib; histiocytic neoplasms
Crizotinib	PF2341066	Pfizer	Xalkori	2011	ALK, ROS1	ALK^+ (i) NSCLC,(ii) anaplastic large cell lymphoma, (iii) inflammatory myofibroblastic tumors, (iv) anaplastic large cell lymphoma; $ROS1^+$ NSCLC
Dabrafenib	GSK2118436	GSK	Tafinlar	2013	B-Raf	*BRAF* mutation-positive (i) melanomas (V600K/E), (ii) NSCLC (V600E), (iii) anaplastic thyroid cancers (V600E); pediatric glioma (V600E)
Dacomitinib	PF00299804	Pfizer	Visimpro	2018	EGFR	*EGFR*-mutant NSCLC with an exon 19 deletion or exon 21 L858R substitution
Dasatinib	BMS354825	Bristol Myers Squibb	Sprycel	2006	BCR-Abl	Ph^+ CML or ALL
Defactinib	PF-04554878	Verastem	Faczinia	2025	FAK	Second-line treatment of *KRAS* mutant low grade serous ovarian carcinoma in combination with avutometinib
Delgocitinib	JTE-052	LEO Pharm	Anzupgo	2025	JAK family	Topically for hand eczema
Deucravacitinib	BMS986165	Bristol Myers Squibb	Sotyktu	2022	TYK2	Psoriasis
Deuruxolitinib	CTP-543	Sun Pharma-ceutical Industries, Inc.	Leqselvi	2024	JAK1/2	Alopecia areata
Encorafenib	LGX818	Array BioPharma	Braftovi	2018	B-Raf	*BRAF* mutant melanoma (V600E/K) or NSCLC (V600E) in combination with binimetinib; *BRAF* mutant colorectal cancer (V600E) in combination with cetuximab
Ensartinib	LGX818	Xcovery Holdings, Inc.	Ensacove	2024	ALK	First-line treatment of ALK^+ NSCLC
Entrectinib	RXDX101	Genentech	Rozlytrek	2019	TRKA/B/C, ROS1	Solid tumors with NTRK fusion proteins, $ROS1^+$ NSCLC
Erdafitinib	JNJ42756493	Jansen Pharm	Balversa	2019	FGFR1/2/3/4	Second-line treatment of urothelial bladder cancer with *FGFR3* gene alterations
Erlotinib	OSI-774	Genentech	Tarceva	2004	EGFR	NSCLC, pancreatic cancer
Everolimus	RAD001	Novartis	Afinitor	2009	FKBP12/mTOR	HER2-negative breast cancer, pancreatic neuroendocrine tumors, RCC, renal angiomyolipoma, subependymal giant cell astrocytoma
Fedratinib	TG101348	Celgene	Inrebic	2019	JAK2	Primary or secondary myelofibrosis
Fostamatinib	R788	Rigel Pharma.	Tavalisse	2018	Syk	Chronic immune thrombocytopenia
Fruquintinib	HMPL013	Takeda	Fruzaqla	2023	VEGFR2	CRC
Futibatinib	TAS120	Tiaho Pharma	Lytgobi	2022	FGFR2	Bile duct cancers (cholangiocarcinomas) with FGFR2 fusion proteins or other rearrangements
Gefitinib	ZD1839	AstraZeneca	Iressa	2003	EGFR	NSCLC with exon 19 deletions or exon 21 L848R substitutions
Gilteritinib	ASP2215	Astellas Pharma	Xospata	2018	Flt3	*FLT3*-mutation positive AML
Ibrutinib	PCI-32765	Johnson & Johnson	Imbruvica	2013	BTK	CLL,SLL, graft vs. host disease, Waldenström macroglobulinemia
Imatinib	STI571	Novartis	Gleevec	2001	BCR-Abl	Ph^+ CML or ALL, aggressive systemic mastocytosis, chronic eosinophilic leukemia, dermatofibrosarcoma protuberans,

(*continued on next page*)

Table 2 (*continued*)

Drug	Code	Company	Trade name	Year approved	Primary targets[b]	Therapeutic indications[c]
						hypereosinophilic syndrome, GIST, myelodysplastic/ myeloproliferative disease
Infigratinib	BGJ398	QED Therapeutics	Truseltiq	2021	FGFR2	Cholangiocarcinomas with FGFR2 fusions or other rearrangement
Lapatinib	GW572016	GSK	Tykerb	2007	EGFR, ErbB2/ HER2	$HER2^+$ breast cancer in combination with capecitabine or letrozole
Larotrectinib	LOXO-101	Bayer	Vitrakvi	2018	TRKA/B/C	Solid tumors with NTRK fusion proteins
Lazertinib	GNS1480	Janssen Biotech, Inc.	Lazcluze	2024	Mutant *EGFR*	NSCLC with exon19 deletions or exon 21 L858R substitutions in combination with amivantamab
Lenvatinib	AK175809	Easai Co.	Lenvima	2015	VEGFR, RET	Differentiated thyroid cancer, HCC, RCC, endometrial carcinoma
Lorlatinib	PF06463922	Pfizer	Lorbrena	2018	ALK	ALK^+ NSCLC
Midostaurin	CPG 41251	Novartis	Rydapt	2017	Flt3	*FLT3* mutation positive AML, mastocytosis, mast cell leukemia
Mirdametinib	PD0325901	SpringWorks Therapeutics, Inc.	Gomekli	2025	MEK1/2	Type I neurofibromatosis
Mobocertinib	TAK-788	Takeda Pharm.	Exkivity	2021	EGFR	NSCLC with *EGFR*-positive exon 20 insertions
Momelotinib	CYT 387	GSK	Ojjaara	2023	JAK1/2	Primary or secondary myelofibrosis patients with anemia
Neratinib	HKI-272	Puma Biotech	Nerlynx	2017	ErbB2/ HER2	Second and third-line treatment of $HER2^+$ breast cancer
Netarsudil	AR11324	Aerie Pharma	Rhopressa	2018	ROCK1/2	Glaucoma
Nilotinib	AMN107	Novartis	Tasigna	2007	BCR-Abl	First or second-line treatment of Ph^+ CML
Nintedanib	BIBF-1120	Boehringer Ingelheim	Vargatef	2014	FGFR1/2/3	Idiopathic pulmonary fibrosis, chronic fibrosing interstitial lung diseases
Osimertinib	AZD-9292	AstraZeneca	Tagrisso	2015	EGFR	NSCLC with exon 19 deletions, exon 21 substitutions (L858R), or T790M mutations
Pacritinib	SB1518	CTI BioPharma	Vonjo	2022	JAK2	Primary or secondary myelofibrosis with a low platelet count
Palbociclib	PD0332991	Parke-Davis	Ibrance	2015	CDK4/6	HR^+ and $HER2^-$ breast cancer in combination with (i) an aromatase inhibitor or (ii) fulvestrant
Pazopanib	GW786034	GSK	Votrient	2009	VEGFR1/2/ 3	RCC, soft tissue sarcomas
Pemigatinib	INCB054828	Incyte Corp.	Pemazyre	2020	FGFR2	Advanced cholangiocarcinoma with a FGFR2 fusions or rearrangements
Pexidartinib	PLX3397	Plexxikon Inc	Turalio	2019	CSF1R	Tenosynovial giant cell tumors
Pirtobrutinib	LOXO-305	Lilly	Jaypirca	2023	BTK	Mantle cell lymphoma, CLL, SLL
Ponatinib	AP 24534	Ariad Pharm	Iclusig	2012	BCR-Abl	Ph^+ ALL, CML, $T315I^+$ CML
Pralsetinib	Blu-667	Blueprint Medicines	Gavreto	2020	RET	RET-fusion protein NSCLC, RET- fusion protein thyroid cancer
Quizartinib	ASP-2869	Daiichi Sankyo	Vanflyta	2023	Flt3	*FLT3* internal tandem duplication positive AML in combination with cytarabine and daunorubicin
Regorafenib	BAY 734506	Bayer	Stivarga	2012	VEGFR1/2/ 3	Second-line treatment of CRC, HCC, GIST
Remibrutinib	LUO064	Novartis	Rapsido	2025	BTK	Chronic spontaneous urticaria
Repotrectinib	TX-0005	Bayer	Augtyro	2023	ROS1	$ROS1^+$ NSCLC and solid tumors with NTRK fusion proteins
Ribociclib	LEE011	Novartis	Kisqali	2017	CDK4/6	HR^+ /$HER2^-$ breast cancer combination therapy
Rilzabrutinib	PRN1088	Genzyme	Wayritz	2025	BTK	Chronic immune thrombocytopenia
Ripretinib	DCC-2618	Decipera Pharma.	Qinlock	2020	Kit, PDGFRα	Fourth-line treatment of GIST
Ritlecitinib	PF06651600	Pfizer	Litfulo	2023	JAK3	Alopecia areata
Ruxolitinib	INCB018424	Incyte Corp.	Jakafi	2011	JAK family	Myelofibrosis, polycythemia vera, graft vs. host disease, atopic dermatitis (applied topically)
Selpercatinib	CEGM9YBNG	Lilly	Retevmo	2020	RET	RET fusion (i) NSCLC, (ii) solid tumors and (iii) thyroid cancers; *RET* mutant medullary thyroid cancer
Selumetinib	AZD6224	AstraZeneca	Koselugo	2020	MEK1/2	Type I neurofibromatosis
Sirolimus	AY 22989	Wyeth, LLC	Rapamycin	1999	FKBP12/ mTOR	Kidney transplant, lymphangioleiomyomatosis
Sorafenib	BAY 439006	Bayer	Nexavar	2005	VEGFR1/2/ 3	HCC, RCC, differentiated thyroid cancer
Sunitinib	SU11248	Pfizer	Sutent	2006	VEGFR2	GIST, RCC, pancreatic neuroendocrine tumors
Sunvozertinib	PZD9008	Dizal Pharm	Zegfrovy	2025	EGFR	Exon 21 *EGFR* insertion NSCLC
Taletrectinib	AB106	Nuvation Bio	Ibtrovi	2025	ROS1	ROS1 NSCLC
Temsirolimus	CCI-779	Wyeth, LLC	Torisel	2007	FKBP12/ mTOR	RCC
Tepotinib	EMD1214063	EMD Serono Inc.	Tepmetko	2021	c-MET (HGFR)	NSCLC with *MET*-exon skipping alterations
Tivozanib	AV951	AVEO Pharma	Fotvida	2021	VEGFR2	Third-line treatment of RCC
Tofacitinib	CP-690550	Pfizer	Tasocitinib	2012	JAK3	Rheumatoid, psoriatic, and juvenile idiopathic arthritis, ulcerative colitis, ankylosing spondylitis
Tovorafenib	DAY101	Pfizer	Ojemda	2024	B-/C-Raf	Pediatric low grade glioma in patients older than six months harboring a *BRAF* fusion or rearrangement or a *BRAF* V600 mutation
Trametinib	GSK1120212	GSK	Mekinist	2013	MEK1/2	Melanoma with *BRAF V600E* or *V600K* mutations with dabrafenib; NSCLC, anaplastic thyroid cancer, and low grade glioma in children with *BRAF* V600E mutations with dabrafenib
Trilaciclib	G1T28	G1 Therapeutics	Cosela	2021	CDK4/6	Chemotherapy-induced myelosuppression when administered prior to a cytotoxic regimen for small cell lung cancer
Tucatinib	ONT-380	Seattle Genetics	Tukysa	2020	ErbB2/ HER2	$HER2^+$ breast cancer, CRC

(*continued on next page*)

Table 2 (*continued*)

Drug	Code	Company	Trade name	Year approved	Primary targets[b]	Therapeutic indications[c]
Upadacitinib	ABT-494	AbbVie	Rinvoq	2019	JAK1	Second-line treatment for rheumatoid arthritis, psoriatic arthritis, atopic dermatitis, ulcerative colitis
Vandetanib	ZD6474	Sanofi	Zactima	2011	RET	Medullary thyroid cancer
Vemurafenib	PLX-4032	Genentech	Zelboraf	2011	B-Raf	*BRAF V600E* mutation positive melanoma, *BRAF V600* Chester-Erdheim disease
Vimseltinib	DCC-3014	Decifera	Romvisma	2025	CSF1R	Adult patients with symptomatic tenosynovial giant cell tumors for which surgical resection will potentially cause worsening functional limitation or severe morbidity
Zanubrutinib	BGB3111	BeiGene	Brukinsa	2019	BTK	Mantle cell lymphoma, Waldenström macroglobulinemia, marginal zone lymphoma, CLL, SLL, follicular lympmphoma
Zongertinib	884–819–6	Boehringer	Hernexeos	2025	ErbB2/ HER2	Mutant *HER2* NSCLC

[a] Data from Refs. [10–16] and www.brimr.org/PKI/PKIs.htm.
[b] Although many of these drugs are multikinase inhibitors, only the initial FDA-approved therapeutic targets are given here.
[c] ALK$^+$, ALK-positive; ALL, acute lymphoblastic leukemia; AML, acute myelogenous leukemia; CLL, chronic lymphocytic leukemia; CML, chronic myelogenous leukemia; ErbB2/HER2, human epidermal growth factor receptor-2; GIST, gastrointestinal stromal tumor; HCC, hepatocellular carcinoma; HER2$^+$, human epidermal growth factor receptor-2 positive; HR$^+$, hormone receptor postive; c-MET (HGFR), hepatocyte growth factor receptor; NSCLC, non-small cell lung cancer; Ph$^+$, Philadelphia chromosome positive; RCC, renal cell carcinoma; SLL, small lymphocytic lymphoma.

rearrangements in cholangiocarcinomas). EGFR (aka ErbB1) and ErbB4 of the ErbB1/2/3/4 epidermal growth factor receptor family are the predominant mutation-bearing protein kinases found in numerous cancers [3]. For a review of the characteristics of small molecule protein kinase blockers that were FDA-approved prior to 2025, see Refs. [10–16].

Of the 94 FDA-approved protein kinase antagonists, thirty-two are used for the treatment of more than one malady. For example, imatinib is approved for the treatment of eight different disorders (Table 2). This therapeutic blocks the nonreceptor protein-tyrosine kinase Abl (and the

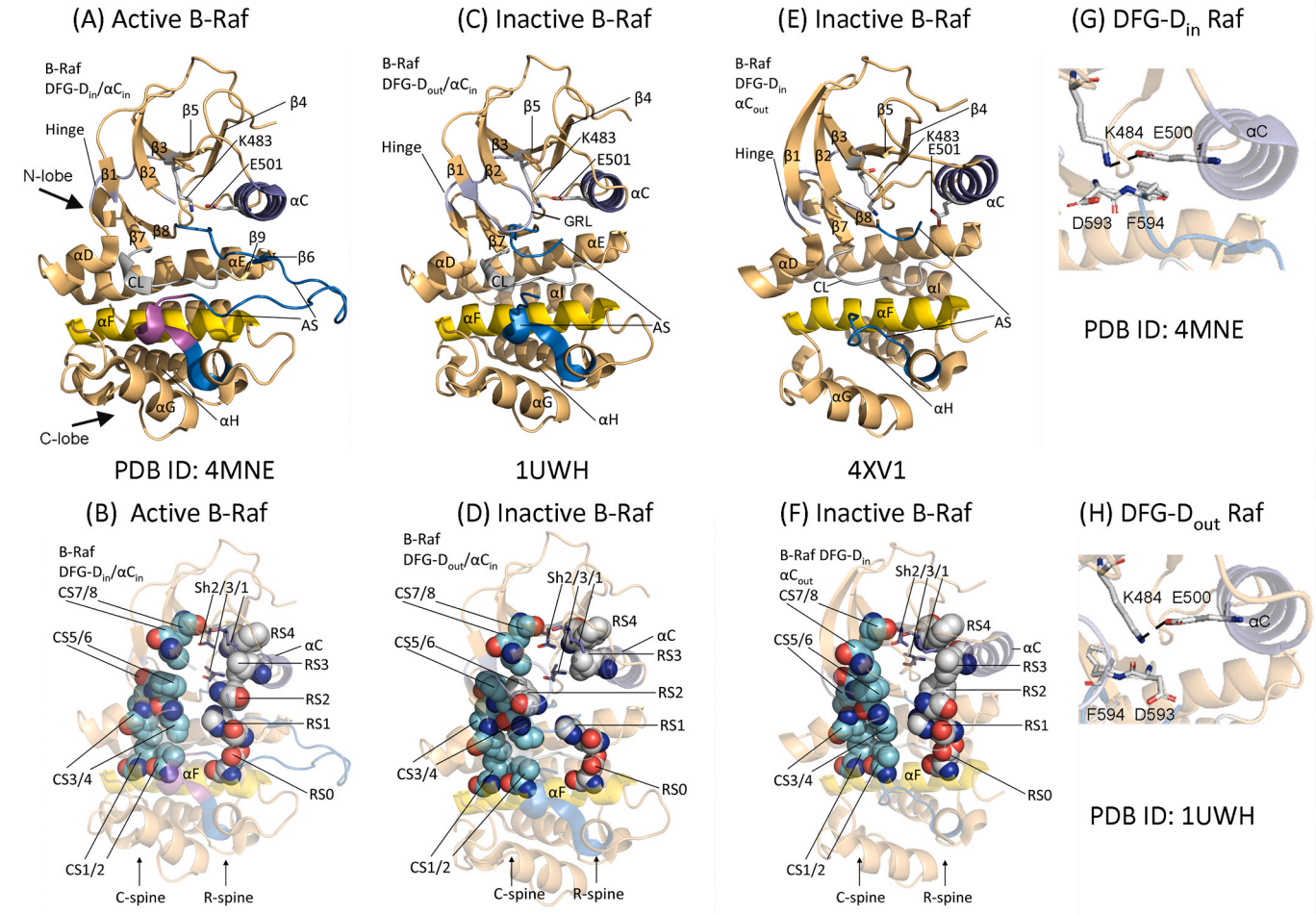

Fig. 2. (A) Overview of active B-Raf and (B) its C-spine, R-spine, and shell residues. (C) The DFG-D$_{out}$ and αC$_{in}$ structure of dormant B-Raf and (D) its C-spine, R-spine, and shell residues. (E) Overview of the DGF-D$_{in}$ and αC$_{out}$ structure of B-Raf and (F) its C-spine, R-spine, and shell residues. (G) The DFG-D$_{in}$ conformation. (H) The DFG-D$_{out}$ conformation. Dashes represent electrostatic bonds. AS, activation segment; CL, catalytic loop. GRL, glycine-rich loop. Figs. 3, 6, and 9 were prepared using the PyMOL Molecular Graphics System Version 2.5.4 Schrödinger, LLC.

BCR-Abl chimera – responsible for the development of chronic myelogenous leukemia or CML), Abl2, PDGFRα/β, Kit (the stem cell factor receptor), and epithelial discoidin domain-containing receptor-1 (DDR1) and receptor-2 (DDR2). DDR1/2, which are activated by collagen, participate in cell proliferation, differentiation, migration, and extracellular matrix remodeling. Imatinib is used for the management of (i) the first-line treatment of Philadelphia chromosome-positive CML, (ii) acute lymphoblastic leukemia or ALL, (iii) myelodysplastic/myeloproliferative diseases with *PDGFR* gene-rearrangements, (iv) hypereosinophilic syndrome, (v) chronic eosinophilic leukemia, (vi) *KIT* mutation-positive gastrointestinal stromal tumors (GIST), (vii) dermatofibrosarcoma protuberans, and (viii) as a second-line treatment for aggressive systemic mastocytosis without the KIT^{D816V} mutation [2,10]. Furthermore, imatinib is used off-label for the treatment of CML following allogeneic stem cell transplantation, desmoid tumors, chordomas, and advanced *KIT*-mutant melanomas. Accordingly, imatinib is a validated broad-spectrum antagonist.

2. The structure and mechanism of protein kinases

2.1. Primary, secondary, and tertiary structures

Because the recently approved drugs described in this article interact with (i) the MEK1/2 dual specificity kinases (ii) the nonreceptor protein-tyrosines JAK1/2/3 and FAK, and (iii) the receptor protein-tyrosine kinases ROS1, CSF1R, and ErbB2/HER2, the following description is of a general nature. As observed initially in protein kinase A (PKA), protein kinases have a small amino-terminal lobe and large carboxyterminal lobe (Fig. 2A) [21]. The N-terminal lobe contains a five-stranded antiparallel β-sheet (β1–β5) (Fig. 2A) [21,22]. The small-lobe contains a glycine-rich loop (GRL), sometimes called the P-loop (for the phosphates of ATP), which connects the β1- and β2-strands of the N-terminal lobe (Fig. 2C); the loop contains a GxGxΦG signature where the Φ residue is usually hydrophobic in nature. A conserved valine occurs two residues after the G-rich loop and it interacts hydrophobically with the adenine base of ATP and numerous small molecule protein kinase antagonists. Protein kinases possess an AxK signature within the N-terminal β3-strand and a conserved glutamate near the midpoint of the αC-helix. An electrostatic bond links the cationic β3-strand lysine (K) and the anionic αC-glutamate (E) in active protein kinases and such assemblies correspond to an "αC_{in}" conformation (Fig. 2A/C). The αC_{in} assembly is necessary, but not sufficient, for the expression of maximal catalytic activity. Furthermore, enzymes lacking this electrostatic bond are catalytically dormant and such assemblies constitute the "αC_{out}" conformation (Fig. 2E). The conversion of the αC_{out} to the αC_{in} structure is required for the expression of full catalytic activity.

The carboxyterminal lobe is primarily α-helical in nature (Fig. 2C) with six conserved helices (αD–αI) [23]. The C-terminal lobe of catalytically active protein kinases contains four small β-strands (β6–β9) (Fig. 2A). The second residue of the β7-strand corresponds to the floor of the adenine binding pocket, and this residue interacts hydrophobically with all known ATP-competitive protein kinase blockers [24]. The carboxyterminal lobe contains a catalytic loop (CL) that mediates the transfer of the ATP γ-phosphoryl group to its protein substrates. The large lobe also selects and places the protein substrate into the active site to promote catalysis.

Hanks and Hunter identified a dozen subdomains (I–VIa, VIb–XI) that represent the functional modules of protein kinases [25]. A K/E/D/D (Lys/Glu/Asp/Asp) tetrad performs an essential role in protein kinase catalysis. The initial *K* corresponds to the β3-strand lysine that forms electrostatic bonds with the α- and β-phosphates of ATP as well as the αC-glutamate residue that creates the active αC_{in} structure. The protein kinase activation loop or activation segment places the phosphorylatable protein substrate into the active site. Moreover, Madhusudan et al. hypothesized that the catalytic loop HRD-*D* (the first *D* of the K/E/*D*/D tetrad) functions as a Lowry-Brönsted base (a H^+ acceptor) and extracts a proton from the protein substrate –OH [26]. Furthermore, Zhou and Adams hypothesized that the catalytic HRD-*D* positions the protein substrate –OH group to facilitate the in-line nucleophilic attack of the substrate oxygen with the ATP γ-phosphoryl group (Fig. 3) [27]. See Table 3 for a list of the essential residues of the main protein kinases considered in this article.

The second *D* of the K/E/D/*D* tetrad represents the first residue of the protein kinase large lobe activation segment (AS). This portion of all protein kinases starts with DFG and ends with APE or a similar triad such as SPE or PPE. Activation segments, which vary in length (~ 33–44 residues), make up critical structural and regulatory elements of all protein kinases [28]. An $HRD(x)_4N$ conserved signature comprises the catalytic loop of functional protein kinases. The AS occurs after the catalytic loop. Two Mg^{2+} ions – labeled $Mg^{2+}(1)$ and $Mg^{2+}(2)$ – are essential for the activity of nearly all protein kinases. $Mg^{2+}(1)$ binds to the activation segment DFG-D and $Mg^{2+}(2)$ links with the catalytic loop asparagine terminus (Fig. 3).

The primary structure and length of the activation segment vary significantly in the protein kinase superfamily [2]. The AS of all protein kinases generally contains one or more phosphorylatable residues. Moreover, AS phosphorylation is required for the manifestation of maximal activity of nearly all protein kinases. The activation segment DFG occurs near the canonical catalytic loop HRD and the αC-helix. The regulatory αC-helix, which is found within the small lobe, nonetheless occurs in a strategically important site between the two lobes. The protein kinase activation segment possesses an open and extended structure in the active form of all protein kinases (Fig. 2A) and a closed structure in many inactive enzymes (not shown in Fig. 2C/E owing to disorder in the X-ray crystal structure) [2]. The first two AS residues (aspartate and phenylalanine) occur in different conformations. The DFG-D side chain of active kinases points inward toward the ATP-binding site and binds $Mg^{2+}(1)$. This structure is called the "DFG-D_{in}" configuration (Fig. 2G). The DFG-D side chain in many dormant protein kinases points away from the ATP-binding site. Such conformations are known as the "DFG-D_{out}" structure (Fig. 2H). It is the capability of DFG-D to interact with (DFG-D_{in}) or not interact with (DFG-D_{out}) active-site $Mg^{2+}(1)$ that is of importance.

Modi and Dunbrack investigated the interaction of ligands and drugs with active and inactive conformations of protein kinases based upon the structure of the activation segment beginning with the canonical

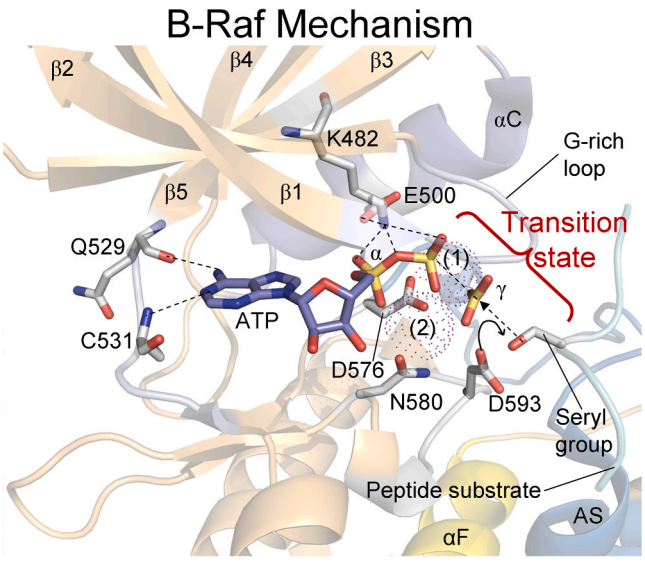

Fig. 3. Postulated mechanism of B-Raf mediated phosphorylation of MEK1. Adapted and derived from PDB ID: 3qhr. Dashes depict polar bonds and the dotted circles represent Mg^{2+}.

Table 3
Important residues in selected human protein kinase residues.

	Comments	B-RAF	MEK1	JAK3	BTK	CSF1R
UniProtKB accession no.		P15056	Q02750	P52333	Q06187	P07333
No. of residues		765	392	1124	659	972
Protein kinase domain		457–717	68–361	822–1111	402–655	582–910
Molecular Wt (kDa)		84.4	43.4	125.1	76.3	108.0
N-lobe						
Glycine-rich loop: GxGxxG	Anchors ATP β-phosphate	^{464}GSGSFG^{469}	^{75}GAGNGG^{80}	^{829}GKGNFG^{834}	^{409}GTGQFG^{414}	^{589}GAGAFG^{595}
β3-lysine (K of K/E/D/D)	Forms salt bridges with ATP α- and β-phosphates	K483	K97	K855	K430	K616
αC-glutamate (E of K/E/D/D)	Forms ion pair with β3-K	E501	E114	E871	E445	E633
Hinge residues between the N- and C-lobes	Connects N- and C-lobes	^{530}QWCEGSS^{536}	^{144}EHMDGGS^{150}	^{903}EYLPSGC^{909}	^{475}EYMANGC^{481}	^{664}EYCTYGD^{670}
C-lobe						
Catalytic loop HRD (first D of K/E/D/D)	Catalytic base (abstracts proton)	D576	D190	D949	D521	778
Catalytic loop Asn (N)	Chelates Mg^{2+}(2)	N581	N195	N954	N526	783
Activation segment	Positions protein substrate	594–623	208–233	967–997	521–567	802–825
AS DFG (second D of K/E/D/D)	Chelates Mg^{2+}(1)	D594	D208	D967	D539	D802
AS phosphorylation sites	Stabilizes the AS after phosphorylation	T599, S602	S218, S222	Y980/Y981	Y551	Y809
End of activation segment		^{621}APE^{623}	^{231}SPE^{233}	995–997	^{565}PPE^{567}	^{823}APE^{825}

DFG sequence [29,30]. With DFG-D_{in}, phenylalanine interacts hydrophobically with the αC-helix of the small lobe; with DFG-D_{out}, phenylalanine translates to a portion of the normal ATP-binding site leaving an αC-helix pocket. These authors observed groups of protein kinases based upon the positions of the phenylalanine side chain (DFG-D_{in}, DFG-D_{out}, and DFG-$D_{intermediate}$) and the backbone dihedral angles of xDF where x is the residue preceding DFG. These investigators observed eight different assemblies and grouped them according to the conformation (χ1) of the phenylalanine rotamer (plus, minus, trans) and on the Ramachandran plot regions (A, alpha; B, beta; L, left) of the xDF motif. Their classification divides the DFG-D_{in} conformation into six clusters including BLAminus – which represents an active structure – as well as two common inactive forms, ABAminus and BLBplus. The DFG-D_{out} structures are found mainly in the BBAminus configuration. The inactive enzyme conformations retain features that hinder their binding with ATP, Mg^{2+}, and/or their protein substrates. Modi and Dunbrack constructed a useful searchable and noncommercial web site (http://dunbrack3.fccc.edu/kincore/) that permits parties of interest to determine whether a known protein kinase structure corresponds to an active or to an inactive enzyme. We used this web site to determine whether our various drug-enzyme combinations correspond to an active (DFG-D_{in}, BLAminus) or inactive (otherwise) enzyme.

2.2. The hydrophobic skeletons and associated shell residues of protein kinases

Kornev et al. explored the three-dimensional structures of active and dormant conformations of about two dozen protein kinases with a goal of identifying critical structural residues [31,32]. Their investigation revealed a tetrad of four amino acids that constitute a regulatory spine (R-spine) an octad of eight amino acids along with the adenine base of ATP that constitute a catalytic spine (C-spine). These residues occur in both the small and large lobes. These spines form a stable, but flexible, catalytically proficient enzyme. The C-spine includes ATP and the R-spine helps to position the protein substrate to enable catalysis. The R-spine includes portions of both the αC-helix and the activation segment, whose structures are crucial in determining active and inactive enzyme conformations. The exact placement and arrangement of each spine are necessary, but not sufficient, for the fabrication of a catalytically competent protein kinase.

The R-spine contains the first amino acid of the β4-strand and the amino acid that is four residues after the conserved αC-helix glutamate, both of which are within the small lobe [31]. The R-spine also contains the HRD-His of the catalytic loop and the DFG-Phe of the activation segment, both within the large lobe. The HRD-His N–H backbone hydrogen bonds with the side chain of a conserved aspartate within the hydrophobic αF-helix. From the base to the apex, Meharena et al. labeled the R-spine residues RS0, RS1, RS2, RS3, and RS4 [33]. We later labeled the C-spine residues from the bottom to top apex as residues CS1–8 (Fig. 2B/D/F) [34]. We observed that both spines of active protein kinases are straight (Fig. 2B). In kinases in the DFG-D_{out} conformation, the DFG-D residue (RS2) is translated leftward and the R-spine is fractured (Fig. 2D). The RS3 residue occurs rightward in protein kinases with the αC_{out} conformation (Fig. 2F). The C-spine, R-spine, and shell residues of the five protein kinases detailed in this review are listed in Table 4.

The location of the spine and shell residues plays an important role in determining the activity of protein kinases; one cannot overemphasize their importance in supporting the activity of this enzyme family as well as their interactions with small molecule protein kinase blockers. For a summary of the properties of the spine and shell residues and their interactions with small molecule inhibitors, see the following commentaries: Refs. [35–37] for the epidermal growth factor receptor family (ErbB1/2/3/4) of protein-tyrosine kinases, Refs. [38–40] for the ALK pleotrophin and midkine receptor protein-tyrosine kinase, Ref. [41] for protein-tyrosine kinases of the FGFR family, Ref. [42] for the PDGFRα/β protein-tyrosine kinases, Ref. [43] for the RET glial-cell derived receptor protein-tyrosine kinase, Ref. [44] for the Kit stem cell receptor protein-tyrosine kinase, Ref. [45] for the Flt3 receptor protein-tyrosine kinase, Ref. [46] for the ROS1 orphan receptor protein-tyrosine kinase, Ref. [47] for the VEGFR1/2/3 protein-tyrosine kinases, Refs. [48,49] for the Janus kinase (JAK) nonreceptor protein-tyrosine kinase, Ref. [50] for the nonreceptor Bruton protein-tyrosine kinase, Refs. [51,52] for the nonreceptor Src protein-tyrosine kinase, Ref. [53] for the BCR-Abl nonreceptor protein tyrosine kinase, Ref. [54] for the dual MEK1/2 dual specificity protein kinases, Ref. [55] for the CDK4/6 protein-serine/threonine kinases, Refs. [56–58] for the ERK1/2 protein-serine/threonine kinases, Refs. [59,60] for the atypical RAF protein-serine/threonine kinases, and Ref. [9] for phosphatidylinositol 3-kinase (PI3K), a member of the atypical protein kinase family. PI3K catalyzes the phosphorylation of lipids, but its structure is related to that of the protein kinase family.

The C-spine of protein kinases contains two residues from the small lobe and six residues from the large lobe. The adenine moiety of ATP links two parts of the C-spine and expedites the unification of the two lobes to enable catalysis [32]. The two N-terminal lobe residues that bind to the ATP adenine include the canonical β2-strand valine (CS7) following the glycine-rich loop and the canonical β3-strand alanine (CS8) of the AxK signature. A hydrophobic amino acid R-group from the midpoint of the carboxyterminal lobe β7-strand (CS6) interacts with the

Table 4
Spine and shell residues of selected human kinase domains [a].

	Symbol	KLIFS No.	B-Raf	MEK1	JAK3	CSF1R	BTK
Regulatory spine							
β4-strand (N-lobe)	RS4	38	F516	F129	Y886	L649	L460
C-helix (N-lobe)	RS3	28	L505	L118	L875	M637	M449
Activation loop DFG-F (C-lobe)	RS2	82	F595	F209	F968	F797	F540
Catalytic loop HRD-H (C-lobe)	RS1	68	H574	H188	H947	H776	H519
F-helix (C-lobe)	RS0	None	D638	D245	D1009	D837	D579
R-Shell					*R-shell*	*R-shell*	
Two residues upstream from the gatekeeper	Sh3	43	I527	I141	L900	V661	I472
Gatekeeper, end of β5-strand	Sh2	45	T529	M143	M902	T663	T474
αC-β4 loop	Sh1	36	V511	V127	V884	V647	V458
Catalytic Spine							
β2-strand (N-lobe)	CS8	15	V471	V82	V863	A614	A428
β3-AxK-A (N-lobe)	CS7	11	A481	A95	A853	V596	V416
β7-strand (C-lobe)	CS6	77	F583	L197	L956	L785	L528
β7-strand (C-lobe)	CS5	78	L584	V198	V057	L786	V529
β7-strand (C-lobe)	CS4	76	I582	I196	I955	V784	C527
D-helix (C-lobe)	CS3	53	L537	L151	L910	L671	L482
F-helix (C-lobe)	CS2	None	V645	S252	S1012	L844	I590
F-helix (C-lobe)	CS1	None	L649	M256	V1016	I848	L586

[a] From Refs. [15,22,23], https://klifs.net/, and https://www.uniprot.org/uniprotkb/.

ATP adenine. Furthermore, the CS4 and CS5 β-7 strand amino acids interact with the CS3 residue occurring near the initial portion of the αD-helix. MoreoverFurthermore, the CS3 residue interacts hydrophobically with (i) its CS4 neighbor and (ii) with CS1 below it within the αF-helix. The R- and C-spines both interact with the hydrophobic αF-helix below them; the αF-helix contains RS0, CS1, and CS2 and this helix serves as a foundation that stabilizes and supports the entire protein kinase domain (Fig. 2B). The hinge and following linker residues connect the N-terminal and C-terminal protein kinase lobes and the 6-amino N–H group of ATP hydrogen bonds with the backbone carbonyl moiety of the first hinge residue (not shown). Furthermore, the adenine *N*1 group of ATP hydrogen bonds with the backbone N–H moiety of the third hinge residue (not shown). Essentially all ATP small-molecule steady-state competitive protein kinase inhibitors form hydrogen bonds with the backbone of the hinge residues, most commonly with the third hinge residue [34]. In contrast, allosteric protein kinase antagonists fail to interact with the first three hinge residues.

Based on site-directed mutagenesis experiments, Meharena et al. discovered three residues in murine PKA that strengthen and stabilize the R-spine, which they identified as Sh1, Sh2, and Sh3 where Sh represents shell (Fig. 2B/D/F) [33]. Their Sh1 V104G mutant expressed 5 % of wildtype activity and their M120G/M118G Sh2/Sh3 double mutant was kinase dead. These data show that the shell residues support PKA catalytic activity. We assume that the equivalent amino acids in other protein kinases implement a similar stabilizing function. The Sh1 residue occurs in the loop connecting the αC-helix with the β4-strand, which is dubbed the back loop. The Sh2 residue (the gatekeeper) occurs at the end of the β5-strand immediately before the hinge and the Sh3 residue is found within the β5-strand two residues upstream from the Sh2 gatekeeper residue.

The title gatekeeper signifies the role that this residue plays in controlling access to a hydrophobic region contiguous with the adenine binding pocket [61,62] and the gatekeeper interacts with many small molecule protein kinase antagonists. Extensive data demonstrate that numerous small molecule ATP-competitive steady-state protein kinase antagonists interact with the C-spine (CS6/7/8), the R-spine (RS2/3), and shell (Sh1 and Sh2) residues. Ung et al. reported that approximately three-quarters of all protein kinases have a relatively large gatekeeper residue (e.g., Leu, Met, Phe) while approximately one-quarter a have smaller gatekeeper residue (e.g., Thr, Val) [63]. Of significance in terms of long-term drug effectiveness, the gatekeeper residues of target protein kinases are frequent sites of mutations leading to drug-resistance [3,64].

3. An overview of selected receptor-mediated signal transduction pathways

3.1. The Ras-Raf-MEK-ERK (MAP kinase) signaling pathway

Protein kinases execute essential roles in nearly every phase of cellular and molecular biology [65–67]. Kinases regulate transcription, cellular growth, metabolism, mitosis, migration, immune responses, and nervous system function. Dysregulation of protein kinase activity is involved in the pathogenesis of many disorders including inflammatory diseases and cancer. Regulatory protein phosphorylation is based upon the action of both protein kinases and phosphoprotein phosphatases so that phosphorylation-dephosphorylation constitutes an overall reversible process – in contrast to unidirectional regulatory proteolytic cascades. The MAP kinase signal transduction module is among the more important oncogenic pathways operative in human neoplasms [8–11, 68–73]. This canonical pathway transmits signals from extracellular growth factors, cytokines, and chemokines into the intracellular compartment. The MAP kinase signaling module is regulated by numerous transmembrane receptors. Activated receptor protein-tyrosine kinases such as EGFR, HER2, c-MET, and PDGFR become phosphorylated at tyrosine residues and these phosphorylated sites attract various adapter proteins and GEFs (guanine nucleotide exchange factors) such as SOS (from *Drosophila* son of sevenless). The GEFs accelerate the conversion of dormant Ras-GDP to active Ras-GTP within the inner bilayer of the plasma membrane [9]. The *RAS* (Rat sarcoma) gene family consists of three members: *KRAS* (Kirsten rat sarcoma viral oncogene homolog), *HRAS* (Harvey rat sarcoma viral oncogene homolog), and *NRAS* (neuroblastoma RAS viral (v-ras) oncogene homolog). These proteins switch between functional and dormant forms; the transformation of dormant Ras-GDP to functional Ras-GTP turns the switch on while intrinsic Ras-GTPase activity stimulated by GAPs (GTPase activating proteins) such as NF1 (neurofibromin-1) turns the switch off (Fig. 4).

The K-Ras, H-Ras, and N-Ras molecular weights are small (21 kDa) [9]. In contrast, GEFs and GAPs are large (150–300 kDa) multidomain proteins proficient in a wide variety of actions involving various proteins and regulatory molecules that regulate the ratio of active and dormant Ras. To activate downstream components of the MAP kinase pathway, Ras-GTP facilitates the formation of operational homodimers or heterodimers consisting of A-Raf, B-Raf, or C-Raf by an intricate process (the Raf acronym corresponds to Rapidly accelerated fibrosarcoma, first described in mice). A/B/C-Raf are protein-serine/threonine kinases that are tyrosine-kinase like and catalyze the phosphorylation and activation

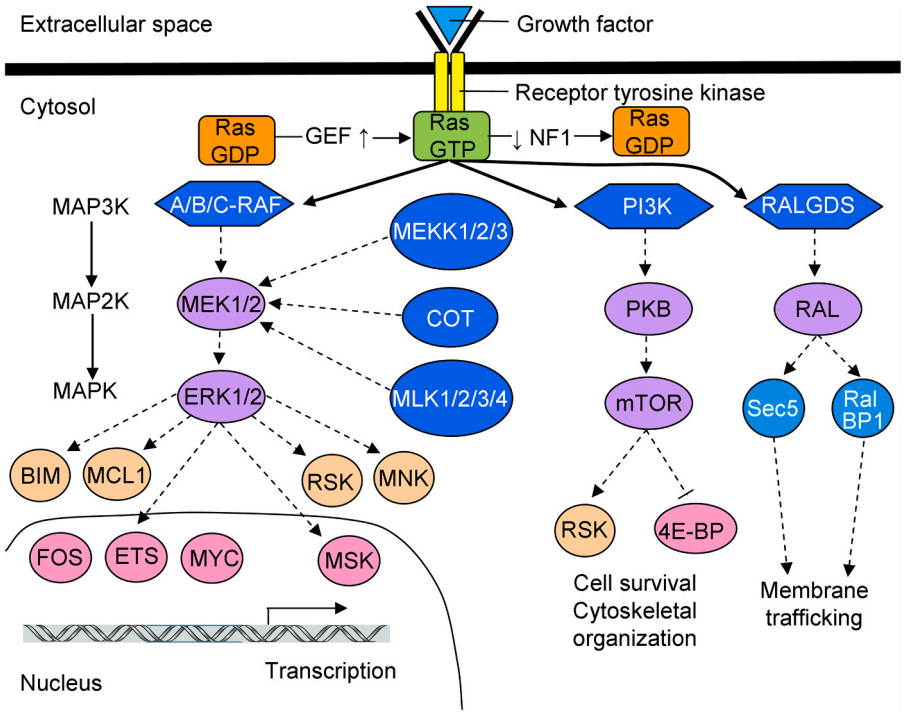

Fig. 4. Overview of the growth factor signal transduction pathway. Adapted from Ref. [57].

of MEK1/2 where MEK represents MAP/ERK Kinase. MEK1/2, in turn, catalyze the phosphorylation and stimulation of ERK1/2 (Extracellular signal-Regulated protein Kinase) enzyme activity.

A/B/C-Raf and MEK1/2 exhibit narrow substrate specificity [74,75]. The only established substrates of the Raf proteins are MEK1/2 and the only established substrates of MEK1/2 are ERK1/2. To further confirm their narrow substrate specificity, MEK1/2 are unable to catalyze the phosphorylation of denatured ERK1/2 nor do they catalyze the phosphorylation of peptides with sequences matching the activation segments of ERK1/2, the physiological substrates. In contradistinction to A/B/C-Raf and MEK1/2, ERK1/2 exhibit broad substrate specificity and ERK1/2 are able to catalyze the phosphorylation of hundreds of different proteins [11]. The Kinase Suppressor of Ras protein kinases (KSR1/2) are tyrosine-kinase like and evolutionarily close to A/B/C-Raf [4]. KSR1/2 exhibit reduced protein kinase activity – but they are not kinase dead – and they serve as platforms to facilitate the assembly of Raf, MEK, and ERK to control cell signaling [11]. The result of KSR1/2 action is context-dependent and varies with the level of the different components of the MAP kinase pathway; as a result, KSR1/2 can be stimulatory or inhibitory.

The MAP kinase signaling cascade contains a tier of three protein kinases: (i) MAPK kinase kinase (MAP3K), (ii) MAPK kinase (MAP2K), and (iii) and MAPK [54]. Even though A/B/C-Raf are found at the beginning of the MAP kinase cascade, other MAP3Ks including MEKK1/2/3, COT (also known as cancer Osaka thyroid kinase or MAP3K8), and MLK1/2/3/4 function in dedicated cell type and stimulation specific reactions (Fig. 4) [54]. Ras-GTP has additional downstream effector cascades including the JAK-STAT (signal transducer and activator of transcription) module.

3.2. *JAK/STAT signaling pathways*

The JAK (Janus kinase) nonreceptor protein-tyrosine kinase family includes four members: JAK1/2/3 and TYK2 (Tyrosine Kinase 2) [76]. These proteins possess a dormant pseudokinase domain (JH2) upstream from a functional C-terminal protein kinase domain (JH1). The pseudokinase domain down-regulates the activity of the JH1 domain. Janus is a two-faced Roman God (looking forwards and backwards) whose name was given to these enzymes owing to the occurrence of two protein kinase segments within a single polypeptide chain. JAK was whimsically expressed as Just Another Kinase [77]. JAK1/2 and TYK2 are found in nearly all cell types while JAK3 is restricted to lymphoid, myeloid, and hematopoietic cells [78]. The JAK-STAT pathway transmits extracellular signals from a variety of chemokines, cytokines, hormones, and growth factors to the nucleus and is tasked with the expression of hundreds of protein-encoding genes [79]. The Janus kinases interact with the intracellular juxtamembrane portion of their specific cytokine receptors.

The JAK-STAT signaling module regulates the expression of hundreds, if not thousands, of protein-encoding genes (Fig. 5) [79]. The Janus kinases interact with the intracellular juxtamembrane region of specific cytokine, chemokine, and G-protein coupled receptors (GPCR). Numerous actions are required for the transmission of an extracellular signal into a transcriptional response. Ligand, cytokine, or chemokine binding produces conformational changes in cognate receptors that foster protein-tyrosine kinase activation as a result of the phosphorylation of dual tyrosine residues within the activation loop of the JH1 domain as catalyzed by a partner Janus kinase JH1 enzyme. Following this stimulation, the JH1 protein kinase domains catalyze the phosphorylation of receptor tyrosines that interact with the SH2 domain of intracellular STATs. The activated JH1 enzyme then mediates the phosphorylation of downstream STAT molecules. These phosphorylated STATS dimerize and then are translocated into the nucleus where they promote the transcription of target genes. Alternatively, existing STAT dimers may preexist, and their phosphorylation may produce a conformational change that results in activation [80]. Besides the MAP kinase cascade, ROS1, CSF1R, and ErbB2/HER2 action often results in the activation of JAK-STAT pathway [79,81].

Humans have seven STAT genes including *STAT1, STAT2, STAT3, STAT4, STAT5A, STAT5B,* and *STAT6*. Each protein contains six domains (from the amino-terminus to the carboxyterminus) consisting of an amino-terminal component, a coiled-coil domain, a DNA-binding segment, a linker portion, an SH2 domain, and finally a transcriptional activation domain (TAD), all of which were identified first in

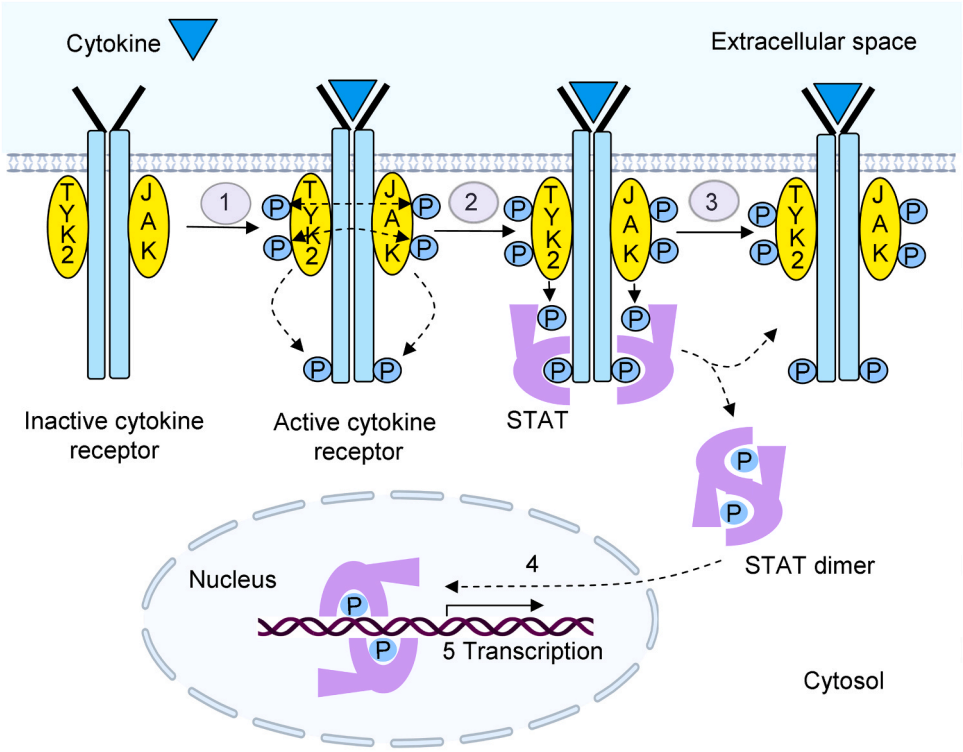

Fig. 5. Overview of the JAK/STAT signaling pathway. The JAK enzymes work in pairs. JAK1 pairs with JAK2/3 and TYK2; JAK2 pairs with JAK1/2 and TYK2 (not JAK3); JAK3 pairs with JAK1 only; TYK2 pairs with JAK1/2. Adapted from Ref. [79].

STAT1 [82]. The transcriptional activation domain contains a tyrosine residue (Y) that can be phosphorylated by an upstream Janus kinase. After phosphorylation, STATs can form homo- or heterodimers following the binding of the phosphotyrosine (pY) to the SH2 domain of their partner. The active dimer translocates into the nucleus where it interacts with target DNA sequences alone or in combination with other transcription factors that may augment or curb DNA transcription.

The STAT family has characteristic roles in cell signaling. For example, STAT1 participates in interleukin-9/10 (IL-9/10), interferon, and thrombopoietin signaling while STAT2 principally participates in interferon-α/β and IL-28/29 signaling [48,49]. STAT3 engages in the signaling pathways supported by various Type I, II, and IL-10 families of cytokines. STAT4 contributes to the downstream signaling of the Type II interferon family cytokines (IL-28/29) along with IFN-α/β. Type I heterodimeric cytokines (IL-12/23) and STAT5A/B participate in the signaling modules initiated by the Type I cytokines with common β-chain or common γ-chain receptor subunits and the hormone-like cytokines including prolactin and growth hormone. STAT6 engages in inflammatory cytokine (IL-3/5) signaling. See Ref. [49] for a summary of JAK/STAT signaling modules.

4. A description of protein kinase-inhibitor complexes and inhibitor-binding pockets

Based upon earlier work [62,83–86], we classified small molecule protein kinase inhibitors into seven main categories including reversible (Groups I, I½, II, III, IV, and V) and targeted covalent inhibitors (VI) as shown in Table 5. The newly approved rilzabrutinib is a reversible covalent blocker whereas most targeted covalent inhibitors are irreversible in nature. We separated type I½ and type II antagonists into A and B subtypes [34]. Subtype A inhibitors, initially described in the imatinib-Abl complex, extend beyond the gatekeeper residue into the back cleft. In contradistinction, subtype B drugs, which were described later, fail to enter the back cleft. The potential significance of this difference, based upon preliminary observations, is that subtype A antagonists bind to their kinase target with longer residence times as compared with subtype B inhibitors [34]. For example, sorafenib is a type IIA VEGFR blocker and sunitinib is a type IIB VEGFR antagonist, both of which are approved by the FDA for the management of renal cell carcinomas. The type IIA blocker has a residence time greater than 64 min while the type IIB antagonist has a residence time of less than 2.9 min [34].

Table 5
Classification of small molecule protein kinase inhibitors[a].

Inhibitor type	Properties
I	Binds in and around the ATP-binding pocket of an active enzyme
I½ A/B	Binds in and around the ATP-binding pocket of an inactive DFG-D_{in} enzyme
I½ A	Extends into the back cleft
I½ B	Does not extend into the back cleft
II A/B	Bind in and around the ATP-binding site of an inactive DFG-D_{out} enzyme
II A	Extends into the back cleft
II B	Does not extend into the back cleft
III	Allosteric inhibitor bound next to the ATP-binding site
IV	Allosteric inhibitor bound away from the ATP-binding site
V	Bivalent inhibitor spanning two kinase domain regions
VI	Covalent inhibitor

[a] Ref. [34].

We followed the lead of previous investigators [86–89] in analyzing drug-binding pockets. An outline depicting the location of the binding pockets and subpockets is illustrated in Fig. 6 and is described in Table 6. The region between the amino-terminal and carboxyterminal protein kinase lobes is partitioned into a front cleft or front pocket, a gate area, and a back cleft. The back pocket (hydrophobic pocket II, or HPII) contains the gate area and its bordering back cleft. The front cleft includes the N-terminal lobe glycine-rich loop and the C-terminal lobe

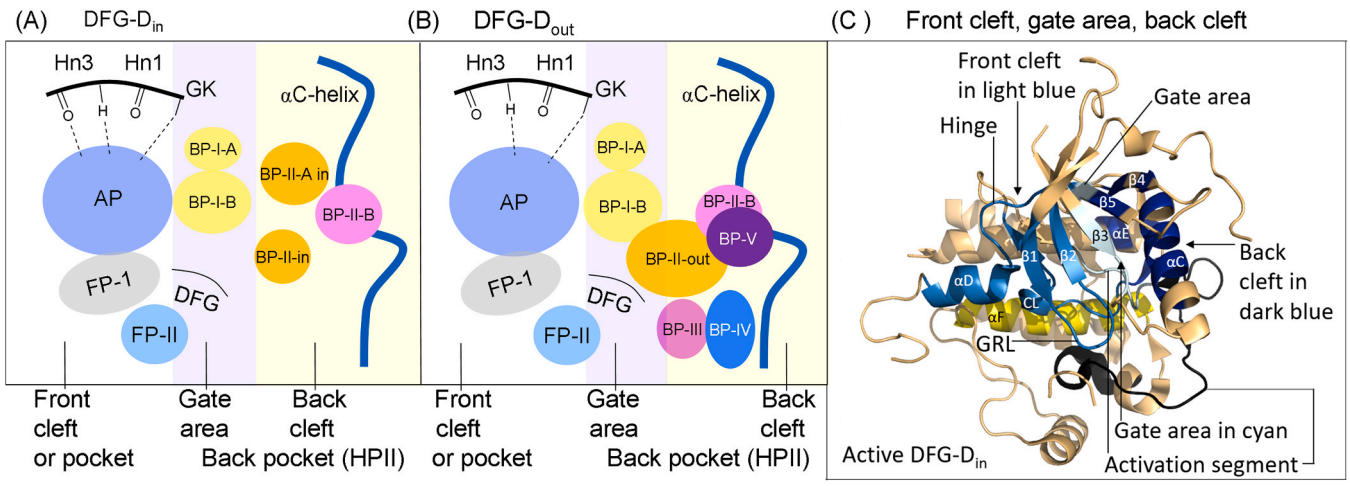

Fig. 6. (A) Location of the protein kinase domain drug-binding pockets in the DFG-D_{in} enzyme form. (B) Location of the drug-binding pockets in the DFG-D_{out} enzyme form. Adapted from Refs. [86–88]. (C) Location of the protein kinase front cleft, gate area, and back cleft. AP, adenine pocket; BP, back pocket; FP, front pocket; Hn, hinge; HPII, hydrophobic pocket II; GK, gatekeeper.

Table 6
Location of important residues within the front cleft, gate area, and back cleft.

Description	Location	KLIFS residue no.[a]
GxGxΦG	Front cleft	4–9
β2-strand V (CS7)	Front cleft	11
β3-strand A (CS8)	Front cleft	15
HRD with DFG-D_{in}	Front cleft	68–70
HRD$(x)_4$N-N	Front cleft	75
β7-strand CS6	Front cleft	77
β3-strand K	Gate area	17
αC-β4 penultimate back loop residue	Gate area	36
Gatekeeper	Gate area	45
The x of xDFG	Gate area	80
DFG	Gate area	81–83
αC-helix E	Back cleft	24
RS3	Back cleft	28
HRD with DFG-D_{out}	Back cleft	68–70

[a] Refs. [88,89].

hinge residues, the linker that connects the hinge residues to the αD-helix, the adenine-binding pocket (AP), and the catalytic loop (HRD$(x)_4$N).

Type I inhibitors interact with residues in the front cleft [86–89]. The gate area includes amino acid residues from both lobes and it includes the last three residues of the β3-strand and the first two residues of the distal β3-αC loop. It also includes the residue directly before the activation segment (the x of xDFG) and the first four residues of the activation segment. The back cleft contains the residues from the midpoint of the αC-helix and the entire β4 and β5-strands. The back cleft also contains the entire αE-helix and the three residues before the catalytic loop HRD. Several type I½ antagonists are found in both the front cleft and a portion of the back cleft. One of the overall goals in the design of small molecule protein kinase blockers is to maximize selectivity and to minimize off-target interactions leading to adverse side effects [84]; this approach is facilitated by comparing drug interactions with target and nontarget enzymes [90–92]. The fabrication of ligand fragments that interact with residues that line the various pockets represents a fundamental part of protein kinase antagonist discovery with the goal of maximizing drug affinity.

Kanev et al. [89] and van Linden et al. [87] described drug and ligand binding to about 6000 human and mouse protein kinases. Their KLIFS (kinase–ligand interaction fingerprint and structure) catalog contains an array of 85 residues occurring in both lobes that interact with various ligands; this information facilitates the evaluation of ligands and drugs based upon their binding properties. Such data aids in the detection of common and unique drug-enzyme interactions. These investigators formulated a standardized amino acid residue numbering system that allows one to compare and contrast different protein kinases and their ligands. The comparison of the KLIFS terminology with the C-spine, R-spine, and shell amino acid residue numbering system are summarized in Table 4 and the location of the KLIFS residues within the protein-kinase domain are depicted in Fig. 7. These investigators created a helpful noncommercial and searchable web site that provides valuable data on the mode of binding of drugs and ligands to their protein kinase targets (klifs.net).

Bournez et al. published an inclusive review of protein kinase antagonists that have been approved by various regulatory agencies or that

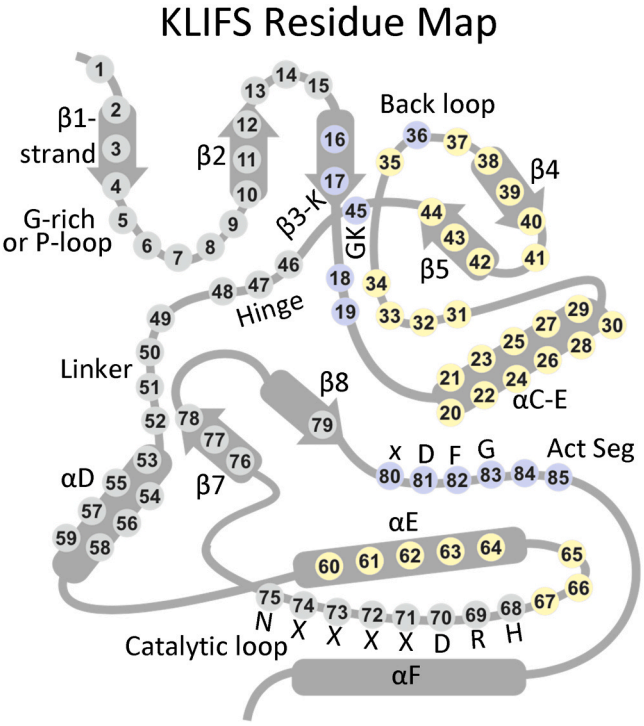

Fig. 7. The location of the KLIFS residues within a generic protein kinase domain. Act Seg, activation segment; GK, gatekeeper. Residues in gray circles are found in the front cleft; blue circles, gate area; yellow circles, back cleft.

are in clinical trials [6]. They created a noncommercial and searchable web site that contains the structures and physicochemical properties of numerous drugs, their protein kinase targets, their therapeutic indications, trade names, and the year of first approval by regulatory agencies (if applicable) (http://www.icoa.fr/pkidb/). Likewise, the Blue Ridge Institute for Medical Research (BRIMR) provides a web site that lists the FDA-approved protein kinase inhibitors and depicts their (i) molecular structures, (ii) the calculated log of the partition coefficients, (iii) the number of hydrogen bond donors/acceptors, (iv) the year of initial approval, (v) the number of rings and rotatable bonds, (vi) their primary protein kinase targets, (vii) and their therapeutic indications. This website (www.brimr.org/PKI/PKIs.htm) is regularly updated following the FDA-approval of new protein kinase antagonists and changes in therapeutic indications.

5. Drug approvals

5.1. Avutometinib and defactinib

Avutometinib is a benzopyran derivative and defactinib is a pyrazine-pyrimidine derivative (Fig. 8A/B) that are approved together by the FDA for the treatment of low grade serous ovarian carcinomas [93]. The estimated number of new ovarian cancers in the United States in 2025 is about 21,000 and of these fewer than 2100 are expected to be low grade serous ovarian cancers [94,95]. Ovarian cancers are heterogeneous diseases with subtypes classified, *in alia*, by cell surface biomarkers, molecular drivers, pathology, and histologic grade. Epithelial ovarian cancers include high grade serous cancer (HGSC), low-grade serous cancer (LGSC), and other histologic subtypes including endometrioid, clear cell, and mucinous varieties. High grade serous cancer is the most common subtype making up about 75 % of epithelial ovarian cancers. They are generally responsive to platinum-based chemotherapy, but most women experience a relapse of their malignancy owing to multiple mechanisms of resistance. Low grade serous cancer occurs less commonly than the high-grade variety and is generally less responsive to platinum-based management; these neoplasms often harbor molecular alterations within the Ras-Raf-MEK-ERK MAP kinase pathway [93,96–98].

In 2020, the World Health Organization (WHO) defined low grade serous ovarian cancer as an invasive serous tumor with low-grade malignant properties [93]. This histologic subtype occurs predominantly in younger patients and may occur in association with premalignant serous borderline neoplasms (SBN). While these premalignant neoplasms are treated surgically, women with advanced stage low grade serous carcinoma (LGSC) are initially treated with both surgery and chemotherapy; however, most women with this disorder suffer from persistent or recurrent disease. While these patients have a more favorable prognosis compared with other ovarian cancers at the time of diagnosis, this cancer is invariably fatal following its spread to the peritoneum. LGSC is accompanied by various *KRAS*, *NRAS*, and *BRAF* mutations and is rather unresponsive to chemotherapy, but is responsive to hormonal therapies and MEK1/2 blockade, which represent standards-of-care for this pathology [96,97].

Genetic modifications in the Ras-Raf-MEK-ERK MAP kinase pathway are common in LGSC, SBN, and mucinous and endometrioid ovarian cancers [93]. A majority of SBNs and LGSCs contain mutually exclusive mutations in either *BRAF*, *KRAS*, or *NRAS*. Reports on *BRAF* mutations range from 0 % to 33 % in LGSCs and 23–48 % in SBNs. *BRAF* mutations are associated with a better prognosis in LGSC and often predict sensitivity to MEK1/2 blockade, BRAF-targeted therapies, or both. The frequency of *KRAS* mutations ranges from 19 % to 54 % in LGSCs and 17–40 % in SBNs. Most of these *KRAS* mutations are non-G12C including G12D or G12V or more rare variants including G12A, G12S, and G12R. In one report, the occurrence of *KRAS* G12D mutation in LGSC was 19.5 % and KRAS G12V was 20.3 %, but the frequency of the *KRAS* G12C mutation was only 0.8 %, a mutant form that is targeted by existing drugs such as sotorasib. *NRAS* mutations occur in about 10 % of women with LGSC, but not in SBN patients. These results implicate *BRAF*, *KRAS*, and *NRAS* as driver mutations in treatment-resistant low grade serous cancer. Moreover, data suggest that MAPK pathway alterations are associated with a better LGSC prognosis.

To date, agents targeting the MAP kinase pathway in LGSC primarily focus on the inhibition of MEK1/2 [93]. For example, trametinib is a MEK1/2 blocker that is used off-label as an National Comprehensive Cancer Network (NCCN) standard-of-care option for the management of recurrent or persistent low grade serous carcinoma. However, new approaches exhibiting potential benefit in the management of LGSC include the Raf-MEK clamp avutometinib combined with the FAK inhibitor defactinib. Avutometinib is an orally bioavailable Raf/MEK dual inhibitor (clamp) that blocks MEK1/2 kinase activity and concurrently prevents the compensatory activation of MEK1/2 by Raf [98]. Specifically, avutometinib (VS-6766) binds directly to MEK1/2 and produces a conformation of MEK1/2 that binds to Raf but is unable to be phosphorylated and released from Raf, thereby producing a stable Raf-MEK complex. As a result, MEK1/2 mimics a dominant negative Raf inhibitor, resulting in the blockade of both Raf and MEK1/2 and thereby preventing downstream ERK signaling [98]. Defactinib (VS-4718) is a selective orally bioavailable FAK antagonist that inhibits parallel pathway signaling. FAK is a nonreceptor protein-tyrosine kinase that is activated as a result of MEK1/2 inhibition and promotes MEK1/2 inhibitor resistance [99].

Combining the Raf/MEK clamp with FAK inhibition represents a

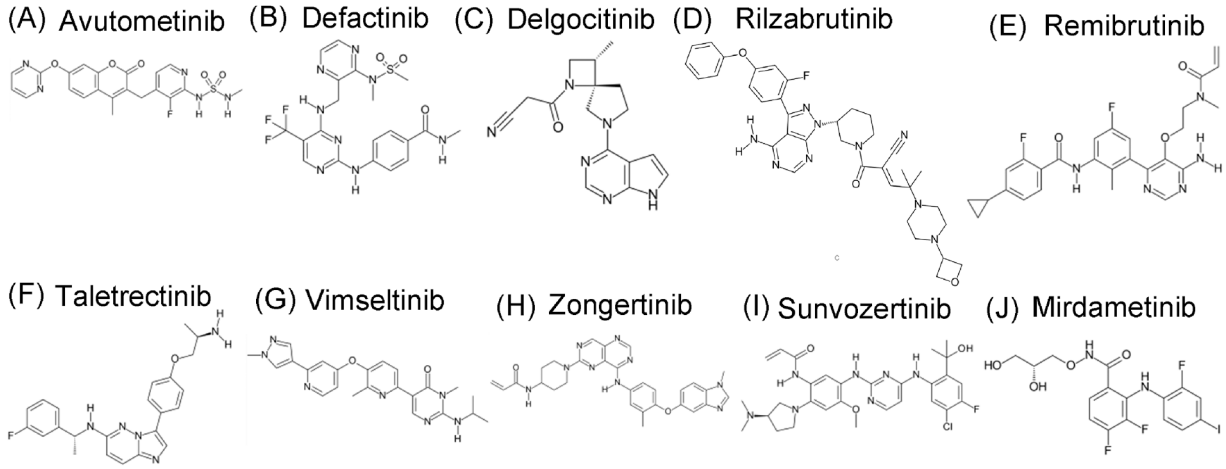

Fig. 8. (A–E). Structures of the small molecule protein kinase antagonists approved by the FDA in 2025.

novel approach in the management of LGSC [93]. This combination has been studied extensively in low grade serous cancer and has demonstrated clinical efficacy [99]. The RAMP201 clinical trial is comparing avutometinib monotherapy and avutometinib and defactinib combination therapy in women with recurrent disease [94,95]. The dosage schedule for the use of these dual inhibitors is unusual. Patients with wildtype *KRAS* or mutant *KRAS* low grade serous cancer were treated with avutometinib monotherapy at a dose of 4 mg twice weekly (three weeks on, one week off) or with the combination of avutometinib 3.2 mg twice weekly and defactinib 200 mg twice daily (three weeks on, one week off). The monotherapy regimen had an overall response rate of 7 % and the combination had an overall response rate of 28 %, values that are not outstanding. For a summary of the clinical trials that led to the approval of the dual inhibitors avutometinib and defactinib, see Refs. [99,100].

Gonzalez-Del Pino et al. determined the X-ray crystal structure of avutometinib and AMP-PNP bound to MEK1; that both a substrate analog and the drug bound simultaneously to the enzyme indicates that avutometinib is an allosteric inhibitor [101]. S212 and V211 within the activation segment hydrogen bond with the benzopyran oxygen, the carbonyl oxygen of R189 of the catalytic loop and the guanidino group of R234 following the activation segment interact with the drug, and the backbone N–H group of DFG-D208 hydrogen bonds with a drug pyrimidine nitrogen (Fig. 9A). L115 and L118 of the αC-helix, V127 and F129 of the backloop, I141 and M143 of the β5-strand, HRD-D190, C207 (the x of xDFG), F209 and G210 (of the DFG signature), L215, I216, and M219 of the activation segment interact hydrophobically with avutometinib. Avutometinib is bound to a dormant BLBplus enzyme with a compact activation segment with DFG-D_{in}, and αC_{out} (http://dunbrack3.fccc.edu/kincore/) [30]. The drug is adjacent to the ATP-binding pocket and is therefore classified as a type III allosteric inhibitor [34]. Type IV allosteric antagonists bind far from the ATP-binding site. Unfortunately, we lack an X-ray crystal structure of defactinib bound to its target FAK.

5.2. Delgocitinib

Delgocitinib is a pyrrolopyrimidine derivative (Fig. 8C) and a Janus kinase antagonist that is FDA approved for the management of moderate to severe chronic hand eczema (CHE) in adults who have had an inadequate response to topical corticosteroids or for whom topical steroids are unsuitable (www.brimr.org/PKI/PKIs.htm). Hand eczema is a common disorder that affects about 9 % of the population in the United States and worldwide [102,103]. It is more common in women than men (12 % vs. 6 %) and this higher frequency in women is caused by environmental and not genetic factors [102]. Chronic hand eczema is a heterogeneous, variable, and long-lasting disease that affects the hands and wrists and adversely affects the quality of life.

Key therapies in the management of hand eczema and atopic dermatitis include topical corticosteroids and calcineurin inhibitors such as tacrolimus [104]. Long-term safety issues of these medicines include skin atrophy and telangiectasia from corticosteroids and local irritation from tacrolimus ointment. For severe chronic hand eczema, topical corticosteroids are often ineffective making this disorder difficult to treat. Consequently, additional treatments are needed including inhibitors of the JAK-STAT pathway [105–107]. Delgocitinib ointment is a topical JAK inhibitor and anti-inflammatory agent useful in the management of chronic hand eczema. Skin atrophy and telangiectasia have not been observed with long-term delgocitinib ointment application, as occurs with topical corticosteroids. Application-site irritation is very rare and usually mild in contrast with tacrolimus. See Refs. [105,107] for a summary of the clinical trials that led to the approval of delgocitinib.

Delgocitinib is a potent pan-JAK family inhibitor with IC_{50} values of 2.8/2.6/13/58 nM for JAK1/2/3/TYK2, respectively [108]. Noji et al. determined the X-ray crystal structure of delgocitinib bound to JAK3 [108] and found that the drug forms hydrogen bonds with the first and third hinge residues (E903, L905) and with G831 of the glycine-rich loop (Fig. 9B). The drug interacts hydrophobically with RS2, Sh1, Sh2 (the gatekeeper), CS6/7/8 and the KLIFS-3 residue. It also interacts hydrophobically with G829, K830, G831, and G834 of the glycine-rich loop,

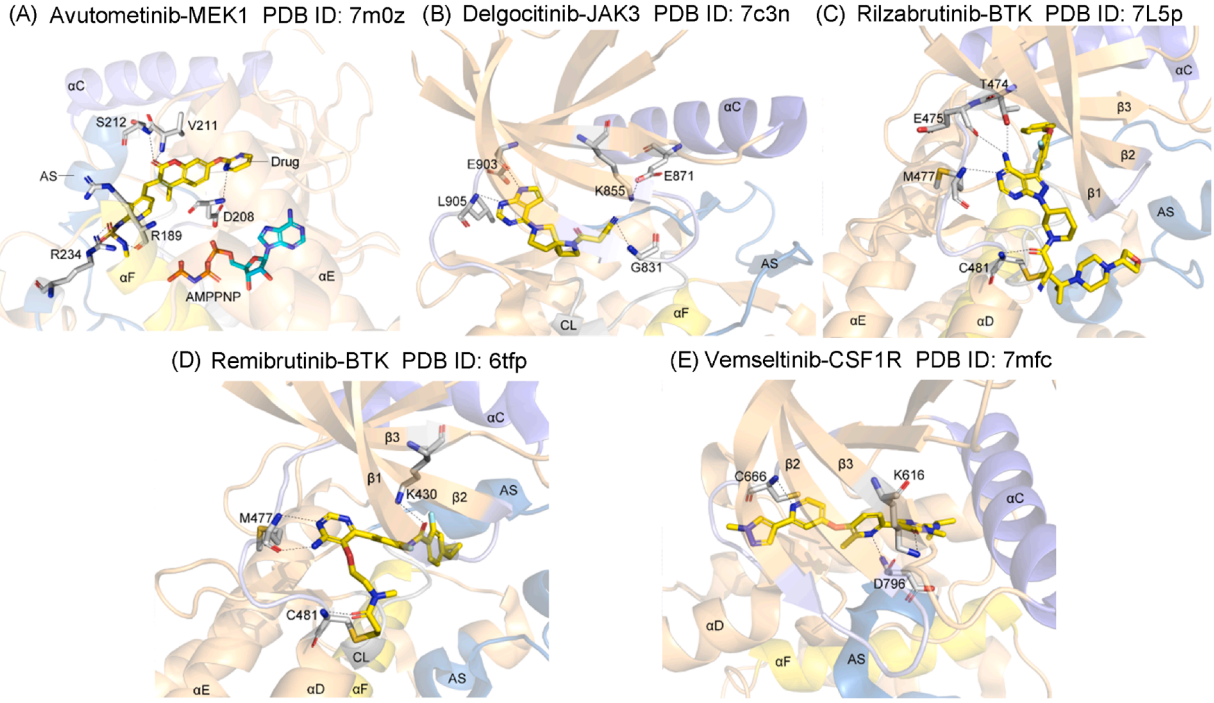

Fig. 9. (A) Avutometinib-MEK. (B) Delgocitinib-JAK3. (C) Rilzabrutinib-BTK. (D) Remibrutinib-BTK (E) Vimseltinib-CSF1R. The respective PDB ID numbers are listed. The drug carbon atoms are colored yellow, the ADP-analog carbon atoms are colored cyan, and the dashed lines represent polar bonds. AS, activation segment; CL, catalytic loop.

S835 of the β2-strand, AxK-K855, Y904 and L905 of the hinge, C909 of the linker, R953 and N954 of the catalytic loop, A966 (the x of xDFG) and DFG-D957. The drug occupies the front pocket and FP-I/II of an inactive ABAminus enzyme structure and is classified as a type I ½ B inhibitor [30,34].

5.3. Rilzabrutinib

Rilzabrutinib is a pyrazolo[3,4-*d*]pyrimidine derivative (phenoxyphenyl-pyrrolopyrimidine Fig. 8D) and a BTK blocker that is FDA approved for the treatment of chronic immune thrombocytopenia in people who have had an insufficient response to previous therapies (www.brimr.org/PKI/PKIs.htm). Chronic immune thrombocytopenia (cITP) is an acquired autoimmune disease characterized by low levels of platelets owing to accelerated immune-mediated platelet destruction and diminished production by megakaryocytes [109]. Mucocutaneous (gingiva, nose, and skin) bleeding, petechiae, and brusing resulting from broken capillaries are common. In severe cases, hemorrhage is life-threatening. The estimated annual incidence in the United States ranges from 100,000–120,000. Chronic immune thrombocytopenia is characterized by repeat episodes of bleeding that result in psychological stress and dependency on immunosuppressive therapies. Conventional therapies include corticosteroids, intravenous immunoglobulin, rituximab, and thrombopoietin receptor agonists that improve platelet levels, but are characterized by relapses, adverse side effects, and incomplete responses. Ironically, besides an increased bleeding risk, people with cITP also have an elevated chance of venous thromboembolism when compared with the general population [110]

Rilzabrutinib is a covalent, but reversible, selective inhibitor of BTK that acts on both B lymphocytes and myeloid cells [109,111]. By reducing B-cell receptor and Fc receptor signaling, it reduces the biosynthesis of autoantibodies as well as decreasing Fc-mediated platelet phagocytosis by macrophages. Rilzabrutinib minimizes the global immune response by specifically targeting disease-driving pathways, in contrast to conventional immunosuppressants that reduce overall immune activity. Orally bioavailable rilzabrutinib is rapidly absorbed and reaches steady-state concentrations in a few days. The drug, which is metabolized by the liver, has not been linked to any significant drug–drug interactions. Twice-daily dosing is used owing to a comparatively short half-life, maintaining a balance between tolerability and effectiveness. See Refs. [110,112] for a summary of the clinical trials that led to the approval of rilzabrutinib.

Owens et al. determined the X-ray crystal structure of rilzabrutinib covalently linked to BTK (Fig. 9 C) and found that the drug forms hydrogen bonds with gatekeeper T474, the first hinge residue (E475), and the third hinge residue (M477) [111]. The drug also forms a covalent and hydrogen bond with C481 (the last linker residue). The drug also interacts hydrophobically with RS2/3/4, Sh1/2/3, CS6/7/8, and the KLIFS-3 residue. It also interacts hydrophobically with G409, T410, and G411 of the glycine-rich loop, I429 of the β3-strand, AxK-K430, V458 of the back loop, L460 of the β4-strand, I452 of the β5-strand, Y476 of the hinge, C481 of the linker, L483 and N484 of the αD-helix, R525 of the catalytic loop, S538 (the x of xDFG), DFG-D539, and L542 of the activation segment. The drug occurs in the front pocket, the gate area, and BP-I-A/B. The enzyme structure corresponds to an inactive BLBplus conformation with DFG-D_{in} and αC_{out} [30]. We classify this interaction as a type VI inhibition owing to the covalent linkage of the drug to the enzyme [34].

5.4. Remibrutinib

Remibrutinib is a pyrimidine-benzamide derivative (Fig. 8E) that is FDA approved for the treatment of chronic spontaneous urticaria (CSU) in adult patients who remain symptomatic despite H1 antihistamine treatment (www.brimr.org/PKI/PKIs.htm). Chronic spontaneous urticaria is an inflammatory skin disease accompanied with pruritic wheals, hives, or welts and localized edema – or both – that last for more than six weeks [113]. The lesions are red or skin-colored that change shape and often disappear within hours. The disorder affects about 0.5–1.0 % of the general population worldwide and is more common in women aged 30–50. Second-generation H1-antihistamines such as loratadine (Claritin) or fexofenadine (Allegra) represent the first-line therapy for chronic spontaneous urticaria, followed by omalizumab, a monoclonal antibody that blocks and targets IgE; it is prescribed for people who are refractory to antihistamines. Omalizumab decreases IgE levels, downregulates the expression of FcεRI, and attenuates mast cell and basophil activity. Because many people fail to respond to these treatments, there is a need for innovative targeted therapies. Mast cells are responsible for the pathogenesis of this disorder involving autoimmune and autoallergic signaling via IgG and IgE autoantibodies, respectively. Besides mast cells, B cells and basophils also have integral roles in the pathophysiology of this disorder. BTK is a key intracellular signaling component of these three cell types and its therapeutic blockade is under clinical investigation in autoimmune and allergic diseases.

The unwanted side effects associated with remibrutinib are less severe than those of first generation BTK antagonists owing to its greater specificity and its preference for the inactive conformation of BTK [114]. Remibrutinib has marked activity against BTK, minimal activity against TEC and BMX, and no activity against other kinases. The IC_{50} of remibrutinib for BTK is 1.3 nM [115]. Clinical improvement with remibrutinib is rapid, with onsets as early as one week and robust activity regardless of prior omalizumab responsiveness [113]. See Ref. [116] for a summary of the clinical trials that led to the FDA approval of remibrutinib.

Angst et al. determined the X-ray crystal structure of the remibrutinib-BTK complex [115] and found that the drug forms hydrogen bonds with M477 (the third hinge residue) and AxK-K430 (Fig. 9D). The drug forms a covalent and hydrogen bond with C481 (the last linker residue). Remibrutinib interacts hydrophobically with CS6/7/8 and the KLIFS-3 residue. It also interacts hydrophobically with ^{409}GTGQF^{413} of the glycine-rich loop, Y476 and M477 of the hinge, G480 and C481 of the linker, N484 of the αD-helix, HRD-D521, N526 of the catalytic loop, S538 (the x of xDFG), DFG-D539, and L542 and S543 of the activation segment. The drug is found in the front pocket and FP-II and the enzyme has the inactive BLBplus conformation with DFG-D_{in} and αC_{out} [30]. Remibrutinib is a type VI irreversible covalent antagonist [34].

5.5. Taletrectinib

Taletrectinib is an imidazo[1,2-*b*]pyridazine derivative (Fig. 8F) that is FDA approved for the management of locally advanced or metastatic NSCLC with ROS1 rearrangements (www.brimr.org/PKI/PKIs.htm). Proto-oncogene protein-tyrosine kinase-1 (ROS1) gene fusions, which were first reported in 2007, are oncogenic drivers producing constitutive activation of the ROS1 kinase domain and stimulating persistent downstream signaling and dysregulated cell differentiation, proliferation, and survival [117–119]. These ROS1 fusions are rare genetic events that occur in various solid tumors, including NSCLC, where the prevalence ranges from 0.9 % to 2.6 %. Patients with ROS1 fusion–positive NSCLC are likely to be female, are diagnosed at an advanced stage (III-IV), are younger than individuals without driver alterations, have adenocarcinoma histology, and occur mostly in never smokers. About one third of people with ROS1$^+$ NSCLC have brain metastases at the time of diagnosis, the incidence of which can be as high as 50 % in previously treated patients.

ROS1 protein-tyrosine kinase inhibitors have improved the clinical outcomes for ROS1$^+$ NSCLC; however, patients treated with first-generation ROS1 antagonists generally progress owing to (i) off-target bypass pathway activation leading to intractable disease, (ii) development of on-target acquired resistance mutations such as G2032R, or (iii) brain metastases [117]. Presently, three kinase blockers are approved by

the FDA for ROS1$^+$ NSCLC including crizotinib, entrectinib, and repotrectinib. While a higher objective response rate and longer median progression-free survival were seen with first-line crizotinib treatment versus chemotherapy, CNS metastases developed in nearly half of the crizotinib-treated patients with ROS1$^+$ NSCLC. Entrectinib was formulated to cross the bloodbrain barrier (BBB), made up of endothelial cells lining the cerebral microvessels with unique tight junctions. The BBB is essential for providing neural homeostasis and shielding the CNS from toxic substances. Unfortunately, the entrectinib responses were marginal in people with previous CNS progression and against the most common acquired resistance mutation (G2023R) found after crizotinib treatment, a mutation that occurs in 30–40 % of patients.

Repotrectinib, which is FDA approved for advanced ROS1$^+$ NSCLC, has CNS activity and was formulated to be effective against ROS1 resistance mutations [117]. While active against the *G2032R* mutation and brain metastases, a wide range of neurologic side effects occurs in many patients receiving repotrectinib. Unmet needs remain for effective and well-tolerated therapies for patients needing robust overall and intracranial responses, lengthened disease control, blockade of secondary on-target resistance mutations, while possessing no or minor neurological side effects.

Taletrectinib is an orally bioavailable, CNS-active, next-generation ROS1 inhibitor that produced a robust clinical overall response rate (88.8 %) and duration of response (44.2 months) in protein-tyrosine kinase inhibitor naïve patients and led to relatively long-lasting outcomes in most patients with advanced ROS1$^+$ NSCLC [117–119]. Taletrectinib produced a median progression-free survival of 45.6 months in kinase inhibitor naïve patients. In patients pretreated with entrectinib or crizotinib, taletrectinib reliably produced the intended, beneficial therapeutic effects (overall response rate of 55.8 %; median duration of response of 16.6 months) and a median progression-free survival of 9.7 months. Responses were observed regardless of ethnicity, region of the world, or whether patients had prior systemic treatments. These data show that taletrectinib provides clinically significant tumor reduction and persistent disease control for advanced ROS1$^+$ NSCLC notwithstanding treatment history. These results indicate that taletrectinib provides clinically meaningful tumor shrinkage and prolonged disease control as a treatment option for advanced ROS1$^+$ NSCLC regardless of treatment history. See Ref. [118–120] for a summary of the clinical trials that led to the approval of taletrectinib.

5.6. Vimseltinib

Vimseltinib is a methyl pyrazole-pyridine derivative (Fig. 8G) that is FDA approved for the management of adult patients with symptomatic tenosynovial giant cell tumors (TGCT) for which surgical resection will possibly produce worsening functional limitation or severe illness (www.brimr.org/PKI/PKIs.htm). These rare tumors are more common in women and are usually diagnosed between ages 35–50 years [121]. These locally aggressive neoplasms are the result of dysregulation of the colony stimulating factor 1 (*CSF1*) gene and overexpression of the CSF1 ligand [122]. Tenosynovial giant cell tumors were previously known as pigmented villonodular synovitis or giant cell tumor of the tendon sheath and are locally aggressive neoplasms affecting the synovium, bursae, and tendon sheath [122]. These tumors are classified as (i) localized or (ii) diffuse, based upon the tumor location and size. The standard-of-care for most patients is surgical resection, with about 90 % of localized disease being cured with surgery; however, not all patients are amenable to surgery. Recurrence rates for the diffuse TGCTs are as high as 50 %, and patients who have a recurrence are considerably more likely to suffer additional recurrences.

Treatment options for people with tenosynovial giant cell tumors who are not candidates for surgery are limited. One orally effective protein kinase antagonist, pexidartinib, is approved in the USA, Taiwan, and South Korea [122]. It can only be prescribed in the US under a risk evaluation mitigation strategy owing to its associated rare, but potentially fatal, off-target cholestatic hepatoxicity. Pexidartinib failed to gain regulatory approval in Europe owing to these safety concerns and risks over the durability and extent of symptomatic improvements. Patients with these tumors require long-term treatment and need therapeutic options that can improve symptoms and the overall quality of life with manageable toxicity profiles.

In a multicenter, randomized, double-blind clinical trial (MOTION), the antitumor effect of vimseltinib was robust and four (5 %) of 83 patients had a complete response [122,123]. For patients in the vimseltinib arm at a dose of 30 mg twice weekly during a 24-week treatment cycle, the objective response rate at week 25 was 40 % (33 of 83 patients) and 0 % in the placebo arm. In the clinical trial, 85 % with an objective response had a duration of response greater than or equal to six months and 58 % had a duration of response greater than or equal to nine months. At the 25-week evaluation, the vimseltinib arm had statistically significant benefits in functional outcomes when compared to the placebo group. The most common side effects were rash, fatigue, peripheral, facial, and periorbital edema, leukopenia, neutropenia, pruritus, and increased serum alanine aminotransferase, aspartate aminotransferase, and cholesterol. Moreover, vimseltinib provided statistically significant and clinically meaningful improvements in health status, active range of motion, stiffness, physical function, and pain compared with the placebo arm.

Caldwell et al. determined the X-ray crystal structure of the vemseltinib-CSF1R complex [124] and found that the drug forms a hydrogen bond with C666 (the third hinge residue), AxK-K616, and DFG-D796. The drug interacts hydrophobically with RS1/2/3, Sh1/2, CS6/7/8, and the KLIFS-3 residue found proximally to the glycine-rich loop. It also interacts hydrophobically with AxK-K616, E633 and M637 of the αC-helix, L640 and V647 of the back loop, ^{664}EYCT^{667} of the hinge linker, G669 of the linker, L769 of the αF helix, C774 of the β6-strand, L785 of the β7-strand, the x of xDFG (G795), and DFG-D796. The drug interacts with a large portion of CSF1R [125] including the front pocket, gate area, back pocket, FP-I, BP-I-B, BP-II-out and BP-III. Vimseltinib was specifically designed to selectively block CSF1R. By binding to the switch pocket of CSF1R, vimseltinib precludes the occupation of the activation switch and stabilizes the switch in its inactive conformation. Important residues in the switch pocket include W550 in the juxtamembrane domain, M637 of the αC-helix, and the x residue (G795) of xDFG. Vimseltinib inhibits CSF1R activity with nanomolar potency and is $>$ 500-fold more selective for CSF1R versus closely related kinases and $>$ 1,000-fold more selective versus other kinases [122]. The enzyme has a DFG-D$_{out}$ configuration (BBAminus) and extends into the back cleft so that the interaction is characterized as type IIA inhibition [30,34]. See Refs. [121–123,125,126] for a summary of the clinical trials that led to the approval of vimseltinib.

5.7. Zongertinib

Zongertinib is a methylbenzimidazole derivative (Fig. 7H) that is FDA approved for the treatment of adult patients with unresectable or metastatic nonsquamous NSCLC whose tumors have *HER2* (*ERBB2*) protein-tyrosine kinase domain activating mutations and who have received prior systemic therapy (www.brimr.org/PKI/PKIs.htm). Mutations in *ERBB2* (encoding HER2) occur in 2 – 4 % of NSCLC patients and confer a poor prognosis [127,128]. This corresponds to an annual incidence ranging from 4000 to 8000 cases in the United States. Activating *HER2* alterations (mutation, overexpression, or amplification) stimulate downstream signaling pathways including the MAP kinase, PI3K/Akt, phospholipase C, protein kinase C, and Janus kinase (Jak--STAT) pathways [129]. Most *HER2* mutations arise as exon 20 in-frame insertions, the exon of which encodes the αC-β4 loop of the intracellular kinase domain and such mutations produce conformational changes in the ATP-binding pocket. These mutations can respond to irreversible tyrosine kinase inhibitors even when the overexpression is not observed by immunohistochemical staining. *HER2* mutations are associated with

adenocarcinoma histology, never smokers, Caucasians, and are a prognostic factor for worse clinical outcomes. Brain metastases are present in 44 % of patients with *HER2*-mutated NSCLC at the time of diagnosis [130].

Hong et al. performed an analysis of 3000 NSCLC patients with all types of ERBB2 alterations, drawn from two extensive retrospective cohorts: 1719 from Guardant360 (the United States, US) and 1281 from Geneplus (Chinese) [131]. The incidence of all types of ERBB2 alterations was 5.2 % in the US group and 5.6 % in the Chinese group. In both cohorts, among oncogenic alterations of ERBB2, exon 20 oncogenic insertion Y772_A775dupYVMA was the most frequent alteration in both groups (41.6 % in the US cohort and 58 % in the Chinese group), followed by G776delinsVC/LC/VV/IC (9.7 % vs. 10.7 %), and S310X (15.4 % vs. 10.5 %). The most common mutation is an *ERBB2* insertion (83 % of cases) involving a YVMA duplication at codon 775. Certain point mutations in *ERBB2* exon 20 are oncogenic as well, including L755S and G776C. Moreover, mutations in *ERBB2* transmembrane domain (G660D) and juxtamembrane domain have been identified (R678Q, E693K, and Q709L). These activating oncogenic mutations stimulate ErbB2 activity by promoting receptor dimerization or through disinhibition by the juxtamembrane segment.

Results from clinical trials demonstrated that the overall response rate of patients with *HER2*-mutant NSCLC was 71 % with a median duration of response of 14.1 months (n = 75) with subgroup analyses demonstrating an overall response rate of 81 % for patients with a *A775_G776insYVMA* insertion, 75 % for *P780_Y781insGSP*, and 42 % for all other ERBB2 alterations [128,129]. Zongertinib also demonstrated promising intracranial activity; interim analysis demonstrated an intracranial overall response rate (icORR) of 33 % and an intracranial disease control rate (icDCR) of 74 %. The former measures only tumors that have shrunk or disappeared (Partial Response + Complete Response), and the latter measures tumors that have shrunk, disappeared, or stayed the same size (Partial Response + Complete Response + Stable Disease). Zongertinib was also effective in a separate cohort of patients previously treated with the HER2 antibody-drug-conjugate trastuzumab deruxtecan with an overall response rate of 41 % [128]. The most common treatment related zongertinib side effects included diarrhea (56 %), rash (33 %), elevated serum aspartate transaminase activity (24 %), and elevated alanine transaminase activiety (21 %). Unfortunately, we lack an X-ray crystal structure of the zongertinib-HER2 complex; however, the drug is an irreversible covalent inhibitor of its target and is therefore classified as a type VI inhibitor [34].

5.8. Sunvozertinib

Sunvozertinib (DZD9008) is a pyrimidine derivative (Fig. 8I) that is FDA-approved for the management of adult patients with locally advanced or metastatic NSCLC with EGFR exon 20 insertion mutations, as detected by an FDA-approved test, and whose disease has progressed on or after platinum-based chemotherapy (www.brimr.org/PKI/PKIs.htm). These insertion mutations are the third most common *EGFR* mutations (2 % of all *EGFR* mutations) following exon 19 deletions (50 %) and exon 21 L858R point mutations (35 %) [132]. The exon 20 insertion mutations are traditionally associated with a worse patient prognosis than classical *EGFR* mutations. Sunvozertinib is an oral, irreversible EGFR blocker that was developed by Dizal Pharmaceuticals (a joint venture company formed by AstraZeneca and the Chinese Future Industry Investment Fund) for the treatment of NSCLC [133]. The compound contains a flexible anilinophenyl moiety on C-4 of the pyrimidine hinge binding motif that allows it to selectively bind to EGFRexon20ins and other mutants (IC_{50} values near 1 nM) while possessing less activity against wildtype EGFR (IC_{50} value of 230 nM). This approval was based on the results of the phase 2 WU-KONG1 trial, which randomly assigned patients with *EGFR* exon 20 mutations and prior exposure to platinum-based therapy [134–136]. The primary endpoint was an objective response rate, which was observed in 54.3 % of the participants. A complete response occurred in 2.9 % of the patients. Disease control was achieved in more than 90 % of the patients. The median duration of response was 11.1 months. Common drug-related treatment-emergent side effects included diarrhea, skin rash, and elevated serum creatine phosphokinase activity. The drug label includes warnings and precautions for interstitial lung disease, pneumonitis, gastrointestinal, dermatologic, ocular, and embryo-fetal toxicity. See Refs. [134–136] for a summary of the clinical trials that led to the approval of sunvozertinib.

5.9. Mirdametinib

Mirdametinib is an iodoanilino benzamide derivative (Fig. 8J) that antagonizes the dual specificity MEK1/2 protein kinases and is FDA-approved for the treatment of neurofibromatosis type-1 (NF1) with inoperable plexiform neurofibromas. (www.brimr.org/PKI/PKIs.htm). NF1 (von Recklinghausen disease) is an autosomal dominant genetic disease (1/3000 births) that manifests itself in childhood [137]. This neurocutaneous disease is characterized by tumors in the nervous system and skin. Neurofibromas are benign in nature containing various cell types including Schwann cells, perineural cells, and fibroblasts. Most affected children exhibit harmless light-brown café au lait macules that are observed at birth or appear during the first years of life. A finding of more than six café au lait spots strongly suggests a diagnosis of NF1. Additional signs and symptoms of NF1 vary, but they can include short stature, scoliosis (a sideways curvature of the spine), macrocephaly (an unusually large head), and hypertension. Mirdametinib is a selective inhibitor of MEK1/2 with an IC_{50} value of about 0.4 nM (ebi.ac.uk/chembl). The agent was approved by the FDA in 2025 and its properties were reviewed in a previous article [16].

6. Physicochemical properties of orally effective drugs

6.1. Lipinski's rule of five (Ro5)

Medicinal chemists and pharmacologists have investigated the physicochemical properties of drugs that are orally bioavailable to ascertain procedures for formulating new orally effective drugs [138]. Lipinski's rule of five (Ro5) is an algorithmic and experimental procedure that is performed to estimate membrane permeability, solubility, and pharmacologic efficacy in the drug-discovery setting [139]. The Ro5 is a guideline that gauges drug-likeness and determines whether a compound with specific druglike activities has properties indicating that it would be active orally. The Lipinski benchmarks were based on information revealing that most orally efficacious medicines are (i) relatively small and (ii) moderately lipophilic in nature. The paradigm is used during drug discovery as lead compounds, which serve as a starting points, are serially optimized to increase their activity and selectivity (for neophyte medicinal chemists, lead is the opposite of follow and not the metal).

The Ro5 criteria indicate that oral efficacy is more likely to result when (i) the AlogP (atom-based calculated Log P) is ≤ 5, when (ii) there are ≤ 5 hydrogen-bond donors, when (iii) there are $\leq 5 \times 2$ or 10 hydrogen-bond acceptors, and when (iv) the molecular weight is $\leq 5 \times 100$ or 500 [139]. P, the partition coefficient, is the ratio of the concentration of the un-ionized drug in the organic phase divided by its concentration in the aqueous phase of water-saturated *n*-octanol. The P value signifies the hydrophobicity of a compound, the greater the P value, the greater the hydrophobicity. The number of OH and NH groups represents the number of hydrogen-bond donors. The number of hydrogen-bond acceptors corresponds to the number of electronegative nitrogen and oxygen atoms attached to at least one hydrogen atom in its neutral state. In the original paper, the number of hydrogen bond acceptors was simply the number of nitrogens and oxygens, with caveats concerning the use of this criterion [139].

The Ro5 criteria were derived from the physicochemical characteristics of more than two thousand orally bioavailable drugs [139]. Excluding the three macrolides (everolimus, sirolimus, and temsirolimus), the average molecular weight (MW) of the FDA-approved protein kinase inhibitors is 474 with a range of from 285 (ritlecitinib) to 615 (trametinib) (Table 7). The drugs with a molecular weight exceeding 500 include the three macrolides and 29 others including the recently approved defactinib (511), sunvozertinib (584), remibrutinib (508), rilzabrutinib (666), and zongertinib (536). Although these data suggest that there is a propensity for orally bioavailable small molecule protein kinase antagonists to exceed the 500 Da molecular-weight criterion, the masses of most of the larger compounds excepting the macrolides are close to 500 Da. We find that 25 of the 94 approved drugs have an ALogP of greater than 5.0. We also observed that fostamatinib, dabrafenib, tovorafenib, the three macrolides, and the newly approved rilzabrutinib and avutometinib have more than ten hydrogen bond acceptors (Table 7).

In summary, a total of 45 of the 94 FDA-approved small molecule protein kinase antagonists fail to satisfy Lipinski's Ro5 (Fig. 1). Of these 45, temsirolimus, tovorafenib, and the newly approved rilzabrutinib have two Ro5 exceptions (a molecular weight greater than 500 and more than 10 hydrogen bond acceptors) and bosutinib, brigatinib, cabozantinib, ceritinib, entrectinib, infigratinib, lapatinib, midostaurin, mobocertinib, neratinib, nilotinib, quizartinib, ripretinib, and sunvozertinib have two Ro5 exceptions with a molecular weight greater than 500 and a partition coefficient greater than 5. Dabrafenib, everolimus, and sirolimus have three Ro5 deficiencies with a molecular weight greater than 500, more than 10 hydrogen bond acceptors, and an ALogP greater than 5. These are FDA-approved drugs, but drug candidates with two Ro5 exceptions during the discovery process represents an alert that "poor absorption or permeability is possible" [139]. The distribution coefficient ($LogD_{7.4}$) is the ratio of the concentration of the total substance (ionized and un-ionized) in the organic phase divided by that in the aqueous phase of immiscible *n*-octanol/water with a pH of 7.4. For reasons that are unclear, log $D_{7.4}$ data have recently been eliminated from the https://www.ebi.ac.uk/chembl database, but we have used previously posted data when available.

6.2. The importance of lipophilicity and ligand efficiency

6.2.1. Lipophilic efficiency, LipE

Prompted by Lipinski's Ro5 in 2001 [139], additional studies of the physicochemical properties of orally effective drugs have led to numerous additions and refinements [140–147]. For example, lipophilic efficiency, or LipE, is a property that is used during drug discovery that combines potency and lipophilic-mediated binding as an approach to increase binding efficacy. The following equations define lipophilic efficiency:

$$\text{LipE} = \text{p}IC_{50} - \text{ALogP};\ \text{LipE} = \text{p}K_i - \text{ALogP}$$

Like the practice of designating the molar hydrogen ion concentration as pH, the p operator denotes the negative of the logarithm of the IC_{50} or K_i. The ALogP is the atom-based calculated logarithm of the Partition coefficient; this number expresses the ratio of drug concentration in the organic phase divided by its solubility in the aqueous phase of immiscible *n*-octanol/water.

The second component of the equation (– ALogP or minus ALogP) reflects the lipophilicity of a compound and the value is calculated using an algorithm based upon the properties of thousands of reference organic compounds. The greater the concentration of a drug in the organic phase when compared with the aqueous phase of a *n*-octanol/water mixture, the greater its lipophilicity is. Leeson and Springthorpe opined that drug lipophilicity, as assessed by its – ALogP value, is an important fundamental property that should be assessed during drug discovery [141]. Lipophilic moieties include carbon atoms, halogen atoms, and unsaturated bonds [139]. In contrast, hydrophilic moieties include nitrogen atoms and oxygen atoms.

A large lipophilicity value may lead to the binding of a drug to adventitious targets that increase the likelihood of unwanted side effects. A customary goal during drug development and discovery is to increase potency without concurrently increasing lipophilicity. The use of lipophilic efficiency aids in the improvement of lead molecules by comparing a series of drug congeners [143,144]. To cite a pertinent example, Cui et al. recounted the improvement of lead compounds during the creation of crizotinib using lipophilic efficiency as an indicator of binding effectiveness [148]; crizotinib is FDA approved for the management for both $ROS1^+$ and ALK^+ NSCLC.

The ALogP of various lead compounds and drug candidates can be calculated rapidly by computer. Because actual measurements of LogP are labor intensive, such determinations are rarely performed. Hopkins et al. reported that acceptable values for LogP are less than ~ 3 and satisfactory values of lipophilic efficiency are greater than ~ 5 [143]. Substances with these properties are regarded as "druglike.". Note that this definition applies despite the absence of any structural similarity to an approved drug. The average value of lipophilic efficiency (LipE) for 91 FDA-approved small molecule protein kinase inhibitors (omitting the three macrolides) is 4.58 with a range from 1.3 (neratinib) to 7.96 (deucravacitinib) (Table 8). The average AlogP value for the 91 FDA-approved drugs (excluding the three macrolides) was 3.92 with a range from 1.1 (baricitinib) to 6.36 (ceritinib and nilotinib). Improving potency and reducing lipophilicity during drug development usually produces substances with better pharmacodynamic (ADME) properties.

6.2.2. Ligand efficiency, LE

The ligand efficiency (LE) value correlates potency, or binding affinity, to the number (N) of nonhydrogen (heavy) atoms in a compound. The following formula is employed to calculate this value:

$$\text{LE} = \Delta G^{\circ\prime}/\text{N} = -\text{RT ln } K_{eq}/\text{N} = -2.303\text{RT Log } K_{eq}/\text{N}$$

$\Delta G^{\circ\prime}$ is the standard free energy change of an ligand binding to its target protein at neutral pH, R denotes the universal gas constant or energy-temperature coefficient (1.98×10^{-3} kcal/degree-mol), T is the temperature in degrees Kelvin, K_{eq} is the value of the equilibrium constant, and N denotes the number of nonhydrogen or heavy atoms in the drug. The IC_{50} or K_i values are proxies for the equilibrium constant. At a body temperature of 37°C (310 K), this equation becomes $-(2.303 \times (1.98 \times 10^{-3}/\text{K}) \times 310\text{ K Log } K_{eq})/\text{N}$ or $-1.41 \text{ Log } K_{eq}/\text{N}$. Some investigators employ a temperature of 300 K corresponding to a factor of –1.37 [143,147]. Ligand efficiency is a surrogate of drug potency based upon the average binding energy per nonhydrogen atom. Ligand efficiency is helpful in fragment-based drug discovery methodologies and, like lipophilic efficiency, it assists in the design and choice of congeners of lead compounds for further development [145].

Ligand efficiency mirrors the binding affinity per heavy atom of the ligand or drug of interest. The value of N serves as a surrogate for the molecular mass. The equation used to compute ligand efficiency shows that its value is directly proportional to the binding affinity ($-\text{Log } K_{eq}$, a positive number) and is inversely proportional to the number of heavy atoms. Hopkins et al. reported that reasonable values for ligand efficiency (LE) are greater than 0.3 kcal per mole per heavy atom [140,143]. Ligand efficiency values for the FDA-approved small molecule protein kinase blockers based upon representative K_i or IC_{50} values are included in Table 8. The average ligand efficiency value for 91 of the FDA-approved protein kinase inhibitors (excluding the three macrolides) was 0.393 with a range from 0.237 (mobocertinib) to 0.631 (ritlecitinib). Twelve drugs had values of less than 0.3 including fostamatinib, lazertinib, mobocertinib, midostaurin, neratinib, nintedanib, nilotinib, pacritinib, tovorafenib and three newly approved drugs (avutometinib, rilzabrutinib, zongertinib). The values for lipophilic efficiency and ligand efficiency provided in Table 8 are based on findings

Table 7
Properties of FDA-approved small molecule inhibitors.

Drug	PubMED CID	MW (Da)	HD[a]	HA[b]	ALogP[c]	Log $D_{7.4}$[d]	PSA (Å^2)[e]	nStereo[f]	Cplx[g]
Abemaciclib@	46220502	**507**	1	9	4.94	3.76	75	0	723
Abrocitinib	78323835	323	2	6	1.3	0.79	99.4	0	474
Acalabrutinib	71226662	466	2	6	3.31	2.56	119	1	845
Afatinib	10184653	486	2	8	4.39	2.34	88.6	1	702
Alectinib	49806720	483	1	5	4.77	4.75	72.4	0	867
Asciminib	72165228	450	3	8	3.46	3.86	103	1	626
Avapritinib	118023034	499	1	9	2.61	2.12	106	1	752
Avutometinib@	16719221	471	2	**11**	2.68	1.96	141	0	844
Axitinib	6450551	386	2	4	4.64	4.15	96	0	557
Baricitinib	44205240	371	1	7	1.10	-0.19	129	0	678
Belumosudil	11950170	452	3	6	4.82	4.65	105	0	678
Binimetinib	10288191	441	3	7	3.01	3.81	88.4	0	521
Bosutinib@	5328940	**530**	1	8	**5.19**	3.37	82.9	0	734
Brigatinib@	68165256	**584**	2	9	**5.09**	2.49	85.9	0	835
Cabozantinib@	25102847	**501**	2	7	**5.54**	4.65	98.8	0	795
Capivasertib	25227436	429	4	6	2.10	–0.16	120	0	580
Capmatinib	25145656	412	1	6	3.43	2.96	85.1	0	637
Ceritinib@	57379345	**558**	3	8	**6.36**	3.38	114	0	835
Cobimetinib@	16222096	**531**	3	7	3.78	2.73	64.6	1	624
Crizotinib@	11626560	450	2	6	**5.04**	0.95	78	1	558
Dabrafenib@	44462760	**520**	2	**11**	**5.36**	5.10	147	0	817
Dacomitinib@	11511120	470	2	7	**5.16**	3.53	79.4	0	665
Dasatinib	3062316	488	3	9	3.31	3.74	135	0	642
Defactinib@	25117126	**511**	3	**13**	2.40	0.75	150	0	804
Delgocitinib	50914062	310	1	5	1.30	0.6	88.9	0	544
Deucravacitinib	134821691	426	3	8	1.73	2.10	136	0	648
Deuruxolitinib	72704611	314	1	4	3.47	2.48	83.2	1	453
Encorafenib@	50922675	**540**	3	10	3.91	2.61	149	1	836
Ensartinib@	56960363	**561**	3	8	4.72	3.26	122	3	812
Entrectinib@	25141092	**561**	3	8	**5.03**	4.87	85.5	0	847
Erdafitinib	67462786	446	1	7	4.18	1.25	77.3	0	583
Erlotinib	176870	393	1	7	3.41	3.20	74.7	0	525
Everolimus@	6442177	**958**	3	**14**	**6.20**	7.40	205	15	1810
Fedratinib@	16722836	**525**	3	9	4.82	3.23	117	0	787
Fostamatinib@	11671467	**580**	4	**15**	3.09	-0.52	187	0	904
Fruquintinib	44480399	393	1	7	3.85	2.64	95.7	0	579
Futibatinib	71621331	418	1	7	1.78	1.77	108	1	723
Gefitinib	123631	447	1	8	4.28	3.64	68.7	0	545
Gilteritinib@	49803313	**552**	3	10	2.70	1.69	121	0	785
Ibrutinib	24821094	441	1	6	4.22	3.63	99.2	1	678
Imatinib	5291	494	2	7	4.59	3.80	86.3	0	706
Infigratinib@	53235510	**560**	2	8	**5.35**	3.99	95.1	0	724
Lapatinib@	208908	**580**	2	9	**6.14**	4.40	115	0	898
Larotrectinib	46188928	428	2	7	2.95	2.44	86	0	659
Lazertinib@	121269225	**555**	2	9	4.10	3.56	110	0	837
Lenvatinib	9823820	427	3	5	4.07	2.52	116	0	634
Lorlatinib	71731823	406	1	7	2.80	1.62	110	1	700
Midostaurin@	9829523	**571**	1	4	**5.91**	5.43	77.7	4	1140
Mirdametinib	9826528	482	4	8	2.47	3.98	90.8	1	465
Mobocertinib@	118607832	**586**	2	9	**5.08**	3.79	114	0	935
Momelotinib	25062766	414	2	7	2.98	2.70	103	0	615
Neratinib@	9915743	**557**	2	8	**5.93**	3.05	112	0	881
Netarsudil	66599893	454	2	5	4.89	3.42	94.3	1	678
Nilotinib@	644241	**530**	2	9	**6.36**	5.35	97.6	0	817
Nintedanib@	135423438	**540**	2	7	3.62	2.57	101	0	892
Osimertinib	71496458	500	2	7	4.51	3.01	87.6	0	752
Pacritinib	46216796	473	1	7	4.47	1.96	67.7	0	644
Palbociclib	5330286	448	2	8	2.97	1.30	103	0	775
Pazopanib	10113978	438	2	8	3.14	3.55	127	0	717
Pemigatinib	86705695	487	1	8	3.66	1.80	83.2	0	731
Pexidartinib	25151352	417	2	7	**5.23**	4.45	66.5	0	537
Pirtobrutinib	129269915	479	3	9	3.43	3.35	125	1	719
Ponatinib@	24826799	**533**	1	8	4.46	4.54	65.8	0	910
Pralsetinib@	129073603	**534**	3	9	4.20	3.64	136	1	816
Quizartinib@	24889392	**561**	2	9	**5.86**	5.05	106	0	849
Regorafenib	11167602	483	3	8	**5.69**	4.49	92.4	0	686
Remibrutinib@	118107483	**508**	2	8	3.0	3.29	110.4	0	815
Repotrectinib	135565923	355	2	6	2.55	2.17	80.6	0	524
Ribociclib	44631912	435	2	7	2.80	0.91	91.2	0	636
Rilzabrutinib@	73388818	**666**	1	**11**	4.42	3.44	139	0	1230
Ripretinib@	71584930	**510**	3	5	**5.67**	4.38	86.4	0	746
Ritlecitinib	118115473	285	2	4	1.94	1.40	73.9	2	402
Ruxolitinib	25126798	306	1	4	3.47	2.48	83.2	1	453
Selpercatinib@	134436906	**526**	1	9	3.28	3.11	112	0	885

(*continued on next page*)

Table 7 (*continued*)

Drug	PubMED CID	MW (Da)	HD[a]	HA[b]	ALogP[c]	Log $D_{7.4}$[d]	PSA (Å^2)[e]	nStereo[f]	Cplx[g]
Selumetinib	10127622	458	3	6	3.53	4.27	88.4	0	523
Sirolimus@	5284616	**914**	3	**13**	**6.18**	7.45	195	15	1760
Sorafenib	216239	465	3	7	**5.55**	4.34	92.4	0	646
Sunitinib	5329102	398	3	4	3.33	1.28	77.2	0	636
Sunvozertinib	139377809	**584**	4	9	**5.26**	?	115	1	885
Taletrectinib	72202474	405	4	7	4.43	1.9	77.5	0	532
Temsirolimus@	6918289	**1030**	4	**16**	4.39	?	242	15	2010
Tepotinib	25171648	493	0	7	4.01	2.26	94.7	0	880
Tivozanib@	9911830	455	2	7	**5.64**	4.16	108	0	631
Tofacitinib	9926791	312	1	5	1.54	1.19	88.9	2	488
Tovorafenib@	25161177	**506**	3	**11**	3.98	2.99	164	1	695
Trametinib@	11707110	**615**	2	6	3.94	3.18	102	0	1090
Trilaciclib	68029832	447	2	7	2.72	2.29	91.2	0	707
Tucatinib@	51039094	481	2	8	**5.09**	5.25	111	0	796
Upadacitinib	58557659	380	2	6	2.91	0.85	78.3	2	561
Vandetanib	3081361	475	1	7	4.43	2.14	59.5	0	539
Vemurafenib@	42611257	490	2	7	**5.54**	4.61	100	0	790
Vimseltinib	86267612	432	1	6	3.56	2.20	97.5	0	740
Zanubrutinib	135565884	472	2	5	4.22	3.42	103	0	756
Zongertinib@	160283094	**536**	2	9	4.42	3.8	123	0	870

[a] HD, no. of hydrogen bond donors.
[b] HA, no. of hydrogen bond acceptors.
[c] ALogP, values for atom-based log of the partition coefficient from https://www.ebi.ac.uk/chembl/.
[d] Log $D_{7.4}$, values for the log of the distribution coefficients at pH 7.4 obtained from https://www.ebi.ac.uk/chembl/.
[e] PSA, polar surface area values from https://pubchem.ncbi.nlm.nih.gov/.
[f] Defined atom stereocenter count.
[g] Complexity values obtained from https://pubchem.ncbi.nlm.nih.gov/.

obtained using different methodologies. Accordingly, these data cannot be used to make head-to-head comparisons of the drugs because different procedures were used to obtain the data. These data were acquired from diverse drug discovery studies and hence provide representative values.

6.2.3. *Additional chemical descriptors of orally effective drugs*

To verify drug attributes linked to oral bioavailability, the Ro5 has stimulated the development of numerous modifications. For example, Veber et al. found that the number of rotatable bonds and the polar surface area (PSA) varies between orally active and inactive drugs in rats [145]. They observed that 10 rotatable bonds or fewer are optimal. This property influences passive membrane permeation and reflects molecular flexibility and degrees of freedom. Furthermore, molecular flexibility is correlated with the entropy change that results from ligand binding and it controls the extent of drug binding to its targets. With the exception of five drugs with 11 rotatable bonds (temsirolimus, neratinib, lapatinib, fedratinib, erlotinib) and mobocertinib with 13 rotatable bonds, the remaining drugs have 10 or fewer of these bonds (Table 8). The average number of rotatable bonds is 6.49 and ranges from 0 (repotrectinib, lorlatinib) to 13 (mobocertinib). Furthermore, these investigators found that most orally effective drugs have a polar surface area less than or equal to 140 Å^2 [145]. This parameter is the total surface over all polar atoms, primarily nitrogen and oxygen, and it also encompasses connected hydrogen atoms. Omitting the three macrolides, the average value for the surface area is 100.9 Å^2 with a range from 59.5 (vandetanib) to 187 (fostamatinib). Dabrafenib, encorafenib, fostamatinib, tovorafenib, and the recently approved avutometinib are the only drugs with a polar surface area exceeding 140 Å^2 (Table 7). Furthermore, Oprea observed that the total number of ring structures (aromatic and nonaromatic) in most approved orally effective drugs is three or more [146]. All FDA approved small molecule protein kinase antagonists including the macrolides have three or more rings (except mirdametinib) with an average value of 4.26 and a range from two (mirdametinib) to seven (midostaurin) (Table 8). Except for netarsudil (an eye drop), trilaciclib and temsirolimus (which are given intravenously), and delgocitinib (applied topically) all the FDA-approved drugs are orally bioavailable. Ruxolitinib, moreover, is used both orally and topically.

The molecular complexity of a molecule is determined by its structure, its component elements, and its symmetry. The complexity is calculated by the Bertz/Hendrickson/Ihlenfelt algorithm [149,150]. The calculation is based upon the number of constituent atoms, the bonding arrangement, and the nature of the chemical bonds (single, double, triple, aromatic). Molecular complexity ranges from zero for ions to several thousand for elaborate naturally occurring organic chemicals. Larger compounds usually display a greater molecular complexity than smaller substances. In contradistinction, chemicals that are very symmetric and contain few elements have smaller molecular complexity values. The complexity values for the FDA-approved drugs reviewed in this article were downloaded from PubChem (https://pubchem.ncbi.nlm.nih.gov/). For the 94 FDA-approved kinase inhibitors, the average complexity value is 751 with a range from 402 (ritlecitinib) to 2010 (temsirolimus) (Table 7). As expected, the three larger macrolide derivatives have the largest molecular complexity values. There are no optimal molecular complexity values for orally bioavailable drugs; however, this characteristic may be helpful in anticipating the ease or difficulty of drug production, an important factor in the manufacture of commercial pharmaceuticals.

Ritchie and Macdonald investigated the role that aromatic character plays in determining the pharmacokinetic (ADME) properties of various medicines [151]. They regarded aromatic bicyclic and tricyclic agents as drugs that contain two and three aromatic rings, respectively. Aromatic compounds include molecules containing carbon alone or carbon with nitrogen or sulfur heteroatoms. These authors reported that increasing the number of carboaromatic rings had a detrimental influence on druglike properties by increasing binding to serum albumin, decreasing aqueous solubility, and inhibiting cytochrome P450. We find that the average number of aromatic rings in the 94-approved protein kinase inhibitors was 3.3 and the average number of benzene moieties was 1.07 (Table 8). The FDA-approved protein kinase inhibitors, except for the three macrolides, have between two and five aromatic rings. Twenty-three of the drugs lacked benzene components and the number with one or two benzenes was evenly distributed among the remainder (Table 8).

Bayliss et al. examined the dosage of orally bioavailable drug and

Table 8
Properties of FDA-approved small molecule protein kinases inhibitors.

Drug	Target, kinase family[a]	K_i nM[b]	pK_i	LipE[c]	N*[d]	LE[e]	Dose[f]	Sol[g]	nRotB[h]	nRng[i]	nAr[j]	nBnz[k]	QED[l]
Abemaciclib	CDK4, S/T	0.6	9.22	4.28	37	0.351	400*	15.9	7	5	4	0	0.38
Abrocitinib	JAK1, NRY	5.1	8.29	7.04	22	0.531	100	420	6	3	2	0	0.83
Acalbrutinib	BTK, NRY	3.1	8.51	5.20	35	0.343	200*	10.9	4	5	4	1	0.45
Afatinib	EGFR, RY	0.5	9.33	4.94	34	0.387	40	12.8	8	4	3	1	0.46
Alectinib	ALK, RY	1.9	8.72	3.95	36	0.342	1200*	10.5	3	6	3	0	0.58
Asciminib	BCR-Abl, NRY	0.5	9.3	5.84	31	0.300	80	55	6	4	3	1	0.50
Avapritinib	PDGFRα, RY	0.18	9.7	7.09	37	0.370	300	30.1	5	6	5	1	0.39
Avutometinib	MEK1/2, DS	160	6.2	3.52	33	0.265	3.2***	17.7	7	4	4	1	0.39
Axitinib	VEGFR2, RY	0.25	9.6	4.96	28	0.483	300	0.55	5	4	4	1	0.52
Baricitinib	JAK2, NRY	7	8.15	7.05	26	0.442	2	357	5	4	3	0	0.72
Belumosudil	ROCK2, S/T	53.9	7.3	2.48	34	0.303	200	2.89	7	5	5	1	0.33
Binimetinib	MEK1/2, DS	12	7.92	4.91	27	0.414	90*	49.9	6	3	3	1	0.40
Bosutinib	BCR-Abl, NRY	20	7.7	2.51	36	0.302	500	9.5	9	4	3	1	0.38
Brigatinib	ALK, RY	0.398	9.4	4.31	40	0.331	180	22	8	5	3	2	0.35
Cabozantinib	RET, RY	5	8.3	2.76	37	0.316	40	1.99	8	5	4	2	0.31
Capivasertib	AKT=PKB, S/T	3	8.52	6.42	30	0.400	800	> 1000	6	4	3	1	0.48
Capmatinib	MET, RY	0.13	9.89	6.46	31	0.450	800*	5.29	4	5	5	1	0.49
Ceritinib	ALK, RY	0.2	9.7	3.34	38	0.360	750	2.22	9	4	3	2	0.28
Cobimetinib	MEK1/2, DS	0.79	9.1	5.32	30	0.428	60	42.2	4	4	2	2	0.53
Crizotinib	ALK, RY	0.63	9.2	4.16	30	0.432	500*	6.11	5	4	3	1	0.53
Dabrafenib	B-Raf, S/T	0.4	9.4	4.04	35	0.379	300*	3.27	6	4	4	2	0.37
Dacomitinib	EGFR, RY	2	8.7	3.54	33	0.372	45	8.74	7	4	3	1	0.47
Dasatinib	BCR-Abl, NRY	0.16	9.8	6.49	33	0.419	100	12.8	7	4	3	1	0.47
Defactinib	FAK, NRY	0.6	9.22	6.8	35	0.371	400	18.4	8	3	3	1	0.42
Delgocitinib	JAK3, NRY	2.8	8.60	7.30	23	0.527	Topical	552	2	4	2	0	0.90
Deucravacitinib	TYK2, NRY	0.2	9.69	7.96	31	0.441	6	0.159	7	4	3	1	0.52
Deuruxolitinib	JAK2/1, NRY	0.7	9.15	5.68	23	0.561	16*	120	4	4	3	0	0.80
Encorafenib	B-Raf, S/T	0.3	9.52	5.61	36	0.373	450	11.2	10	3	3	1	0.37
Ensartinib	ALK, RY	0.4	9.4	4.68	38	0.349	225	6.4	6	4	3	2	0.37
Entrectinib	TRK, RY	1	9	3.97	41	0.310	600	8.9	7	6	4	2	0.29
Erdafitinib	FGFR1, RY	2	8.7	4.52	33	0.372	8	13	9	4	4	1	0.41
Erlotinib	EGFR, RY	0.32	9.5	6.09	29	0.462	150	8.91	11	3	3	1	0.42
Everolimus	FKBP12/mTOR, S/T	2	8.70	2.5	68	0.180	10	1.63	9	3	0	0	0.13
Fedratinib	JAK2, NRY	6	8.22	3.40	37	0.313	400	9.49	11	4	3	2	0.35
Fostamatinib	Syk, NRY	17	7.77	4.68	40	0.274	300*	52	10	4	3	1	0.26
Fruquintinib	VEGFR2, RY	35	7.46	3.61	29	0.363	5	0.0803	5	4	4	0	0.55
Futibatinib	FGFR2, RY	4	8.4	6.62	31	0.382	20	40	6	4	3	1	0.51
Gefitinib	EGFR, RY	0.5	9.3	5.02	31	0.423	250	27	8	4	3	1	0.52
Gilteritinib	Flt3, RY	0.41	9.39	6.69	40	0.331	120	22.3	9	5	2	1	0.43
Ibrutinib	BTK, NRY	12.6	7.9	3.68	33	0.338	560	20.3	5	5	4	2	0.47
Imatinib	BCR-Abl, NRY	1	9	4.41	37	0.343	600	14.6	7	5	4	2	0.39
Infigratinib	FGFRs, RY	5	8.3	2.95	38	0.308	125	29.9	8	4	3	2	0.38
Lapatinib	EGFR, RY	1	9	2.86	40	0.317	1250	22.3	11	5	5	2	0.18
Larotrectinib	TRK, RY	9.7	8.01	5.06	31	0.364	200*	238	3	5	3	1	0.67
Lazertinib	EGFR, RY	10.2	7.99	3.88	41	2.75	240	25	10	5	4	2	0.28
Lenvatinib	VEGFR2, RY	3.98	8.4	4.33	30	0.395	24	6.22	6	4	3	1	0.55
Lorlatinib	ALK, RY	9	8.05	5.25	30	0.378	100	108	0	3	3	1	0.61
Midostaurin	Flt3, RY	37	7.43	1.52	43	0.244	200*	15.7	3	7	4	1	0.29
Mirdametinib	MEK1/2, DS	0.4	9.4	6.76	26	0.510	2	31.3	7	2	2	2	0.36
Mobocertinib	EGFR, RY	60	7.22	2.14	43	0.237	160	13.6	1*	4	4	1	0.17
Momelotinib	JAK2/1, NRY	1.4	8.85	5.87	31	0.402	200	32.5	6	4	3	2	0.60*
Neratinib	ErbB2/HER2, RY	59	7.23	1.30	40	0.255	240	6.74	11	4	4	1	0.22
Netarsudil	ROCK1/2, S/T	1	9	4.11	34	0.373	0.01	0.23	8	4	4	2	0.39
Nilotinib	BCR-Abl, NRY	12.5	7.9	1.54	39	0.286	600*	2.01	6	5	5	2	0.27
Nintedanib	FGFR, RY	39.8	7.4	3.78	40	0.261	300*	30.9	8	5	4	2	0.35
Osimertinib	EGFR, RY	7	8.15	3.64	37	0.311	80	22.4	10	4	4	1	0.31
Pacritinib	JAK2, NRY	19	7.72	2.21	35	0.289	100	38	4	4	2	1	0.67*
Palbociclib	CDK4, S/T	10	8	5.03	33	0.342	125	17.4	5	5	3	0	0.58
Pazopanib	VEGFR2, RY	30	7.52	4.38	31	0.342	800	43.3	5	4	4	1	0.49
Pemigatinib	FGFR, RY	0.5	9.3	5.64	35	0.375	13.5	144	6	5	3	1	0.57
Pexidartinib	CSF1R, RY	13	7.89	2.66	29	0.384	800*	3.15	5	4	4	0	0.47
Pirtobrutinib	BTK, NRY	0.5	9.3	5.87	34	0.386	200	3.84	7	3	3	2	0.45
Ponatinib	BCR-Abl, NRY	1	9	4.54	39	0.325	45	2.95	6*	5	4	2	0.39
Pralsetinib	RET, RY	0.5	9.3	5.10	39	0.336	400	10.1	8	5	4	0	0.31
Quizartinib	Flt3, RY	3.3	8.48	2.62	40	0.299	35.4	50.9	8	5	3	1	0.26
Regorafenib	VEGFR2, RY	4.2	8.4	2.71	33	0.359	160	1.02	5	3	3	2	0.41
Remibrutinib	BTK, NRY	1.3	8.89	4.99	37	0.339	50*	5	9	4	3	2	0.41
Repotrectinib	ROS1, RY	0.07	11.2	8.60	26	0.607	320*	49.8	0*	3	3	1	0.65
Ribociclib	CDK4, S/T	10	8	5.20	32	0.353	600	231	5	5	3	0	0.64
Rilzabrutinib	BTK, NRY	1.3	8.89	4.47	49	0.256	800*	slight	8	7	4	2	0.21
Ripretinib	Kit, RY	3	8.52	2.85	33	0.364	150	5.83	5	4	4	2	0.32
Ritlecitinib	JAK3, NRY	33.1	7.48	5.54	21	0.502	50	457	3	3	2	0	0.85
Ruxolitinib	JAK1, NRY	1.2	8.92	5.45	23	0.547	20*	116	4	4	3	0	0.8
Selpercatinib	RET, RY	1	9	5.72	39	0.325	320*	29.9	8	4	4	0	0.37

(*continued on next page*)

Table 8 (*continued*)

Drug	Target, kinase family[a]	K_i nM[b]	pK_i	LipE[c]	N*[d]	LE[e]	Dose[f]	Sol[g]	nRotB[h]	nRng[i]	nAr[j]	nBnz[k]	QED[l]
Selumetinib	MEK1/2, DS	14	7.85	4.32	27	0.410	80*	21	6	3	3	1	0.39
Sirolimus	FKBP12/mTOR, S/T	0.1	10	3.82	65	0.217	2	1.73	6	3	0	0	0.16
Sorafenib	VEGFR1, RY	15.8	7.8	2.25	32	0.344	800*	1.71	5	3	3	2	0.46
Sunitinib	VEGFR2, RY	3.98	8.4	5.07	29	0.408	50	30.8	7	3	2	0	0.63
Sunvozertinib	EGFR, RY	1.1	8.89	4.62	41	0.306	200	slight	10	4	3	2	0.24
Taletrectinib	ROS1, RY	0.21	9.68	5.25	30	0.455	600	slight	7	4	4	2	0.48
Temsirolimus	FKBP12/mTOR, S/T	8	8.1	3.71	73	0.156	25**	2.35	11	4	0	0	?
Tepotinib	MET, RY	1	9	4.99	37	0.343	450	0.5	7	5	4	2	0.38
Tivozanib	VEGFR2, RY	6.5	8.19	2.55	32*	0.312	1.34	52.1	6	4	4	1	0.39
Tofacitinib	JAK1, NRY	0.79	9.1	7.56	23	0.558	10*	299	3	3	2	0	0.93
Tovorafenib	B-Raf, S/T	10	8	4.02	32	0.285	600**	1.94	5	3	3	0	0.48
Trametinib	MEK1/2, DS	3.4	8.47	4.53	37	0.323	2	30.7	5	5	3	2	0.33
Trilaciclib	CDK4/6, S/T	1	9	6.28	33	0.385	480	260	3	6	3	0	0.64
Tucatinib	ErbB2/HER2, RY	8	8.1	3.01	36	0.317	600*	4	6	6	5	1	0.36
Upadacitinib	JAK1, NRY	43	7.37	4.46	27	0.385	15	70.7	3	4	3	0	0.73
Vandetanib	RET, RY	50	7.3	2.30	30	0.343	300	10.2	6	4	3	1	0.59*
Vemurafenib	B-Raf, S/T	3.98	8.4	2.86	33	0.359	1920*	0.36	7	4	4	2	0.33
Vimseltinib	CSF1R, RY	19	7.72	4.16	32	0.34	30***	68.4	6	4	4	0	0.50
Zanubrutinib	BTK, NRY	0.3	9.52	5.30	35	0.384	320*	10.3	6	5	3	2	0.52
Zongertinib	ErbB2/HER2, RY	9	8.04	3.63	40	0.283	120	slight	7	6	5	1	0.29

[a] NRY, non-receptor protein-tyrosine kinase; RY, receptor protein-tyrosine kinase; S/T, protein-serine/threonine kinase; DS; dual specificity protein kinase (catalyzes protein-tyrosine and then threonine phosphorylation of target kinase activation segments but evolutionarily in the protein-serine/threonine kinase family).
[b] Representative values obtained from www.ebi.ac.ug/chembl/ and from klifs.net.
[c] LipE (lipophilic efficiency) = $p\mathrm{IC}_{50}$ – ALogP
[d] N*, Number of heavy (nonhydrogen) atoms.
[e] LE (ligand efficiency) = – 2.303 RT Log_{10} K_i/N where N is the number of heavy (non-hydrogen) atoms in the drug
[f] Dosage in mg/day from FDA label; *, total daily dose taken in one-half increments twice a day (bid); **, once weekly, ***, twice weekly
[g] Sol, solubility (μg/ml) in water (go.drugbank.com/drugs/)
[h] nRotB, number of Rotatable Bond values obtained from https://pubchem.ncbi.nlm.nih.gov/.
[i] nRng, number of rings
[j] nAr, number of Aromatic rings
[k] nBnz, number of benzene moieties
[l] QED, summed, weighted desirability (scores using MW + ALogP + HD + HA + PSA + nRotB + nAr) obtained from https://www.ebi.ac.uk/chembl/; see Refs. [147] for a full explanation.

drug candidates [152]. They noted that daily intakes of 100 mg or less lowered the risk of toxicity. The daily dosages of orally bioavailable FDA-approved protein kinase inhibitors range from 1.34 mg (tivozanib) to 1920 mg (vemurafenib) with a mean of about 290 mg and a median of 200 mg (Table 8). Only 35 of the 94 FDA-approved kinase antagonists meet the 100 mg or less criterion. Bayliss et al. found that drugs with a water solubility of 100 μg/ml or less are associated with an increased risk of failure [152]. We examined the water solubility of the FDA-approved protein kinase antagonists and found a range from slight (< 0.1 μg/ml for fruquintinib and the recently approved rilzabrutinib, taletrectinib, and zongertinib) to > 1000 μg/ml for capivasertib with a mean value of about 55 μg/ml. Only 11 of the 94 drugs have a water solubility greater than 100 μg/ml. The dosages and solubilities of the FDA-approved kinase antagonists range over three orders of magnitude.

7. Epilogue and perspective

Although scientists have achieved major breakthroughs in the discovery and development of orally bioavailable small molecule protein kinase antagonists since the FDA-approval of sirolimus in 1999 and imatinib in 2001, this field is still in its infancy. Oprea et al. suggested that the dysregulation of many understudied protein kinases (dark kinases) plays an essential part in the pathogenesis of various neoplasms [153]. Moreover, such understudied kinases represent potential drug targets. Examples include ribosomal protein brain selective kinase-1/2 (BSK1/2), S6 kinase δ1 (RPS6KC1), mitogen-activated protein kinase kinase kinase 1/13 (MAP3K1/13), cyclin-dependent protein kinase 12 (CDK12), and eukaryotic elongation factor 2 kinase (EEF2K). Most of the FDA-approved protein kinase inhibitors target neoplasms or the immune system [10,154–157]. Owing to inherent genetic changes in benign and malignant neoplasms, resistance to protein kinase blockers occurs on a nearly universal basis. Such resistance motivated the formulation of second, third, and later generation antagonists that target (i) the initial enzyme or its mutants and (ii) activators of bypass pathways (e.g., defactinib blockade of FAK in low grade serous ovarian cancer). Gatekeeper mutations occurring in the initial protein kinase target are often the reason for acquired drug resistance [3]. For example, the *EGFR* (T790M) gatekeeper mutation occurs in lung cancers. Moreover, this substitution accounts for about half of all acquired *EGFR* inhibitor resistance mutations.

Because 244 protein kinase genes align with cancer amplicons or disease loci [8], we anticipate that (i) there will be a substantial growth in the number of drugs inhibiting additional protein kinases and (ii) new drugs will be fabricated for the management of many more diseases [158–161]. Adding more protein kinase targets to the medicinal weaponry will require the characterization of signaling pathways besides the MAP kinase, PI3K/AKT/mTOR, and JAK-STAT pathways such as Hedgehog, Hippo, Notch, Wnt, cAMP, and Ca^{+2} signaling modules [162]. Besides the 94 protein kinase blockers covered in this article, the FDA has approved five orally bioavailable drugs that inhibit PI3Ks (these are components of the atypical protein kinase family with lipid substrates) [9]. These PI3K antagonists include alpelisib – a PI3K-α blocker that is used for the management of breast cancer – and copanlisib, duvelisib, idelalisib, and umbralisib which are PI3K-δ antagonists that are used for the third-line treatment of follicular lymphomas and other hematological diseases. As the protein kinase inhibitor discipline progresses, it is likely that protein kinase blockers with new chemical entities, scaffolds, heterocycles, and pharmacophores will be forthcoming [163]. We anticipate that a variety of allosteric inhibitors will be developed that inhibit enzymes besides MEK1/2 [164,165]. Furthermore, it is quite likely that more targeted covalent irreversible inhibitors of protein kinases will become developed. We foresee major efforts in combining protein kinase inhibitor therapies with various immunomodulators for the management of breast, lung, renal, and other

malignancies [166–168].

Of the 94 FDA-approved drugs, receptor protein-tyrosine kinases are the chief targets of 48 of them followed by nonreceptor protein-tyrosine kinases (26), protein-serine/threonine kinases (14), and dual-specificity protein kinases (6) (Table 1). The timeline for the approval of the protein kinases is depicted in Fig. 1 A; note that 2025 was a banner year with ten FDA approvals. The JAK family of nonreceptor protein-tyrosine kinases ranked first with 11 inhibitors, followed by EGFR/ErbB1 with nine antagonists, the VEGFR family with eight blockers, followed by ALK and BCR-Abl each with six inhibitors. The dual specificity (MEK1/2) protein kinases, which inhibit the Ras-Raf-MEK-ERK MAP kinase module, include cobimetinib (used in combination with vemurafenib for the treatment of melanoma), binimetinib (used in combination with encorafenib for the management of melanoma), trametinib (used in combination with dabrafenib for the treatment of melanoma, NSCLC with *BRAF* V600E/K mutations, and advanced thyroid cancer), newly approved avutometinib (used in combination with defactinib for the treatment of low grade serous cancer of the ovary), and selumetinib and mirdametinib (each prescribed for the management of neurofibromatosis I). CDK4/6 is inhibited by four of the FDA-approved drugs that are used for the treatment of breast cancer.

The clinical success of drugs that are FDA-approved for the treatment of chronic myelogenous leukemia (CML) is much greater than that of other protein kinase inhibitors that are used for the management of other maladies. People with CML treated with BCR-Abl blockers have an annual mortality rate of 0.5 % or less when compared with age-matched control groups [169,170]. Such data indicate that BCR-Abl antagonists normalize the life span of CML patients, which is an unbelievable result for a life-threatening disease. Imatinib (first generation), bosutinib, nilotinib, and dasatinib (second generation) are FDA-approved for first-line therapy while asciminib and ponatinib (third generation) are given to patients with resistant disease and a T315I gatekeeper mutation or after failure with at least two other protein-tyrosine kinase antagonists [171]. Asciminib is a STAMP (Specifically Targeting the Abl Myristoyl Pocket) type IV allosteric inhibitor given for (i) the third-line treatment of CML or (ii) the first-line treatment of CML patients with the *T315I* mutation [157].

Dasatinib was an early drug used in the treatment of CML following its approval in 2006. It was discovered by high throughput screening (HTS) initiated by the Pfizer pharmaceutical company in 1986 [172]. HTS methodology uses 96-well plates with assay volumes of 50–100 μL. By 1992 HTS produced successful starting components for approximately 40 % of the drug discovery portfolio. By 1999 ADMET (Absorption, Distribution, Metabolism, Excretion, and Toxicity) HTS was incorporated into the drug discovery methodology. The Ro5 methodology was established at the time to maximize successful drug development and to minimize the attrition of drug precursors that were identified by HTS. The primary goal of drug discovery is to find a molecule with favorable pharmacodynamics, suitable pharmacokinetics, low toxicity, and low synthetic complexity. The pharmaceutical industry faces difficulties achieving this goal as indicated by the high failure rates of lead compounds (> 90 %) during the development process. Erlotinib, gefitinib, lapatinib and sorafenib are other early FDA-approved protein kinase antagonists that were produced from HTS hits. Before the introduction of high throughput screening, drug development depended upon experiments performed in live animals. Although experiments with live animals are currently used, efforts to minimize their necessity and use are now in vogue.

The generally used drug properties and descriptors used by medicinal chemists and pharmacologists are listed in Table 9. Beyond Ro5 (bRo5) descriptors include the potency, polar surface area, the number of rings, stereocenters, and rotatable bonds, ligand efficiency metrics, and composite metrics such as quantitative estimate of drug likeness (QED) [147,173–176]. Weak passive cell permeability, minimal solubility, and metabolic concerns are correlated with greater lipophilicity and higher molecular weights. These difficulties must be overcome when operating in the bRo5 arena. Increased molecular complexity often increases water solubility and decreases unwanted binding to off-targets. The protein kinase inhibitor discipline is relatively recent and 45 of the 94 FDA-approved drugs (47 %) have a least one Ro5 violation. When the five FDA-approved atypical protein kinase blockers (alpelisib, copanlisib, duvelisib, idelalisib, umbralisib) that target PI3K are included, 46 of the 99 drugs have Ro5 violations (umbralisib has two violations with a MW of 572 and a CLogP value of 5.02) [9,177]. As stated by Hartung et al. “Playing by the rules is thus not always advisable when pushing for success in drug discovery. Rather, successful drug hunters must follow a mindset of pushing the limits of what is possible. Now, 25 years after the publication of the Ro5, small-molecule drug discovery is looking at an exciting future of clinical impact that must not be restricted by the number 5” (note that the 25 in this sentence equals 5 × 5) [178].

Table 9
Drug properties and descriptors[a].

Category	Properties and descriptions
Size	Molecular weight (MW) and heavy atom count (N)
Lipophilicity	Calculated octanol–water partition coefficients (ALogP and Log $D_{7.4}$)
Polarity	Polar surface area (PSA), hydrogen-bond donors (HD) and hydrogen-bond acceptors (HA)
Aromatic and aliphatic descriptors	Number of rings (nRng), number of aromatic rings (nAr), number of benzene rings (nBnz), fraction of carbon atoms that are sp^3 hybridized (Fsp3), number of stereocenters (nStereo)
Flexibility	Number of rotatable bonds (nRotB)
Potency	– Log_{10} molar concentration IC_{50} or K_i as pIC_{50} or pK_i
Ligand efficiency metrics	Lipophilic ligand efficiency or LipE = pIC_{50} – AlogP or pIC_{50} – Log $D_{7.4;}$ Ligand efficiency or LE = pIC_{50} /N
Composite physicochemical descriptors	Quantitative estimate of drug-likeness or QED = summed, weighted desirability (scores using MW + ALogP + HD + HA + PSA + nRotB + nAr)

[a] Adapted from Ref. [147].

CRediT authorship contribution statement

Robert Roskoski: Conceptualization, Writing – original draft, Writing – review & editing.

Declaration of Competing Interest

The author is unaware of any affiliations, memberships, or financial holdings that might be perceived as affecting the objectivity of this review.

Acknowledgments

I thank Dr. Albert J. Kooistra for providing the template depicted in Fig. 7 and Laura M. Roskoski for providing editorial and bibliographic assistance. I also thank Jasper Martinsek and Josie Rudnicki for their help in preparing the figures and W.S. Sheppard and Pasha Brezina for their help in the analyses of drug properties. The colored figures in this paper were evaluated to ensure that their perception was accurately conveyed to colorblind readers [179].

Appendix A. Supporting information

Supplementary data associated with this article can be found in the online version at doi:10.1016/j.phrs.2026.108107.

Data availability

No data was used for the research described in the article.

References

[1] P. Cohen, Protein kinases – the major drug targets of the twenty-first century, Nat. Rev. Drug Discov. 1 (2002) 309–315, https://doi.org/10.1038/nrd773.
[2] R. Roskoski Jr, A historical overview of protein kinases and their targeted small molecule inhibitors, Pharm. Res 100 (2015) 1–23, https://doi.org/10.1016/j.phrs.2015.07.010.
[3] P. Cohen, D. Cross, P.A. Jänne, Kinase drug discovery 20 years after imatinib: progress and future directions, Nat. Rev. Drug Discov. 20 (2021) 551–569, https://doi.org/10.1038/s41573-021-00195-4.
[4] M.M. Attwood, D. Fabbro, A.V. Sokolov, S. Knapp, H.B. Schiöth, Trends in kinase drug discovery: targets, indications and inhibitor design, Nat. Rev. Drug Discov. 20 (2021) 839–861, https://doi.org/10.1038/s41573-021-00252-y.
[5] G.K. Kanev, C. de Graaf, I.J.P. de Esch, R. Leurs, T. Würdinger, B.A. Westerman, A.J. Kooistra, The landscape of atypical and eukaryotic protein kinases, Trends Pharm. Sci. 40 (2019) 818–832, https://doi.org/10.1016/j.tips.2019.09.002.
[6] C. Bournez, F. Carles, G. Peyrat, S. Aci-Sèche, S. Bourg, C. Meyer, P. Bonnet, Comparative assessment of protein kinase inhibitors in public databases and in PKIDB, Molecules 25 (2020) 3226, https://doi.org/10.3390/molecules25143226.
[7] J.J. Adashek, M. Nikanjam, R. Kurzrock, Tumour-agnostic kinase inhibitors, Nat. Rev. Drug Discov. 24 (2025) 504–520, https://doi.org/10.1038/s41573-025-01147-y.
[8] G. Manning, D.B. Whyte, R. Martinez, T. Hunter, S. Sudarsanam, The protein kinase complement of the human genome, Science 298 (2002) 1912–1934, https://doi.org/10.1126/science.1075762.
[9] R. Roskoski Jr, Properties of FDA-approved small molecule phosphatidylinositol 3-kinase inhibitors prescribed for the treatment of malignancies, Pharm. Res 168 (2021) 105579, https://doi.org/10.1016/j.phrs.2021.105579.
[10] R. Roskoski Jr, Properties of FDA-approved small molecule protein kinase inhibitors, Pharm. Res 144 (2019) 19–50, https://doi.org/10.1016/j.phrs.2019.03.006.
[11] R. Roskoski Jr, Properties of FDA-approved small molecule protein kinase inhibitors: a 2020 update, Pharm. Res 152 (2020) 104609, https://doi.org/10.1016/j.phrs.2019.104609.
[12] R. Roskoski Jr, Properties of FDA-approved small molecule protein kinase inhibitors: a 2021 update, Pharm. Res 165 (2021) 105463, https://doi.org/10.1016/j.phrs.2021.105463.
[13] R. Roskoski Jr, Properties of FDA-approved small molecule protein kinase inhibitors: a 2022 update, Pharm. Res 175 (2022) 106037, https://doi.org/10.1016/j.phrs.2021.106037.
[14] R. Roskoski Jr, Properties of FDA-approved small molecule protein kinase inhibitors: a 2023 update, Pharm. Res 187 (2023) 106552, https://doi.org/10.1016/j.phrs.2022.106552.
[15] R. Roskoski Jr, Properties of FDA-approved small molecule protein kinase inhibitors: a 2024 update, Pharm. Res 200 (2024) 107059, https://doi.org/10.1016/j.phrs.2024.107059.
[16] R. Roskoski Jr, Properties of FDA-approved small molecule protein kinase inhibitors: a 2025 update, Pharm. Res 216 (2025) 107723, https://doi.org/10.1016/j.phrs.2025.107723.
[17] S.H. Myers, V.G. Brunton, A. Unciti-Broceta, AXL inhibitors in cancer: a medicinal chemistry perspective, J. Med. Chem. 59 (2016) 3593–3608, https://doi.org/10.1021/acs.jmedchem.5b01273.
[18] B.L. Roth, D.J. Sheffler, W.K. Kroeze, Magic shotguns versus magic bullets: selectively non-selective drugs for mood disorders and schizophrenia, Nat. Rev. Drug Discov. 3 (2004) 353–359, https://doi.org/10.1038/nrd1346.
[19] R. Roskoski Jr, Orally effective FDA-approved protein kinase targeted covalent inhibitors (TCIs), Pharm. Res 165 (2021) 105422, https://doi.org/10.1016/j.phrs.2021.105422.
[20] R. Roskoski Jr, Futibatinib (Lytgobi) for cholangiocarcinoma, Trends Pharm. Sci. 44 (2023) 190–191, https://doi.org/10.1016/j.tips.2022.12.007.
[21] D.R. Knighton, J.H. Zheng, L.F. Ten Eyck, V.A. Ashford, N.H. Xuong, S.S. Taylor, J.M. Sowadski, Crystal structure of the catalytic subunit of cyclic adenosine monophosphate-dependent protein kinase, Science 253 (1991) 407–414, https://doi.org/10.1126/science.1862342.
[22] A.P. Kornev, S.S. Taylor, Dynamics-driven allostery in protein kinases, Trends Biochem Sci. 40 (2015) 628–647, https://doi.org/10.1016/j.tibs.2015.09.002.
[23] R. Roskoski Jr, Cyclin-dependent protein serine/threonine kinase inhibitors as anticancer drugs, Pharm. Res 139 (2019) 471–488, https://doi.org/10.1016/j.phrs.2018.11.035.
[24] R. Roskoski Jr, Hydrophobic and polar interactions of FDA-approved small molecule protein kinase inhibitors with their target enzymes, Pharm. Res 169 (2021) 105660, https://doi.org/10.1016/j.phrs.2021.105660.
[25] S.K. Hanks, T. Hunter, Protein kinases 6. The eukaryotic protein kinase superfamily: kinase (catalytic) domain structure and classification, FASEB J. 9 (1995) 576–596.
[26] Madhusudan, E.A. Trafny, N.H. Xuong, J.A. Adams, L.F. Ten Eyck, S.S. Taylor, J. M. Sowadski, cAMP-dependent protein kinase: crystallographic insights into substrate recognition and phosphotransfer, Protein Sci. 3 (1994) 176–187, https://doi.org/10.1002/pro.5560030203.
[27] J. Zhou, J.A. Adams, Participation of ADP dissociation in the rate-determining step in cAMP-dependent protein kinase, Biochemistry 36 (1997) 15733–15738, https://doi.org/10.1021/bi971438n.
[28] A.P. Kornev, S.S. Taylor, Defining the conserved internal architecture of a protein kinase, Biochim Biophys. Acta 1804 (2010) 440–444, https://doi.org/10.1016/j.bbapap.2009.10.017.
[29] V. Modi, R.L. Dunbrack Jr, Defining a new nomenclature for the structures of active and inactive kinases, Proc. Natl. Acad. Sci. USA 116 (2019) 6818–6827, https://doi.org/10.1073/pnas.1814279116.
[30] V. Modi, R.L. Dunbrack Jr, Kincore: a web resource for structural classification of protein kinases and their inhibitors, Nucleic Acids Res. 50 (2022) D654–D664, https://doi.org/10.1093/nar/gkab920.
[31] A.P. Kornev, N.M. Haste, S.S. Taylor, L.F. Ten Eyck, Surface comparison of active and inactive protein kinases identifies a conserved activation mechanism, Proc. Natl. Acad. Sci. USA 103 (2006) 17783–17788, https://doi.org/10.1073/pnas.0607656103.
[32] A.P. Kornev, S.S. Taylor, L.F. Ten Eyck, A helix scaffold for the assembly of active protein kinases, Proc. Natl. Acad. Sci. USA 105 (2008) 14377–14382, https://doi.org/10.1073/pnas.0807988105.
[33] H.S. Meharena, P. Chang, M.M. Keshwani, K. Oruganty, A.K. Nene, N. Kannan, S. S. Taylor, A.P. Kornev, Deciphering the structural basis of eukaryotic protein kinase regulation, PLoS Biol. 11 (2013) e1001690, https://doi.org/10.1371/journal.pbio.1001680.
[34] R. Roskoski Jr, Classification of small molecule protein kinase inhibitors based upon the structures of their drug-enzyme complexes, Pharm. Res 103 (2016) 26–48, https://doi.org/10.1016/j.phrs.2015.10.021.
[35] R. Roskoski Jr, The ErbB/HER family of protein-tyrosine kinases and cancer, Pharm. Res 79 (2014) 34–74, https://doi.org/10.1016/j.phrs.2013.11.002.
[36] R. Roskoski Jr, ErbB/HER protein-tyrosine kinases: structure and small molecule inhibitors, Pharm. Res 87 (2014) 42–59, https://doi.org/10.1016/j.phrs.2014.06.001.
[37] R. Roskoski Jr, Small molecule inhibitors targeting the EGFR/ErbB family of protein-tyrosine kinases in human cancers, Pharm. Res. 139 (2019) 395–411, https://doi.org/10.1016/j.phrs.2018.11.014.
[38] R. Roskoski Jr, Anaplastic lymphoma kinase (ALK): structure, oncogenic activation, and pharmacological inhibition, Pharm. Res. 68 (2013) 68–94, https://doi.org/10.1016/j.phrs.2012.11.007.
[39] R. Roskoski Jr, Anaplastic lymphoma kinase (ALK) inhibitors in the treatment of ALK-driven lung cancers, Pharm. Res. 117 (2017) 343–356, https://doi.org/10.1016/j.phrs.2017.01.007.
[40] R. Roskoski Jr, The preclinical profile of crizotinib in the treatment of non-small cell lung cancer and other neoplastic disorders, Expert Opin. Drug Dis. 8 (2013) 1165–1179, https://doi.org/10.1517/17460441.2013.813015.
[41] R. Roskoski Jr, The role of fibroblast growth factor receptor (FGFR) protein-tyrosine kinase inhibitors in the treatment of cancers including those of the urinary bladder, Pharm. Res. 151 (2020) 104567, https://doi.org/10.1016/j.phrs.2019.104567.
[42] R. Roskoski Jr, The role of small molecule platelet-derived growth factor receptor (PDGFR) inhibitors in the treatment of neoplastic disorders, Pharm. Res. 129 (2018) 65–83, https://doi.org/10.1016/j.phrs.2018.01.021.
[43] R. Roskoski Jr, A. Sadeghi-Nejad, Role of RET protein-tyrosine kinase inhibitors in the treatment RET-driven thyroid and lung cancers, Pharm. Res. 128 (2018) 1–17, https://doi.org/10.1016/j.phrs.2017.12.021.
[44] R. Roskoski Jr, The role of small molecule Kit protein-tyrosine kinase inhibitors in the treatment of neoplastic disorders, Pharm. Res. 133 (2018) 35–52, https://doi.org/10.1016/j.phrs.2018.04.020.
[45] R. Roskoski Jr, The role of small molecule Flt3 receptor protein-tyrosine kinase inhibitors in the treatment of Flt3-positive acute myelogenous leukemias, Pharm. Res. 155 (2020) 104725, https://doi.org/10.1016/j.phrs.2020.104725.
[46] R. Roskoski Jr, ROS1 protein-tyrosine kinase inhibitors in the treatment of ROS1 fusion protein-driven non-small cell lung cancers, Pharm. Res. 121 (2017) 202–212, https://doi.org/10.1016/j.phrs.2017.04.022.
[47] R. Roskoski Jr, Vascular endothelial growth factor (VEGF) and VEGF receptor inhibitors in the treatment of renal cell carcinomas, Pharm. Res. 120 (2017) 116–132, https://doi.org/10.1016/j.phrs.2017.03.010.
[48] R. Roskoski Jr, Janus kinase (JAK) inhibitors in the treatment of inflammatory and neoplastic diseases, Pharm. Res. 111 (2016) 784–803, https://doi.org/10.1016/j.phrs.2016.07.038.
[49] R. Roskoski Jr, Janus kinase (JAK) inhibitors in the treatment of neoplastic and inflammatory disorders, Pharm. Res. 183 (2022) 106362, https://doi.org/10.1016/j.phrs.2022.106362.
[50] R. Roskoski Jr, Ibrutinib inhibition of Bruton protein-tyrosine kinase (BTK) in the treatment of B cell neoplasms, Pharm. Res. 113 (2016) 395–408, https://doi.org/10.1016/j.phrs.2016.09.011.
[51] R. Roskoski Jr, Src protein-tyrosine kinase structure, mechanism, and small molecule inhibitors, Pharm. Res. 94 (2015) 9–25, https://doi.org/10.1016/j.phrs.2015.01.003.
[52] M.C. Frame, R. Roskoski Jr, Src family tyrosine kinases. Reference module in life sciences, Elsevier, Amsterdam, 2017, pp. 1–11, https://doi.org/10.1016/B978-0-12-809633-8.07199-5.
[53] R. Roskoski Jr, Targeting BCR-Abl in the treatment of Philadelphia-chromosome positive chronic myelogenous leukemia, Pharm. Res. 178 (2022) 106156, https://doi.org/10.1016/j.phrs.2022.106156.
[54] R. Roskoski Jr, Allosteric MEK1/2 inhibitors including cobimetanib and trametinib in the treatment of cutaneous melanomas, Pharm. Res. 117 (2017) 20–31, https://doi.org/10.1016/j.phrs.2016.12.009.
[55] R. Roskoski Jr, Cyclin-dependent protein kinase inhibitors including palbociclib as anticancer drugs, Pharm. Res 107 (2016) 249–275, https://doi.org/10.1016/j.phrs.2016.03.012.
[56] R. Roskoski Jr, ERK1/2 MAP kinases: structure, function, and regulation, Pharm. Res. 66 (2012) 105–143, https://doi.org/10.1016/j.phrs.2012.04.005.

[57] R. Roskoski Jr, Targeting ERK1/2 protein-serine/threonine kinases in human cancers, Pharm. Res. 142 (2019) 151–168, https://doi.org/10.1016/j.phrs.2019.01.039.
[58] A. Martin-Vega, M.H. Cobb, Navigating the ERK1/2 MAPK Cascade, Biomolecules 13 (2023) 1555, https://doi.org/10.3390/biom13101555.
[59] R. Roskoski Jr, Targeting oncogenic Raf protein-serine/threonine kinases in human cancers, Pharm. Res 135 (2018) 239–258, https://doi.org/10.1016/j.phrs.2018.08.013.
[60] R. Roskoski Jr, RAF protein-serine/threonine kinases: structure and regulation, Biochem. Biophys. Res. Commun. 399 (2010) 313–317, https://doi.org/10.1016/j.bbrc.2010.07.092.
[61] Y. Liu, K. Shah, F. Yang, L. Witucki, K.M. Shokat, A molecular gate which controls unnatural ATP analogue recognition by the tyrosine kinase v-Src, Bioorg. Med. Chem. 6 (1998) 1219–1226, https://doi.org/10.1016/s0968-0896(98)00099-6.
[62] A.C. Dar, K.M. Shokat, The evolution of protein kinase inhibitors from antagonists to agonists of cellular signaling, Annu Rev. Biochem. 80 (2011) 769–795, https://doi.org/10.1146/annurev-biochem-090308-173656.
[63] P.M. Ung, R. Rahman, A. Schlessinger, Redefining the protein kinase conformational space with machine learning, Cell Chem. Biol. 25 (2018) 916–924.e2, https://doi.org/10.1016/j.chembiol.2018.05.002.
[64] R. Hu, H. Xu, P. Jia, Z. Zhao, KinaseMD: kinase mutations and drug response database, Nucleic Acids Res 49 (D1) (2021) D552–D561, https://doi.org/10.1093/nar/gkaa945.
[65] D. Fabbro, S.W. Cowan-Jacob, H. Moebitz, Ten things you should know about protein kinases: IUPHAR Review 14, Br. J. Pharm. 172 (2015) 2675–2700, https://doi.org/10.1111/bph.13096.
[66] A.J. Kooistra, A. Volkamer, Kinase-centric computational drug development, Ann. Rep. Med. Chem. 50 (2017) 197–236, https://doi.org/10.1016/bs.armc.2017.08.001.
[67] E. Mavridis, D. Hadjipavlou-Litina, Using a novel consensus-based chemoinformatics approach to predict ADMET properties and druglikeness of tyrosine kinase inhibitors, Int. J. Mol. Sci. 26 (2025) 10207, https://doi.org/10.3390/ijms262010207.
[68] M. Malumbres, M. Barbacid, RAS oncogenes: the first 30 years, Nat. Rev. Cancer 3 (2003) 459–465, https://doi.org/10.1038/nrc1097.
[69] A.G. Stephen, D. Esposito, R.K. Bagni, F. McCormick, Dragging Ras back in the ring, Cancer Cell 25 (2014) 272–281, https://doi.org/10.1016/j.ccr.2014.02.017.
[70] D.K. Simanshu, D.V. Nissley, F. McCormick, RAS proteins and their regulators in human disease, Cell 170 (2017) 17–33, https://doi.org/10.1016/j.cell.2017.06.009.
[71] M. Holderfield, M.M. Deuker, F. McCormick, M. McMahon, Targeting RAF kinases for cancer therapy: BRAF-mutated melanoma and beyond, Nat. Rev. Cancer 14 (2014) 455–467, https://doi.org/10.1038/nrc3760.
[72] G.M. Nitulescu, G. Stancov, O.C. Seremet, G. Nitulescu, D.P. Mihai, C.G. Duta-Bratu, S.F. Barbuceanu, O.T. Olaru, The importance of the pyrazole scaffold in the design of protein kinases inhibitors as targeted anticancer therapies, Molecules 28 (2023) 5359, https://doi.org/10.3390/molecules28145359.
[73] M.A. Hossain, A comprehensive review of targeting RAF kinase in cancer, Eur. J. Pharm. 986 (2025) 177142, https://doi.org/10.1016/j.ejphar.2024.177142.
[74] E.H. Chang, M.A. Gonda, R.W. Ellis, E.M. Scolnick, D.R. Lowy, Human genome contains four genes homologous to transforming genes of Harvey and Kirsten murine sarcoma viruses, Proc. Natl. Acad. Sci. USA 79 (1982) 4848–4852, https://doi.org/10.1073/pnas.79.16.4848.
[75] G.M. Cooper, Cellular transforming genes, Science 217 (1982) 801–806, https://doi.org/10.1126/science.6285471.
[76] N.K. Williams, R.S. Bamert, O. Patel, C. Wang, P.M. Walden, A.F. Wilks, et al., Dissecting specificity in the Janus kinases: the structures of JAK-specific inhibitors complexed to the JAK1 and JAK2 protein tyrosine kinase domains, J. Mol. Biol. 387 (2009) 219–232, https://doi.org/10.1016/j.jmb.2009.01.041.
[77] A.F. Wilks, The JAK kinases: not just another kinase drug discovery target, Semin Cell Dev. Biol. 19 (2008) 319–328, https://doi.org/10.1016/j.semcdb.2008.07.020.
[78] M. Kawamura, D.W. McVicar, J.A. Johnston, T.B. Blake, Y.Q. Chen, B.K. Lal, A. R. Lloyd, D.J. Kelvin, J.E. Staples, Ortaldo Jr, J.J. O'Shea, Molecular cloning of L-JAK, a Janus family protein-tyrosine kinase expressed in natural killer cells and activated leukocytes, Proc. Natl. Acad. Sci. USA 91 (1994) 6374–6378, https://doi.org/10.1073/pnas.91.14.6374.
[79] R. Roskoski Jr, Deucravacitinib is an allosteric TYK2 protein kinase inhibitor FDA-approved for the treatment of psoriasis, Pharm. Res. 189 (2023) 106642, https://doi.org/10.1016/j.phrs.2022.106642.
[80] J.J. Babon, I.S. Lucet, J.M. Murphy, N.A. Nicola, L.N. Varghese, The molecular regulation of Janus kinase (JAK) activation, Biochem. J. 462 (2014) 1–13, https://doi.org/10.1042/BJ20140712.
[81] S. Abroun, N. Saki, M. Ahmadvand, F. Asghari, F. Salari, F. Rahim, STATs: an old story, yet mesmerizing, Cell J. 17 (2015) 395–411, https://doi.org/10.22074/cellj.2015.1.
[82] X. Chen, U. Vinkemeier, Y. Zhao, D. Jeruzalmi, J.E. Darnell Jr, J. Kuriyan, Crystal structure of a tyrosine phosphorylated STAT-1 dimer bound to DNA, Cell 93 (1998) 827–839, https://doi.org/10.1016/s0092-8674(00)81443-9.
[83] F. Zuccotto, E. Ardini, E. Casale, M. Angiolini, Through the "gatekeeper door": exploiting the active kinase conformation, J. Med. Chem. 53 (2010) 2691–2694, https://doi.org/10.1021/jm901443h.
[84] L.K. Gavrin, E. Saiah, Approaches to discover non-ATP site inhibitors, Med. Chem. Commun. 4 (2013) 41–51, https://doi.org/10.1039/C2MD20180A.
[85] V. Lamba, I. Ghosh, New directions in targeting protein kinases: focusing upon true allosteric and bivalent inhibitors, Curr. Pharm. Des. 18 (2012) 2936–2945, https://doi.org/10.2174/138161212800672813.
[86] J.J. Liao, Molecular recognition of protein kinase binding pockets for design of potent and selective kinase inhibitors, J. Med. Chem. 50 (2007) 409–424, https://doi.org/10.1021/jm0608107.
[87] O.P. van Linden, A.J. Kooistra, R. Leurs, I.J. de Esch, C. de Graaf, KLIFS: a knowledge-based structural database to navigate kinase-ligand interaction space, J. Med. Chem. 57 (2014) 249–277, https://doi.org/10.1021/jm400378w.
[88] A.J. Kooistra, G.K. Kanev, O.P. van Linden, R. Leurs, I.J. de Esch, C. de Graaf, KLIFS: a structural kinase-ligand interaction database, Nucleic Acids Res. 44 (D1) (2016) D365–D371, https://doi.org/10.1093/nar/gkv1082.
[89] G.K. Kanev, C. de Graaf, B.A. Westerman, I.J.P. de Esch, A.J. Kooistra, KLIFS: an overhaul after the first 5 years of supporting kinase research, Nucleic Acids Res. 49 (D1) (2021) D562–D569, https://doi.org/10.1093/nar/gkaa895.
[90] B. Wienen-Schmidt, D. Schmidt, H.D. Gerber, A. Heine, H. Gohlke, G. Klebe, Surprising non-additivity of methyl groups in drug-kinase interaction, ACS Chem. Biol. 14 (2019) 2585–2594, https://doi.org/10.1021/acschembio.9b00476.
[91] D. Bajusz, G.G. Ferenczy, G.M. Keserű, Structure-based virtual screening approaches in kinase-directed drug discovery, Curr. Top. Med. Chem. 17 (2017) 2235–2259, https://doi.org/10.2174/1568026617666170224121313.
[92] P. Wu, T.E. Nielsen, M.H. Clausen, FDA-approved small-molecule kinase inhibitors, Trends Pharm. Sci. 36 (2015) 422–439, https://doi.org/10.1016/j.tips.2015.04.005.
[93] E.H. Stover, E.K. Lee, G.I. Shapiro, J.S. Brugge, U.A. Matulonis, J.F. Liu, The RAS-MEK-ERK pathway in low-grade serous ovarian cancer, Gynecol. Oncol. 200 (2025) 22–32, https://doi.org/10.1016/j.ygyno.2025.06.022.
[94] S.N. Banerjee, E. Van Nieuwenhuysen, C. Aghajanian, V. D'Hondt, B.J. Monk, A. Clamp, E. Prendergast, A. Oaknin, K. Ring, N. Colombo, R.W. Holloway, M. Rodrigues, H.S. Chon, C. Gourley, A.D. Santin, P.H. Thaker, C. Gennigens, G. Newman, E. Salinas, H. Youssoufian, K.N. Moore, S. Lustgarten, D.M. O'Malley, T. Van Gorp, R.N. Grisham, Efficacy and safety of avutometinib ± defactinib in recurrent low-grade serous ovarian cancer: primary analysis of ENGOT-OV60/GOG-3052/RAMP 201, J. Clin. Oncol. 43 (2025) 2782–2792, https://doi.org/10.1200/JCO-25-00112.
[95] S.N. Banerjee, E. Van Nieuwenhuysen, C. Aghajanian, V. D'Hondt, B.J. Monk, A. Clamp, E. Prendergast, A. Oaknin, K. Ring, N. Colombo, R.W. Holloway, M. Rodrigues, H.S. Chon, C. Gourley, A.D. Santin, P.H. Thaker, C. Gennigens, G. Newman, E. Salinas, H. Youssoufian, K.N. Moore, S. Lustgarten, D.M. O'Malley, T. Van Gorp, R.N. Grisham, The combination of avutometinib and defactinib in treating recurrent low-grade serous ovarian cancer: a plain language summary of the Phase II clinical trial ENGOT-OV60/GOG-3052/RAMP 201, Future Oncol. 21 (2025) 3859–3871, https://doi.org/10.1080/14796694.2025.2595130.
[96] R.N. Grisham, B.M. Slomovitz, N. Andrews, S. Banerjee, J. Brown, M.S. Carey, H. Chui, R.L. Coleman, A.N. Fader, S. Gaillard, C. Gourley, A.K. Sood, B.J. Monk, K.N. Moore, I. Ray-Coquard, I.M. Shih, S.N. Westin, K.K. Wong, D.M. Gershenson, Low-grade serous ovarian cancer: expert consensus report on the state of the science, Int. J. Gynecol. Cancer 33 (2023) 1331–1344, https://doi.org/10.1136/ijgc-2023-004610.
[97] L. Kelliher, R. Yoeli-Bik, L. Schweizer, E. Lengyel, Molecular changes driving low-grade serous ovarian cancer and implications for treatment, Int. J. Gynecol. Cancer 34 (2024) 1630–1638, https://doi.org/10.1136/ijgc-2024-005305.
[98] N. Ishii, N. Harada, E.W. Joseph, K. Ohara, T. Miura, H. Sakamoto, Y. Matsuda, Y. Tomii, Y. Tachibana-Kondo, H. Iikura, T. Aoki, N. Shimma, M. Arisawa, Y. Sowa, P.I. Poulikakos, N. Rosen, Y. Aoki, T. Sakai, Enhanced inhibition of ERK signaling by a novel allosteric MEK inhibitor, CH5126766, that suppresses feedback reactivation of RAF activity, Cancer Res. 73 (2013) 4050–4060, https://doi.org/10.1158/0008-5472.CAN-12-3937.
[99] B. McNamara, C. Demirkiran, T.M.P. Hartwich, S. Bellone, D. Manavella, L. Mutlu, M. Greenman, M. Zipponi, Y. Yang-Hartwich, K. Yang, E. Ratner, P. E. Schwartz, S. Coma, J.A. Pachter, A.D. Santin, Preclinical efficacy of RAF/MEK clamp avutometinib in combination with FAK inhibition in low grade serous ovarian cancer, Gynecol. Oncol. 183 (2024) 133–140, https://doi.org/10.1016/j.ygyno.2024.01.028.
[100] R. Grisham, B.J. Monk, E. Van Nieuwenhuysen, K.N. Moore, M. Fabbro, D. M. O'Malley, A. Oaknin, P. Thaker, A.M. Oza, N. Colombo, D. Gershenson, C. A. Aghajanian, C.H. Choi, Y.C. Lee, M.R. Mirza, R.L. Coleman, L. Cobb, P. Harter, S. Lustgarten, H. Youssoufian, S. Banerjee, GOG-3097/ENGOT-ov81/GTG-UK/RAMP 301: a phase 3, randomized trial evaluating avutometinib plus defactinib compared with investigator's choice of treatment in patients with recurrent low grade serous ovarian cancer, Int. J. Gynecol. Cancer 35 (2025) 101832, https://doi.org/10.1136/ijgc-2024-005919.
[101] G.L. Gonzalez-Del Pino, K. Li, E. Park, A.M. Schmoker, B.H. Ha, M.J. Eck, Allosteric MEK inhibitors act on BRAF/MEK complexes to block MEK activation, Proc. Natl. Acad. Sci. USA 118 (2021) e2107207118, https://doi.org/10.1073/pnas.2107207118.
[102] R. Bissonnette, T. Agner, S. Molin, E. Guttman-Yassky, Hand eczema-Part 1: epidemiology, pathogenesis, diagnosis, and work-up, J. Am. Acad. Dermatol. 93 (2025) 1201–1210, https://doi.org/10.1016/j.jaad.2024.09.048.
[103] A.S. Quaade, A.B. Simonsen, A.S. Halling, J.P. Thyssen, J.D. Johansen, Prevalence, incidence, and severity of hand eczema in the general population - a systematic review and meta-analysis, Contact Dermat. 84 (2021) 361–374, https://doi.org/10.1111/cod.13804.
[104] E. Haider, L. Tanveer, M. Usman Iqbal, J. Taj, C. Tague, Delgocitinib in dermatology: a topical pan-JAK inhibitor for chronic hand eczema and atopic

dermatitis, Ann. Med. Surg. 87 (2025) 7928–7929, https://doi.org/10.1097/MS9.0000000000004233.
[105] A.M. Giménez-Arnau, A. Pinter, W. Sondermann, Z. Reguiai, R. Woolf, C. Lynde, F.J. Legat, A. Costanzo, J.F. Silvestre, N. Mellerup, M.L. Østerdal, U. Plohberger, L. Ryttig, A. Bauer, trial investigators, Efficacy and safety of topical delgocitinib cream versus oral alitretinoin capsules in adults with severe chronic hand eczema (DELTA FORCE): a 24-week, randomised, head-to-head, phase 3 trial, Lancet 405 (2025) 1676–1688, https://doi.org/10.1016/S0140-6736(25)00001-7.
[106] D. Termini, G. Avallone, G. Tavoletti, J. Beaziz, C. Moltrasio, V. Boero, A. V. Marzano, S.M. Ferrucci, Pan-JAK inhibition across chronic hand eczema and other cutaneous diseases: an updated review on topical delgocitinib, Drugs (2025), https://doi.org/10.1007/s40265-025-02262-1.
[107] Z. Jawaid, M. Khalid, A. Waafira, Delgocitinib 2% cream: a promising FDA-approved therapy for moderate-to-severe chronic hand eczema, Ann. Med Surg. 87 (2025) 6916–6917, https://doi.org/10.1097/MS9.0000000000003771.
[108] S. Noji, Y. Hara, T. Miura, H. Yamanaka, K. Maeda, A. Hori, H. Yamamoto, S. Obika, M. Inoue, Y. Hase, T. Orita, S. Doi, T. Adachi, A. Tanimoto, C. Oki, Y. Kimoto, Y. Ogawa, T. Negoro, H. Hashimoto, M. Shiozaki, Discovery of a Janus kinase inhibitor bearing a highly three-dimensional spiro scaffold: JTE-052 (Delgocitinib) as a new dermatological agent to treat inflammatory skin disorders, J. Med Chem. 63 (2020) 7163–7185, https://doi.org/10.1021/acs.jmedchem.0c00450.
[109] S.F.Z. Hujjat, H.K. Chandani, M.S. Khan, D.K. Chandani, A. Mahmoud, Bruton's tyrosine kinase inhibition in ITP: Wayrilz (rilzabrutinib) as a disease-modifying strategy, Ann. Med. Surg. 87 (2025) 7907–7909, https://doi.org/10.1097/MS9.0000000000004164.
[110] D.J. Kuter, W. Ghanima, Evaluating rilzabrutinib in the treatment of immune thrombocytopenia, Immunotherapy 17 (2025) 767–782, https://doi.org/10.1080/1750743X.2025.2545170.
[111] T.D. Owens, K.A. Brameld, E.J. Verner, T. Ton, X. Li, J. Zhu, M.R. Masjedizadeh, J.M. Bradshaw, R.J. Hill, D. Tam, A. Bisconte, E.O. Kim, M. Francesco, Y. Xing, J. Shu, D. Karr, J. LaStant, D. Finkle, N. Loewenstein, H. Haberstock-Debic, M. J. Taylor, P. Nunn, C.L. Langrish, D.M. Goldstein, Discovery of reversible covalent Bruton's tyrosine kinase inhibitors PRN473 and PRN1008 (Rilzabrutinib), J. Med Chem. 65 (2022) 5300–5316, https://doi.org/10.1021/acs.jmedchem.1c01170.
[112] D.C. Moore, P.C. Parish, Arnall Jr, J.B. Elmes, Rilzabrutinib and Bruton tyrosine kinase inhibition for the treatment of persistent or chronic immune thrombocytopenia, Expert Opin. Pharm. 26 (2025) 1583–1588, https://doi.org/10.1080/14656566.2025.2574850.
[113] J.A. Bernstein, M. Maurer, S.S. Saini, BTK signaling-a crucial link in the pathophysiology of chronic spontaneous urticaria, J. Allergy Clin. Immunol. 153 (2024) 1229–1240, https://doi.org/10.1016/j.jaci.2023.12.008.
[114] E.V. Lin, B. Arce, S. Alvarez-Arango, M.C. Dispenza, Current and future landscape of Bruton tyrosine kinase inhibitors in allergy, J. Allergy Clin. Immunol. 156 (2025) 568–578, https://doi.org/10.1016/j.jaci.2025.05.030.
[115] D. Angst, F. Gessier, P. Janser, A. Vulpetti, R. Wälchli, C. Beerli, A. Littlewood-Evans, J. Dawson, B. Nuesslein-Hildesheim, G. Wieczorek, S. Gutmann, C. Scheufler, A. Hinniger, A. Zimmerlin, E.G. Funhoff, R. Pulz, B. Cenni, Discovery of LOU064 (Remibrutinib), a potent and highly selective covalent inhibitor of Bruton's tyrosine kinase, J. Med. Chem. 63 (2020) 5102–5118, https://doi.org/10.1021/acs.jmedchem.9b01916.
[116] P. Kolkhir, J.S. Fok, E. Kocatürk, P.H. Li, T.L. Okas, J. Marcelino, M. Metz, Update on the treatment of chronic spontaneous urticaria, Drugs 85 (2025) 475–486, https://doi.org/10.1007/s40265-025-02170-4.
[117] M. Pérol, W. Li, N.A. Pennell, G. Liu, Y. Ohe, F. De Braud, M. Nagasaka, E. Felip, A. Xiong, Y. Zhang, H. Fan, X. Wang, S. Li, R.K. Lai, F. Ran, X. Zhang, W. Chen, L. Bazhenova, C. Zhou, Taletrectinib in ROS1+ non-small cell lung cancer: TRUST, J. Clin. Oncol. 43 (2025) 1920–1929, https://doi.org/10.1200/JCO-25-00275.
[118] M. Nagasaka, Y. Ohe, C. Zhou, C.M. Choi, N. Yang, G. Liu, E. Felip, M. Pérol, B. Besse, J. Nieva, L. Raez, N.A. Pennell, A. Dimou, F. Marinis, F. Ciardiello, T. Seto, Z. Hu, M. Pan, W. Wang, S. Li, S.I. Ou, TRUST-II: a global phase II study of taletrectinib in ROS1-positive non-small-cell lung cancer and other solid tumors, Future Oncol. 19 (2023) 123–135, https://doi.org/10.2217/fon-2022-1059.
[119] M. Nagasaka, D. Brazel, S.I. Ou, Taletrectinib for the treatment of ROS-1 positive non-small cell lung cancer: a drug evaluation of phase I and II data, Expert Opin. Invest. Drugs 33 (2024) 79–84, https://doi.org/10.1080/13543784.2024.2305131.
[120] Mankar S., Kumbhare M., Chandak S., Gadekar D. Zhongguo Ying Yong Sheng Li Xue Za Zhi, Next-generation targeted therapy: the evolving role of taletrectinib in fusion-positive malignancies, 2025 41:e20250033, https://doi: ⟨10.62958/j.cjap.2025.033⟩.
[121] S. Stacchiotti, H.R. Dürr, I.M. Schaefer, K. Woertler, R. Haas, A. Trama, A. Caraceni, J. Bajpai, G.G. Baldi, N. Bernthal, J.Y. Blay, K. Boye, J.M. Broto, W. T. Chen, P.A. Dei Tos, J. Desai, S. Emhofer, M. Eriksson, A. Gronchi, H. Gelderblom, J. Hardes, W. Hartmann, J. Healey, A. Italiano, R.L. Jones, A. Kawai, A. Leithner, H. Loong, E. Mascard, C. Morosi, N. Otten, E. Palmerini, S. R. Patel, P. Reichardt, B. Rubin, P. Rutkowski, C. Sangalli, K. Schuster, B. M. Seddon, M. Shkodra, E.L. Staals, W. Tap, M. van de Rijn, K. van Langevelde, F. M.M. Vanhoenacker, A. Wagner, L. Wiltink, S. Stern, V.M. Van de Sande, S. Bauer, Best clinical management of tenosynovial giant cell tumour (TGCT): a consensus paper from the community of experts, Cancer Treat. Rev. 112 (2023) 102491, https://doi.org/10.1016/j.ctrv.2022.102491.
[122] H. Gelderblom, V. Bhadri, S. Stacchiotti, S. Bauer, A.J. Wagner, M. van de Sande, N.M. Bernthal, A. López Pousa, A.A. Razak, A. Italiano, M. Ahmed, A. Le Cesne, G. Tinoco, K. Boye, J. Martín-Broto, E. Palmerini, S. Tafuto, S. Pratap, B. C. Powers, P. Reichardt, A. Casado Herráez, P. Rutkowski, C. Tait, F. Zarins, B. Harrow, M.G. Sharma, R. Ruiz-Soto, M.L. Sherman, J.Y. Blay, W.D. Tap, MOTION investigators, Vimseltinib versus placebo for tenosynovial giant cell tumour (MOTION): a multicentre, randomised, double-blind, placebo-controlled, phase 3 trial, Lancet 403 (2024) 2709–2719, https://doi.org/10.1016/S0140-6736(24)00885-7.
[123] F. Dou, D. Lu, J. Gao, Vimseltinib: a novel colony stimulating factor 1 receptor (CSF1R) inhibitor approved for treatment of tenosynovial giant cell tumors (TGCTs), Intractable Rare Dis. Res. 14 (2025) 143–144, https://doi.org/10.5582/irdr.2025.01010.
[124] T.M. Caldwell, Y.M. Ahn, S.L. Bulfer, C.B. Leary, M.M. Hood, W.P. Lu, L. Vogeti, S. Vogeti, M.D. Kaufman, S.C. Wise, B. Le Bourdonnec, B.D. Smith, D.L. Flynn, Discovery of vimseltinib (DCC-3014), a highly selective CSF1R switch-control kinase inhibitor, in clinical development for the treatment of Tenosynovial Giant Cell Tumor (TGCT), Bioorg. Med. Chem. Lett. 74 (2022) 128928, https://doi.org/10.1016/j.bmcl.2022.128928.
[125] B.D. Smith, M.D. Kaufman, S.C. Wise, Y.M. Ahn, T.M. Caldwell, C.B. Leary, W. P. Lu, G. Tan, L. Vogeti, S. Vogeti, B.A. Wilky, L.E. Davis, M. Sharma, R. Ruiz-Soto, D.L. Flynn, Vimseltinib: a precision CSF1R therapy for tenosynovial giant cell tumors and diseases promoted by macrophages, Mol. Cancer Ther. 20 (2021) 2098–2109, https://doi.org/10.1158/1535-7163.MCT-21-0361.
[126] E. Palmerini, J.C. Trent, F.J. Hornicek Jr, Medical management of tenosynovial giant cell tumor, Curr. Oncol. Rep. 27 (2025) 844–855, https://doi.org/10.1007/s11912-025-01679-x.
[127] B. Wilding, L. Woelflingseder, A. Baum, K. Chylinski, G. Vainorius, N. Gibson, I. C. Waizenegger, D. Gerlach, M. Augsten, F. Spreitzer, Y. Shirai, M. Ikegami, S. Tilandyová, D. Scharn, M.A. Pearson, J. Popow, A.C. Obenauf, N. Yamamoto, S. Kondo, F.L. Opdam, A. Bruining, S. Kohsaka, N. Kraut, J.V. Heymach, F. Solca, R.A. Neumüller, Zongertinib (BI 1810631), an irreversible HER2 TKI, spares EGFR signaling and improves therapeutic response in preclinical models and patients with HER2-driven cancers, Cancer Discov. 15 (2025) 119–138, https://doi.org/10.1158/2159-8290.CD-24-0306.
[128] J.V. Heymach, G. Ruiter, M.J. Ahn, N. Girard, E.F. Smit, D. Planchard, Y.L. Wu, B. C. Cho, N. Yamamoto, J.K. Sabari, Y. Zhao, H.Y. Tu, K. Yoh, E. Nadal, B. Sadrolhefazi, M. Rohrbacher, U. von Wangenheim, S. Eigenbrod-Giese, J. Zugazagoitia, Beamion LUNG-1 Investigators, Zongertinib in previously treated HER2-mutant Non-Small-Cell Lung Cancer, N. Engl. J. Med. 392 (2025) 2321–2333, https://doi.org/10.1056/NEJMoa2503704.
[129] D. Brazel, C.J. Park, M. Nagasaka, The development of Zongertinib for *HER2*-mutant NSCLC, Crit. Rev. Oncol. Hematol. 215 (2025) 104896, https://doi.org/10.1016/j.critrevonc.2025.104896.
[130] S. Waliany, M. Nagasaka, L. Park, C. Lam, Z. Jiang, F. Lin, J.W. Neal, Real-World Prevalence, treatment patterns, and outcomes for patients with HER2 (*ERBB2*)-mutant metastatic Non-Small Cell Lung Cancer, From a US-Based Clinico-Genomic Database, Cancer Med. 13 (2024) e70272, https://doi.org/10.1002/cam4.70272.
[131] L. Hong, S. Patel, L.M. Drusbosky, Y. Xiong, R. Chen, R. Geng, S. Heeke, M. Nilsson, J. Wu, J.V. Heymach, Y. Wang, J. Zhang, X. Le, Molecular landscape of *ERBB2* alterations in 3000 advanced NSCLC patients, NPJ Precis Oncol. 8 (2024) 217, https://doi.org/10.1038/s41698-024-00720-9.
[132] M. Dorta-Suárez, M. de Miguel, O. Amor-Carro, J.M. Calderón, M. González-Ortega, D. Rodríguez-Abreu, The state of the art of EGFR exon 20 insertions in non-small cell lung cancer: diagnosis and future perspectives, Cancer Treat. Rev. 124 (2024) 102671, https://doi.org/10.1016/j.ctrv.2023.102671.
[133] C.S. Gawli, C.R. Patil, H.M. Patel, A clinical review on third and fourth generation EGFR tyrosine kinase inhibitors for the treatment of non-small cell lung cancer, Bioorg. Med. Chem. 123 (2025) 118146, https://doi.org/10.1016/j.bmc.2025.118146.
[134] S. Dhillon, Sunvozertinib: first approval, Drugs 83 (2023) 1629–1634, https://doi.org/10.1007/s40265-023-01959-5.
[135] L. Lawrence, EGFR exon 20-targeting sunvozertinib granted accelerated approval for advanced NSCLC, Cancer 131 (2025) e70091, https://doi.org/10.1002/cncr.70091.
[136] K. Sangwan, G. Agarwal, Sunvozertinib: a promising oral EGFR inhibitor approved for NSCLC with EGFR Ex20ins mutations, Invest. N. Drugs 43 (2025) 1177–1189, https://doi.org/10.1007/s10637-025-01588-7.
[137] R.E. Strowd 3rd, Available therapies for patients with neurofibromatosis-related nervous system tumors, Curr. Treat. Options Oncol. 21 (2020) 81, https://doi.org/10.1007/s11864-020-00779-z.
[138] R. Roskoski Jr, Rule of five violations among the FDA-approved small molecule protein kinase inhibitors, Pharm. Res. 191 (2023) 106774, https://doi.org/10.1016/j.phrs.2023.106774.
[139] C.A. Lipinski, F. Lombardo, B.W. Dominy, P.J. Feeney, Experimental and computational approaches to estimate solubility and permeability in drug discovery and development settings, Adv. Drug Deliv. Rev. 46 (2001) 3–26, https://doi.org/10.1016/s0169-409x(00)00129-0.
[140] A.L. Hopkins, C.R. Groom, A. Alex, Ligand efficiency: a useful metric for lead selection, Drug Discov. Today 9 (2004) 430–431, https://doi.org/10.1016/S1359-6446(04)03069-7.
[141] P.D. Leeson, B. Springthorpe, The influence of drug-like concepts on decision-making in medicinal chemistry, Nat. Rev. Drug Discov. 6 (2007) 881–890, https://doi.org/10.1038/nrd2445.
[142] T.W. Johnson, R.A. Gallego, M.P. Edwards, Lipophilic efficiency as an important metric in drug design, J. Med. Chem. 61 (2018) 6401–6420, https://doi.org/10.1021/acs.jmedchem.8b00077.

[143] A.L. Hopkins, G.M. Keserü, P.D. Leeson, D.C. Rees, C.H. Reynolds, The role of ligand efficiency metrics in drug discovery, Nat. Rev. Drug Discov. 13 (2014) 105–121, https://doi.org/10.1038/nrd4163.
[144] P.D. Leeson, Molecular inflation, attrition, and the rule of five, Adv. Drug Deliv. Rev. 101 (2016) 22–33, https://doi.org/10.1016/j.addr.2016.01.018.
[145] D.F. Veber, S.R. Johnson, H.Y. Cheng, B.R. Smith, K.W. Ward, K.D. Kopple, Molecular properties that influence the oral bioavailability of drug candidates, J. Med. Chem. 45 (2002) 2615–2623, https://doi.org/10.1021/jm020017n.
[146] T.I. Oprea, Property distribution of drug-related chemical databases, J. Comput. Aided Mol. Des. 14 (2000) 251–264, https://doi.org/10.1023/a:1008130001697.
[147] P.D. Leeson, A.P. Bento, A. Gaulton, A. Hersey, E.J. Manners, C.J. Radoux, A. R. Leach, Target-based evaluation of "drug-like" properties and ligand efficiencies, J. Med Chem. 64 (2021) 7210–7230, https://doi.org/10.1021/acs.jmedchem.1c00416.
[148] J.J. Cui, M. McTigue, M. Nambu, M. Tran-Dubé, M. Pairish, H. Shen, L. Jia, H. Cheng, J. Hoffman, P. Le, M. Jalaie, G.H. Goetz, K. Ryan, N. Grodsky, Y. L. Deng, M. Parker, S. Timofeevski, B.W. Murray, S. Yamazaki, S. Aguirre, Q. Li, H. Zou, J. Christensen, Discovery of a novel class of exquisitely selective mesenchymal-epithelial transition factor (c-MET) protein kinase inhibitors and identification of the clinical candidate 2-(4-(1-(quinolin-6-ylmethyl)-1H-[1,2,3]triazolo[4,5-*b*]pyrazin-6-yl)-1H-pyrazol-1-yl)ethanol (PF-04217903) for the treatment of cancer, J. Med. Chem. 55 (2012) 8091–8109, https://doi.org/10.1021/jm300967g.
[149] S.H. Bertz, The first general index of molecular complexity, J. Am. Chem. Soc. 1103 (1981) 3559–3601.
[150] J.B. Hendrickson, P. Huang, A.G. Toczko, Molecular complexity: a simplified formula adapted to individual atoms, J. Chem. Inf. Comput. Sci. 27 (1987) 63–67.
[151] T.J. Ritchie, S.J. Macdonald, Physicochemical descriptors of aromatic character and their use in drug discovery, J. Med. Chem. 57 (2014) 7206–7215, https://doi.org/10.1021/jm500515d.
[152] M.K. Bayliss, J. Butler, P.L. Feldman, D.V. Green, P.D. Leeson, M.R. Palovich, A. J. Taylor, Quality guidelines for oral drug candidates: dose, solubility and lipophilicity, Drug Discov. Today 21 (2016) 1719–1727, https://doi.org/10.1016/j.drudis.2016.07.007.
[153] T.I. Oprea, C.G. Bologa, S. Brunak, A. Campbell, G.N. Gan, A. Gaulton, S. M. Gomez, R. Guha, A. Hersey, J. Holmes, A. Jadhav, L.J. Jensen, G.L. Johnson, A. Karlson, A.R. Leach, A. Ma'ayan, A. Malovannaya, S. Mani, S.L. Mathias, M. T. McManus, T.F. Meehan, C. von Mering, D. Muthas, D.T. Nguyen, J. P. Overington, G. Papadatos, J. Qin, C. Reich, B.L. Roth, S.C. Schürer, A. Simeonov, L.A. Sklar, N. Southall, S. Tomita, I. Tudose, O. Ursu, D. Vidovic, A. Waller, D. Westergaard, J.J. Yang, G. Zahoránszky-Köhalmi, Unexplored therapeutic opportunities in the human genome, Nat. Rev. Drug Discov. 17 (2018) 377, https://doi.org/10.1038/nrd.2018.52.
[154] L. Huang, S. Jiang, Y. Shi, Tyrosine kinase inhibitors for solid tumors in the past 20 years (2001-2020), J. Hematol. Oncol. 13 (2020) 143, https://doi.org/10.1186/s13045-020-00977-0.
[155] K. Bechman, M. Yates, J.B. Galloway, The new entries in the therapeutic armamentarium: the small molecule JAK inhibitors, Pharm. Res 147 (2019) 104392, https://doi.org/10.1016/j.phrs.2019.104392. ⟨10.1016/j.phrs.2020.104634⟩.
[156] M.A. Adas, E. Alveyn, E. Cook, M. Dey, J.B. Galloway, K. Bechman, The infection risks of JAK inhibition, Expert Rev. Clin. Immunol. 18 (2022) 253–261, https://doi.org/10.1080/1744666X.2022.2014323.
[157] R. Roskoski Jr, Cost in the United States of FDA-approved small molecule protein kinase inhibitors used in the treatment of neoplastic and non-neoplastic diseases, Pharm. Res. 199 (2023) 107036, https://doi.org/10.1016/j.phrs.2023.107036.
[158] C.I. Wells, H. Al-Ali, D.M. Andrews, C.R.M. Asquith, A.D. Axtman, I. Dikic, D. Ebner, P. Ettmayer, C. Fischer, M. Frederiksen, R.E. Futrell, N.S. Gray, S. B. Hatch, S. Knapp, U. Lücking, M. Michaelides, C.E. Mills, S. Müller, D. Owen, A. Picado, K.S. Saikatendu, M. Schröder, A. Stolz, M. Tellechea, B.J. Turunen, S. Vilar, J. Wang, W.J. Zuercher, T.M. Willson, D.H. Drewry, The kinase chemogenomic set (KCGS): an open science resource for kinase vulnerability identification, Int. J. Mol. Sci. 22 (2021) 566, https://doi.org/10.3390/ijms22020566.
[159] J. Choo, G. Heo, C. Pothoulakis, E. Im, Posttranslational modifications as therapeutic targets for intestinal disorders, Pharm. Res. (2021) 105412, https://doi.org/10.1016/j.phrs.2020.105412.
[160] C.C. Ayala-Aguilera, T. Valero, Á. Lorente-Macías, D.J. Baillache, S. Croke, A. Unciti-Broceta, Small molecule kinase inhibitor drugs (1995-2021): medical indication, pharmacology, and synthesis, J. Med. Chem. 65 (2022) 1047–1131, https://doi.org/10.1021/acs.jmedchem.1c00963.
[161] Z. Xie, X. Yang, Y. Duan, J. Han, C. Liao, Small-molecule kinase inhibitors for the treatment of nononcologic diseases, J. Med. Chem. 64 (2021) 1283–1345, https://doi.org/10.1021/acs.jmedchem.0c01511.
[162] R. Roskoski Jr, Blockade of mutant RAS oncogenic signaling with a special emphasis on KRAS, Pharm. Res 172 (2021) 105806, https://doi.org/10.1016/j.phrs.2021.105806.
[163] A. Cichońska, B. Ravikumar, R.J. Allaway, F. Wan, S. Park, O. Isayev, S. Li, M. Mason, A. Lamb, Z. Tanoli, M. Jeon, S. Kim, M. Popova, S. Capuzzi, J. Zeng, K. Dang, G. Koytiger, J. Kang, C.I. Wells, T.M. Willson, IDG-DREAM Drug-Kinase Binding Prediction Challenge Consortium, T.I. Oprea, A. Schlessinger, D. H. Drewry, G. Stolovitzky, K. Wennerberg, J. Guinney, T. Aittokallio, Crowdsourced mapping of unexplored target space of kinase inhibitors, Nat. Commun. 12 (2021) 3307, https://doi.org/10.1038/s41467-021-23165-1.
[164] H.Y. Min, H.Y. Lee, Molecular targeted therapy for anticancer treatment, Exp. Mol. Med. (2022), https://doi.org/10.1038/s12276-022-00864-3.
[165] X. Lu, J.B. Smaill, K. Ding, New promise and opportunities for allosteric kinase inhibitors, Angew. Chem. Int. Ed. Engl. 59 (2020) 13764–13776, https://doi.org/10.1002/anie.201914525.
[166] R. Roskoski Jr, Combination immune checkpoint and targeted protein kinase inhibitors for the treatment of renal cell carcinomas, Pharm. Res 203 (2024) 107181, https://doi.org/10.1016/j.phrs.2024.107181.
[167] R. Roskoski Jr, Targeted and cytotoxic inhibitors used in the treatment of breast cancer, Pharm. Res 210 (2024) 107534, https://doi.org/10.1016/j.phrs.2024.107534.
[168] R. Roskoski Jr, Targeted and cytotoxic inhibitors used in the treatment of lung cancers, Pharm. Res 209 (2024) 107465, https://doi.org/10.1016/j.phrs.2024.107465.
[169] K. Sasaki, S.S. Strom, S. O'Brien, E. Jabbour, F. Ravandi, M. Konopleva, G. Borthakur, N. Pemmaraju, N. Daver, P. Jain, S. Pierce, H. Kantarjian, J. E. Cortes, Relative survival in patients with chronic-phase chronic myeloid leukaemia in the tyrosine-kinase inhibitor era: analysis of patient data from six prospective clinical trials, Lancet Haematol. 2 (2015) e186–e193, https://doi.org/10.1016/S2352-3026(15)00048-4.
[170] H.M. Kantarjian, N. Jain, G. Garcia-Manero, M.A. Welch, F. Ravandi, W. G. Wierda, E.J. Jabbour, The cure of leukemia through the optimist's prism, Cancer 128 (2022) 240–259, https://doi.org/10.1002/cncr.33933.
[171] E. Jabbour, H. Kantarjian, J. Cortes, Use of second- and third-generation tyrosine kinase inhibitors in the treatment of chronic myeloid leukemia: an evolving treatment paradigm, Clin. Lymphoma Myeloma Leuk. 15 (2015) 323–334, https://doi.org/10.1016/j.clml.2015.03.006.
[172] R. Macarron, M.N. Banks, D. Bojanic, D.J. Burns, D.A. Cirovic, T. Garyantes, D. V. Green, R.P. Hertzberg, W.P. Janzen, J.W. Paslay, U. Schopfer, G. S. Sittampalam, Impact of high-throughput screening in biomedical research, Nat. Rev. Drug Discov. 10 (2011) 188–195, https://doi.org/10.1038/nrd3368.
[173] R.J. Young, S.L. Flitsch, M. Grigalunas, P.D. Leeson, R.J. Quinn, N.J. Turner, H. Waldmann, The time and place for nature in drug discovery, JACS Au 2 (2022) 2400–2416, https://doi.org/10.1021/jacsau.2c00415.
[174] D.G. Brown, What do oral drugs really look like? Dose regimen, pharmacokinetics, and safety of recently approved small-molecule oral drugs, J. Med. Chem. 68 (2025) 23751–23780, https://doi.org/10.1021/acs.jmedchem.5c02863.
[175] J.W. Collins, M. Abedi, D. Ramirez, L. Philippe-Venec, B. Moore, J.O. Asher, CANDID-CNS: AI unlocks stereochemistry and beyond rule of 5 to predict CNS penetration of small molecules, J. Chem. Inf. Model 65 (2025) 12918–12928, https://doi.org/10.1021/acs.jcim.5c01888.
[176] E. Mavridis, D. Hadjipavlou-Litina, Using a novel consensus-based chemoinformatics approach to predict ADMET properties and druglikeness of tyrosine kinase inhibitors, Int. J. Mol. Sci. 26 (2025) 10207, https://doi.org/10.3390/ijms262010207.
[177] A. Mullard, FDA approves 100th small-molecule kinase inhibitor, Nat. Rev. Drug Discov. 24 (2025) 891–895, https://doi.org/10.1038/d41573-025-00188-7.
[178] I.V. Hartung, B.R. Huck, A. Crespo, Rules were made to be broken, Nat. Rev. Chem. (2023), https://doi.org/10.1038/s41570-022-00451-0.
[179] R. Roskoski Jr, Guidelines for preparing color figures for everyone including the colorblind, Pharm. Res. 119 (2017) 240–241, https://doi.org/10.1016/j.phrs.2017.02.005.